IDENTIFICATION AND CHARACTERIZATION OF GENES ESSENTIAL FOR ONCOLYTIC NEWCASTLE DISEASE VIRUS REPLICATION IN HUMAN TUMOR CELLS

Dissertation zur Erlangung des akademischen Grades des

Doktors der Naturwissenschaften (Dr. rer. nat.)

eingereicht im Fachbereich Biologie, Chemie, Pharmazie

der Freien Universität Berlin

vorgelegt von

Jenny Sarah Puhlmann

aus Potsdam

Oktober 2009

Die Arbeit wurde im Zeitraum von November 2005 bis Oktober 2009 unter der Leitung von Dr. Rudolf Beier und Dr. Florian Pühler in der TRG Oncology, Bayer Schering Pharma AG, Berlin, angefertigt.

1. Gutachter	**Adjunct Prof. Dr. Sanna-Maria Käkönen** University of Turku, Turku, Finland Institute of Biomedicine
2. Gutachter	**Prof. Dr. Rupert Mutzel** Freie Universität Berlin, Berlin, Germany Institut für Pflanzenphysiologie und Mikrobiologie

Disputation am: 22.01.2010

ABSTRACT

Newcastle disease virus (NDV) is an avian paramyxovirus with a negative-stranded RNA genome. It has a natural preference for replicating in tumor cells but not in normal cells. Therefore, NDV is currently under investigations for oncolytic virotherapy.

A defective antiviral response in tumor cells is assumed to be responsible for tumor-selective viral replication. However, the precise link between tumorigenesis and sensitivity to oncolytic viruses is not fully understood and needs to be analyzed in more detail in order to improve therapeutic efficacy.

To address this issue, a human cell line model has been set up based on a non-tumorigenic keratinocyte cell line HaCaT and a derived *Harvey*-Rat sarcoma (H-Ras)-transformed and *in vivo* tumor-passaged clone RT3. In contrast to HaCaT cells, the tumorigenic cell line RT3 was partially susceptible to NDV. A RT3-derived subclone K1 featured an increased tumor growth potential in nude mice and a higher NDV susceptibility compared to the parental cell line RT3.

This model for oncolysis was utilized to systematically analyze pathways which are supposed to promote NDV susceptibility. Investigations of the Interferon (IFN)-signaling pathway as a reason for NDV susceptibility of RT3 and RT3 K1 cells did not show severe tumor cell-specific defects. Nevertheless, retarded induction and expression levels of several IFN-inducible antiviral factors following NDV infection could be observed. However, the most affected antiviral factor “Interferon inducible transmembrane protein I” was demonstrated to be dispensable for counteracting NDV replication. It indicated that oncolytic NDV replication could not exclusively depend on impaired IFN-mediated antiviral activity.

Oncogenic H-Ras, which had been used for tumorigenic transformation, was found to be necessary for virus replication in RT3 K1 cells but was not sufficient to render HaCaT cells NDV-susceptible. A focused siRNA screening approach on the basis of oncolytic NDV replication in RT3 K1 cells revealed additional oncolytic NDV-sensitizing cellular factors. Several genes with NDV-sensitizing properties but no direct connection with the IFN-signaling pathway were confirmed. Some of them were also found to be tumor cell-specifically overexpressed. The NDV-sensitizing Rho GTPase “Ras-related C3 botulinum toxin substrate 1” (Rac1) was demonstrated to be essential for NDV replication not only in H-Ras transformed RT3 K1 cells but also in epithelial cancer cells with *Kirsten*-Ras mutation. Unlike Ras, Rac1 was sufficient to render non-tumorigenic HaCaT cells susceptible to NDV replication. Initial experiments hint to a role for Rac1 in viral uptake and anchorage-

independent growth in RT3 K1 cells. Rac1 activity has been reported to be tightly connected with oncogenic Ras activity. Therefore, increased viral uptake, due to Rac1-mediated elevated endocytotic activity, could provide a link between Ras-induced tumorigenesis and oncolytic virus sensitivity in addition to defects in IFN-mediated antiviral defense.

In summary, this unique epithelial cell line model for NDV oncolysis in combination with the RNA interference screening approach identified novel NDV-sensitizing factors involved in cellular pathways such as clathrin-mediated processes and actin cytoskeleton reorganization. These results provide a basis for the identification of tumor-associated biomarkers for oncolytic virus replication and novel targets for anti-cancer therapy.

ZUSAMMENFASSUNG

Das Newcastle disease virus (NDV) ist ein aviäres Paramyxovirus mit einem RNA-Genom in Negativstrangorientierung. Das Virus zeichnet sich durch eine selektive Replikation in Tumorzellen aus, so dass es gegenwärtig in der onkolytischen Virotherapie klinisch getestet wird.

Es wird vermutet, dass die tumorselektive Replikation auf Defekte in der antiviralen Abwehr beruht. Der genaue Zusammenhang zwischen Tumorigenese und Suszeptibilität für onkolytische Viren ist bisher aber nicht vollständig geklärt. Ein besseres Verständnis dieses Zusammenhangs kann dazu beitragen, die antitumorale Effizienz dieser Viren zu verbessern.

Für diese Untersuchungen wurde ein humanes Zelllinienmodel herangezogen. Es basierte auf der nicht-tumorigenen Keratinozytenzelllinie HaCaT und der durch *Harvey* Rat sarcoma (H-Ras)-transformierten und mehrfach *in vivo* tumorpassagierten HaCaT Zelllinie RT3. Im Gegensatz zu HaCaT Zellen, erwiesen sich RT3 Zellen als partiell NDV-suszeptibel. Der isolierte Subklon K1 zeichnete sich nicht nur durch ein erhöhtes Tumorwachstum in Nacktmäusen aus, sondern auch durch eine verstärkte NDV-Suszeptibilität im Vergleich zu den parentalen RT3 Zellen.

Untersuchungen an diesem Modellsystem für Onkolyse zeigten, dass keine massiven tumorzell-spezifischen Defekte im Interferon (IFN)-Signalweg vorliegen. Allerdings waren die Induktions- und Expressionslevel einiger IFN-stimulierter, antiviraler Proteine tumorzell-spezifisch vermindert. Der am stärksten gehemmte antivirale Faktor „Interferon-stimuliertes Transmembranprotein 1“ zeigte jedoch keine NDV-spezifische antivirale Wirkung.

Im Gegensatz dazu konnte nachgewiesen werden, dass onkogenes H-Ras als NDV-sensitivierende Komponente in den Ras-transformierten RT3 K1 Zellen fungiert. Es bewirkte aber in HaCaT Zellen keine generelle NDV-Suszeptibilität.

Ein fokussiertes siRNA-Screening basierend auf der NDV-Replikation in RT3 K1 Zellen enthüllte zusätzliche NDV-sensitivierende Proteine. Diese zeigten keine direkte Verbindung zum IFN-Signalweg und waren teilweise auch tumorzell-spezifisch überexprimiert.

Die Rho GTPase “RAS-verwandtes C3-Botulinum-Toxin-Substrat 1” (Rac1) stellte sich als notwendige Komponente für die NDV-Replikation in den H-Ras transformierten RT3 K1 Zellen heraus. Auch für andere epitheliale Tumorzelllinien mit *Kirsten*-Ras Mutationen konnte ein Zusammenhang zwischen Rac1-Aktivität und NDV-Suszeptibilität nachgewiesen werden. Im Gegensatz zu H-Ras führte eine Überexpression von Rac1 zur NDV-Suszeptibilität von HaCaT Zellen.

Die Rac1-Aktivität wird durch die onkogene Aktivität von Ras beeinflusst. Tatsächlich verhinderte die dominant negative Rac1-Mutante das kontaktunabhängige Wachstum von RT3 K1 Zellen. Rac1 könnte demnach eine Verbindung zwischen Ras-induzierter Tumorigenese und NDV-Suszeptibilität darstellen. Möglicherweise führt eine verstärkte Rac1-Aktivität zu einer gesteigerten endozytotischen Aktivität und somit zu einer erhöhten Internalisierung von NDV in Tumorzellen. Zusätzlich könnten Defekte in der antiviralen Abwehr die NDV-Replikation in diesen Zellen begünstigen.

Mit Hilfe des epithelialen Zelllinienmodels für NDV Onkolyse kombiniert mit einem siRNA Screening konnten neue NDV-sensitivierende Proteine identifiziert werden. Diese Faktoren sind an verschiedenen zelluläre Signalwegen wie z.B. an Clathrin-vermittelten Prozessen und der Reorganisation des Aktinzytoskeletts beteiligt. Diese Ergebnisse sollten ein guter Ausgangspunkt sein, um tumorassoziierte Biomarker für die Virotherapie und neue therapeutische Zielmoleküle für die Behandlung von Krebs zu finden.

TABLE OF CONTENTS

ABBREVATIONS

Ago-2	Argonaute-2 protein
ALT	alternative lengthening of telomeres
AP	adaptor protein
AP-1	activator protein-1
ATP	adenosine triphosphate
BCA	bicinchoninic acid
CARD	caspase recruiting and activation domain
cDNA	complementary DNA
CHC	clathrin heavy chain
CLTA	clathrin light chain A
Ct	cycle threshold
cv	coefficient variation
DC	dendritic cell
DCCR	DharmaFECT Cell Culture Reagent
DMEM	Dulbecco's Modified Eagle Medium
DN	dominant negative
DNA	deoxyribonucleic acid
ECM	extracellular matrix
EDTA	ethylenediaminetetraacetic acid
e.g.	for example
EGFP	enhanced green fluorescent protein
eIF	eukaryotic initiation factor
F-actin	filamentous actin
FCS	fetal calf serum
FGFR3	fibroblast growth factor receptor 3
F-protein	fusion protein
Fyn	FYN oncogene related to SRC, FGR, YES
GAP	GTPase-activating protein
GAPDH	glyceraldehyde 3-phosphate dehydrogenase
G-CSF	granulocyte-colony stimulating factor
GDP	guanosine diphosphate
GEF	guanine-nucleotide exchange factor
GM-CSF	granulocyte macrophage-colony-stimulating-factor
dsRNA	double-stranded RNA
GTP	guanosine triphosphate
HBV	hepatitis B virus
HCC	hepatocellular carcinoma
HIV	human immunodeficiency virus
HN-protein	hemagglutinin-neuraminidase
H-Ras	Harvey-Ras
HSV-1	Herpes simplex virus-1
H101	genetically engineered adenovirus
IC_{50}	half maximal inhibitory concentration
IFITM1	interferon-induced transmembrane protein 1
IFN	interferon
IFNAR	IFN-α/β receptor
IKKε	inhibitor of kappa light polypeptide gene enhancer in B-cells, kinase epsilon

IPS-1	interferon-beta promoter stimulating factor 1 adaptor protein
ISG	IFN-stimulated genes
ISGF3	interferon-stimulated gene factor 3
ISRE	IFN-stimulated response element
IRF	interferon-regulatory factor
JAK1	Janus-activated kinase 1
K-Ras	Kirsten-Ras
LB	Luria-Bertani
LDS	Lithium dodecyl sulphate
L-protein	large (polymerase) protein
M	matrix protein
MAPK	mitogen activated protein kinase
MDA-5	melanoma-differentiation-associated gene 5
miRNA	micro-RNA
MOI	multiplicity of infection
mRNA	messenger RNA
MTH-68	More than hope 1968
MV	Measles virus
Mx	myxovirus resistance protein
MyD88	myeloid differentiation primary response protein 88
NDV	Newcastle disease virus
NF- κB	nuclear factor kappaB
NP	nucleocapsid protein
N-Ras	Neuroblastoma-Ras
nt	nucleotide
OAS	2´-5´-oligoadenylate synthetase
Pak	p21 activating kinase
Pak1	cell division cycle 42 (Cdc42)/Rac)-activated kinase 1
PAMP	pathogen associated molecular pattern
PBS	phosphate buffered saline
PCR	polymerase chain reaction
pDC	plasmacytoid dendritic cell
PFU	plaque forming unit
p.i.	post infection
PIK3CG	phosphoinositide-3-kinase, catalytic, gamma polypeptide
PIK4CA	phosphatidylinositol 4-kinase, catalytic, alpha
PI3K	phosphatidylinositol 3-kinase
PKB	protein kinase B
PKR	protein kinase R
PMV-1	paramyxovirus type 1
P-protein	phosphoprotein
Rac1	Ras-related C3 botulinum toxin substrate 1
Ras	rat sarcoma
Rb	retinoblastoma
REDOX	reduction-oxidation
reovirus	Respiratory enteric orphan virus
RhoA	Ras homolog gene familiy, member A
RIG-1	RNA helicases retinoic acid inducible gene-1
RISC	RNA-induced silencing complex

RLR	RIG-1-like receptor
RLU	relative luciferase units
RNA	ribonucleic acid
RNAi	RNA interference
RNase	ribonuclease
RTF	reverse transfection
SD	standard deviation
SDS-Page	sodium dodecyl sulfate polyacrylamide gel electrophoresis
siRNA	small interfering RNA
shRNA	short hairpin RNA
STAT	signal transducer and activator of transcription
TAE	Tris-acetate-EDTA
TBK1	Tank binding kinase-1
TBS-T	Tris-Buffered Saline Tween-20
TIAM1	T-cell lymphoma invasion and metastasis 1
TIR	Toll/interleukin-1 receptor
TLR	Toll-like receptor
TRAF3	tumor necrosis factor receptor-associated factor 3
TRIF	TIR domain-containing adaptor inducing IFN-β
TYK2	tyrosine kinase 2
txf.ctr.	transfection control
VSV	Vesicular stomatitis virus
UTR	untranslated region
UV	ultraviolet
wt	wild type
2`-5`-A	2`-5`linked-oligoadenylate

1 INTRODUCTION

1.1 Cancer biology

Cancer, a leading cause of death worldwide, is a complex collection of distinct genetic diseases which arise through multistep, mutagenic processes (http://www.who.int/cancer/en/index.html). It evolves through random mutations and epigenetic changes followed by clonal selection of cells that can survive and proliferate under circumstances that would normally lead to cell death. Hanahan and Weinberg postulated that there exist six essential hallmarks of tumorigenous growth namely (I) self-sufficiency in growth signals, (II) unlimited proliferation potential, (III) resistance to antiproliferative and (IV) apoptotic signaling, (V) sustained angiogenesis to supply with nutrients and oxygens as well as (VI) tissue invasion and metastasis [1]. These phenotypes are mainly provided by reactivating and modifying existing cellular pathways normally utilized for cell development and differentiation during embryogenesis and tissue homeostasis [2]. Many of these aberrant signaling pathways are induced by genetic alterations involving gain-of-function mutations, amplifications and/ or overexpressions of key oncogenes along with the loss-of-function mutation, deletion and/ or epigenetic silencing of key tumor suppressors. Recently, in 2008, Kroemer and colleagues postulated an additional cancer hallmark, the avoidance of immune surveillance and in 2009, Luo and colleagues proposed several cancer characteristics collectively referred to as stress phenotypes [2, 3]. These stress phenotypes including DNA damage/ replication stress, proteotoxic-, mitotic-, metabolic and oxidative stress are neither thought to be responsible for tumor initiation nor unique to cancer cells. However, they probably represent a common set of tumor-associated stresses a cancer cell has to tolerate by activating stress support pathways. Furthermore, the functional interaction among cancer hallmarks supports the tumorigenic state and at the same time suppresses tumor-specific stress [2] (Figure 1-1).

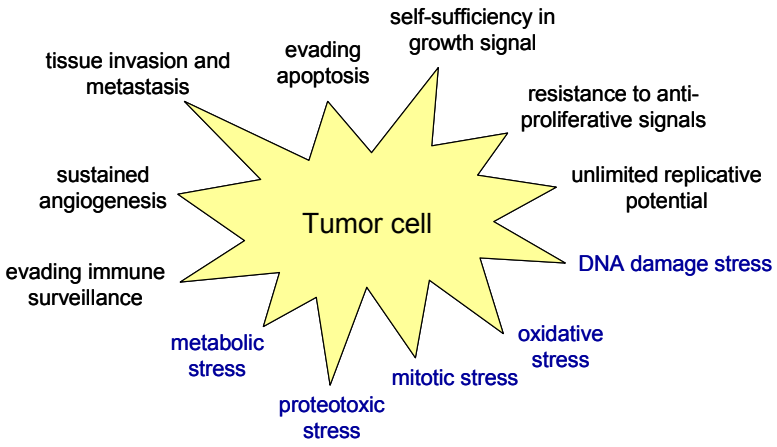

Figure 1-1: Cancer specific phenotypes
Cancer is a complex collection of diverse genetic diseases which can be summarized by common hallmarks. The tumorigenic state is supported by a functional interplay among these hallmarks and suppression of oncogenic stress [2].

1.2 Ras oncoprotein and its role in tumorigenous transformation of cells

Rat sarcoma (Ras) proteins are besides the Rho, Arf, Rab, Ran and Rad subfamilies members of a large family of approximately 21 kDa membrane-associated monomeric GTPases. These hydrolase enzymes cycle between an inactive guanosine diphosphate (GDP)-bound and an active guanosine triphosphate (GTP)-bound state. The GTP/GDP cycle of Ras proteins is regulated by a variety of cell surface receptors belonging to receptor tyrosine kinases, heterotrimeric G-protein-coupled or cytokine receptors and integrins. Guanine-nucleotide exchange factors (GEFs;[4]) promote the release of bound GDP and support binding of GTP whereas GTPase-activating proteins (GAPs; [5]) stimulate the low intrinsic GTPase activity of Ras thereby leading to its deactivation. Active GTP-bound Ras interacts with a variety of effector proteins [6]. The best characterized effectors are Raf kinases [7] and phosphatidylinositol 3-kinases (PI3K; [8]). In addition, certain GEFs and GAPs e.g. the Ras-related C3 botulinum toxin substrate 1 (Rac1) exchange factor T-cell lymphoma invasion and metastasis 1 (TIAM1) and the Ral exchange factor RalGDS have also been shown to serve as effector proteins coupling Ras to GTPases of the Rho and Ral family [9].

Prototypic members of the Ras subfamily are *Harvey* (H)-Ras, *Neuroblastoma* (N)-Ras and the two splice variants of *Kirsten* (K)-Ras. Although ubiquitously expressed, the three Ras isoforms have been postulated to perform distinct biological functions and can differentially activate Ras effector molecules [10]. Ras proteins act as molecular switches of signaling pathways which modulate a diverse range of cell behaviour including cell proliferation, differentiation and survival.

Ras genes are the most frequently mutated oncogenes in human cancer. Aberrant activation of Ras can occur either by mutation of the gene, overexpression or deregulated growth factor receptor signaling. Deregulated Ras signaling has been implicated in supporting virtually all aspects of a malignant phenotype of cells including proliferation, invasion and metastasis [11]. Mutated variants of Ras proteins at codon 12, 13 or 61 are detected in 30 % of all human tumors [12, 13]. These Ras mutants show impaired intrinsic GTPase activity which makes them insensitive to GAP-mediated GTP hydrolysis. These mutants are constitutively activated [14]. This property leads to deregulation of multiple downstream effector pathways which promote cellular transformation leading to deregulated cell growth, survival and differentiation. The two major pathways believed to play a pivotal role in Ras transformation and tumorigenesis are the mitogen activated protein kinase (MAPK)-pathway MAPK kinase kinase (Raf)/ MAPK kinase (MEK)/ MAPK (ERK) [15] and the PI3K-protein kinase B (PKB)- dependent pathway [16]. Aberrant activation of these pathways clearly contribute to oncogenic properties like independence from growth factors, enhanced proliferation and survival [17, 18]. Besides Ras, PI3K can also activate Rac-GEFs to promote activation of the small GTPase Rac [19, 20]. Aberrant Rac-mediated regulation of the actin cytoskeleton can lead to increased cell motility and contribute to tumor cell invasion and metastatis [21].

1.3 Virotherapy

The conventional approach of cancer therapy is cytotoxic chemotherapy either alone or in combination with surgery and radiotherapy. These conventional cancer therapies have many limitations and can cause severe side effects. As a consequence there are new approaches emerging e.g. biological therapies which utilize for example immunomodulatory factors, such as cytokines (e.g. interferons) or monoclonal antibodies to stimulate the patient's immune system to fight cancer. The latter is also used for functional blocking of cancer cell specific antigens or for delivery of toxin, radioisotope or cytokine conjugates into the tumor (http://www.cancer.gov/cancertopics/treatment/types-of-treatment).

One of the alternative approaches is the use of viruses as anti-cancer agents (virotherapy). These specific viruses are termed oncolytic viruses as they infect and destroy cancer cells but not normal cells. Interest in this mode of therapy started in the past century when temporary improvements of cancer following natural infections or vaccinations against viral diseases like rabbies have been reported [22]. In the 1950s human trials with diverse potentially oncolytic viruses were initiated [23, 24]. However, except for some individual cases of tumor regressions, this approach lacked a significant antitumor efficacy. Advanced knowledge with

respect to cancer and virus biology and the discovery of recombinant DNA technology have resulted in the current revival of oncolytic viruses in the field of cancer therapy. Since the 1990s when the first genetically engineered virus was described to selectively replicate in dividing cells, several preclinical as well as clinical studies with different virus species were performed. Currently, a variety of virus types are studied that can be roughly divided into two groups. On the one hand, there are inherently oncolytic wild-type strains (partially genetically engineered or live-attenuated) like Newcastle disease virus (NDV), Vesicular stomatitis virus (VSV), Measles virus (MV) or Respiratory enteric orphan virus (reovirus). On the other hand, there are several virus types rendered tumor-selective by genetic modifications e.g. adenovirus, Herpes simplex virus-1 (HSV-1) or influenza virus [25].

The first marketing approval for an oncolytic virus was granted in China in 2005 for a genetically engineered adenovirus (H101). This virus showed superior response rates in head and neck cancer in patients treated with combined intratumoral H101 and chemotherapy compared to those treated with chemotherapy alone [26]. However, there are no follow up studies under way.

Despite promising results in the field of virotherapy, there is still the need to further understand the molecular mechanism of the interplay between the oncolytic virus and the tumor cell in order to improve antitumor efficacy.

This project concentrated on the investigation of the tumor-selective replication of NDV. In the following section, this virus is further introduced with regard to its molecular biology and oncolytic properties.

1.4 Newcastle disease virus

1.4.1 Newcastle disease

NDV was named after the first described disease outbreak in 1926 as it was discovered on a chicken farm near Newcastle-upon-Tyne (UK) [27, 28]. It can cause a fatal disease in a wide variety of birds, especially in poultry. The disease is characterized by inflammation of the respiratory tract and of either the brain or the gastrointestinal tract [29, 30]. NDV can be considered as human apathogenic because it has only adapted to the avian immune system and can not cope with the immune system of humans [31, 32]. NDV infections of humans have therefore only been reported to cause transient conjunctivitis [33].

1.4.2 Structure of NDV and functions of the viral proteins

NDV is an avian paramyxovirus type 1 (avian PMV-1) which belongs to the Paramyxoviridae-family in the order Mononegaviralis [28, 34]. It used to be classified in the genus Rubulavirus but as it infects birds it was recently reclassified in the genus Avulavirus [35]. This enveloped virus reaches a diameter of 100 to 300 nm and exhibits a pleomorphic spherical shape covered with spikes of glycoproteins. The negative single-stranded RNA genome is non-segmented and of approximately 15-16 kb size [28, 36]. The complete RNA sequence of several NDV strains is already known. Its viral genome codes for 6 gene products. Starting from the 3´-end: nucleocapsid protein (NP, 55 kDa), phosphoprotein (P, 53 kDa), matrix protein (M, 40 kDa), fusion protein (F, 67 kDa), hemagglutinin-neuraminidase (HN, 74 kDa) and the large (polymerase) protein (L, 200 kDa). By means of RNA-editing (insertion of one nontemplate G residue), the P gene encodes for an additional gene product, the V-protein. The F protein is synthesized as an inactive precursor (F_0) and is cleaved by host proteases into biologically active F_1 (55 kDa) and F_2 (12.5 kDa) proteins which remain connected via a disulfide-linkage. Some strains also produce a HN protein precursor (HN_0) which requires proteolytic activation before these strains can attach to receptors on host cells. Cleavage of this HN_0 proteins of the progeny virus is also limited to a restricted range of host cells [37-39].

The surface glycoprotein HN, anchored in the viral envelope, mediates attachment of the virus to sialic acid-containing cell surface molecules such as gangliosides and N-glycoproteins which can be found on most mammalian cells [40]. The F glycoprotein is also anchored in the viral envelope and is required together with the HN protein for viral membrane fusion with the host cell membrane which mediates cell entry [41]. The M-protein, which controls virus assembly before budding, is located between the viral envelope and the nucleocapsid [42]. The nucleocapsid consists of NP, L- and P-proteins which form a complex with the viral RNA genome and thereby providing RNA dependent RNA transcriptase activity. The V-protein, which is incorporated into the virion, significantly contributes to the virus virulence in its natural host as it blocks components of the innate antiviral immune system. These V-protein specific interactions have not been found in humans [43]. The structure of the NDV virion is depicted in Figure 1-2.

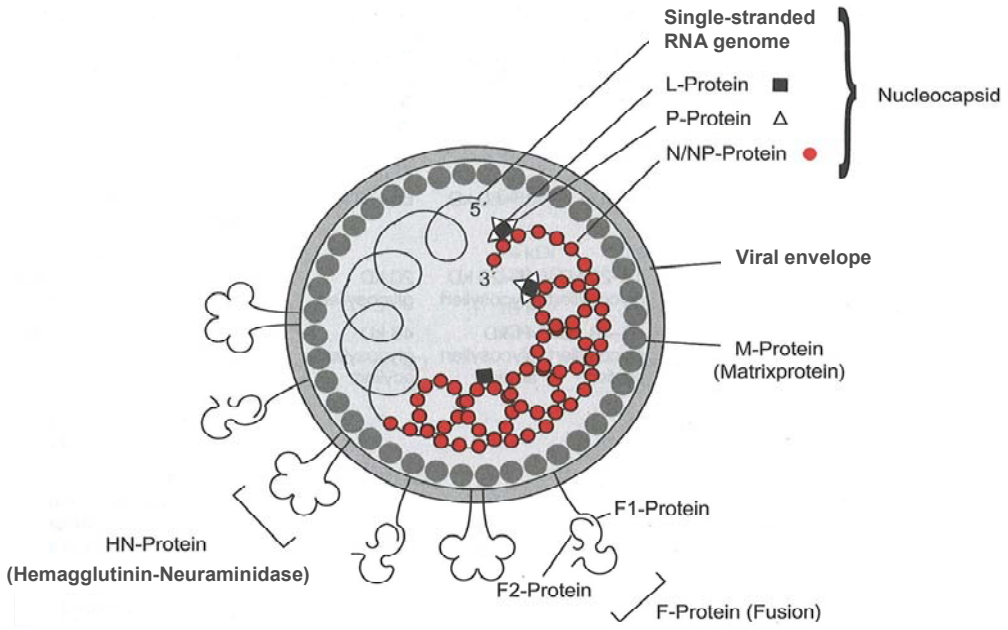

Figure 1-2: Structure of the NDV virion
The enveloped NDV virion contains a single negative-stranded, non-segmented RNA genome which codes for six gene products: NP (nucleocapsid protein), P (phosphoprotein), M (matrix protein), F (fusion protein), HN (hemagglutinin-neuraminidase) and L (large protein). The additional gene product (V-protein) synthetisized following RNA-editing of the P-mRNA is not depicted. Adapted from: [44]

1.4.3 NDV life cycle

The replication of NDV exclusively takes place in the cytoplasm (Figure 1-3). Virus binding and membrane fusion is mediated by HN and F proteins in a ph-independent manner [45]. Recently, it was shown that NDV might also infect cells via an alternative entering pathway using a receptor-mediated, caveolae-dependent endocytic route [46]. Shortly after the nucleocapsid has entered the cytosol, the RNA genome is uncoated and transcribed into mRNAs by the L-NP and P-protein complex. The negative sense RNA genome is transcribed to produce mRNAs corresponding to each individual gene by a stop-restart mechanism. It is caused by intergenic sequences that separate the individual genes but are not copied into mRNA. Transcription continues in this stop-restart manner until the last mRNA (L-mRNA) is transcribed. The viral mRNAs are 5´-capped and 3´-polyadenylated as standard eukaryotic mRNAs.

Translation of the viral mRNA is mediated by the host's translation machinery. Once sufficient NP is translated it binds to the newly transcribed mRNA. This process induces the polymerase complex to produce full-length antigenome (complementay positive strand) RNA

by ignoring the transcription stop signal at the 5´-end of each gene. NDV replication follows "the rule of six" which means that efficient replication can only take place if the genome size is a multiple of 6 nucleotides (nt) [47]. The antigenome serves as replication matrix for the generation of full-length negative-stranded genomes. Finally, the encapsulated viral genome and the posttranslationally modified M, HN and F proteins accumulate at the plasma membrane for virus assembly and subsequent virus budding [48, 49]. Ordered assembly and release of infectious virus particles has been shown to depend on membrane lipid rafts, defined as cholesterol- and sphingolipid-rich microdomains in the lipid layer facing the extracellular space [50].

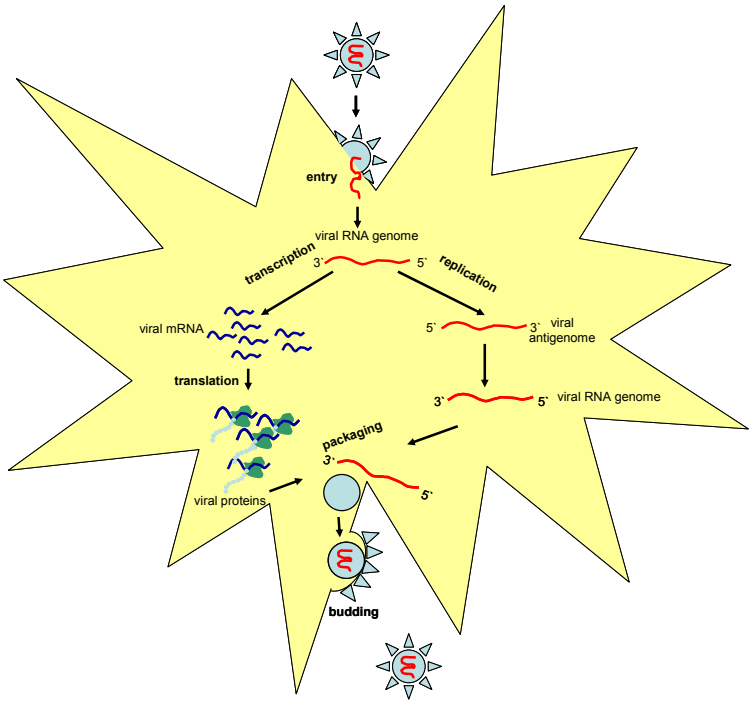

Figure 1-3: Replication cycle of a negative-stranded RNA virus
The negative-stranded RNA virus NDV replicates solely in the cytosol of the infected cell. Viral mRNAs and genomic RNAs are synthesized by the viral L-NP and P-protein complex with RNA-dependent RNA polymerase activity. During viral RNA synthesis, double stranded RNA (dsRNA) is produced as an intermediate product. Following protein translation, virus assembly and budding takes places at the cell membrane of the infected cell.

1.4.4 Classification of NDV strains

NDV strains are classified concerning their virulence in their natural host. They can be devided into a velogenic (highly virulent), mesogenic (intermediate) or lentogenic (non-virulent) category based, for example, on the mean death time of infected embryonated hens' eggs [51]. The virulence of each NDV strain depends primarily on the specific cleavage sites of the F_0 and/ or HN_0 proteins and the cell type dependent recognition by host proteases [52-54].

Furthermore, NDV strains suitable for antineoplastic therapy can be divided into lytic or non-lytic for human cancer cells. Lytic strains actively lyse cancer cells as infectious progeny virus is produced within the infected cell. The production of infectious progeny viruses enables for multicyclic replication as viral offsprings can spread to neighboring cells (Figure 1-4). In contrast, progeny viral particles of non-lytic strains are characterized by non-activated F proteins and or HN proteins. It renders them non-infectious [54] so that thex can only perform a monocyclic replication cycle [36] (Figure 1-4). The infectious or non-infectious property of progeny viruses defines the virulence of the strain.

Nevertheless, lytic as well as non-lytic strains have the potential to kill cancer cells and replicate much more efficiently in most human tumor cells than in normal cells [55-57]. It has been shown that certain NDV strains can replicate up to 10,000 times better in human tumorigenic transformed cells than in normal cells [55]. Lytic strains replicate and spread quickly. They can cause fusion of adjacent cells following plasma membrane budding of progeny virus with activated HN and F proteins. It enables the virus to spread without an extracellular phase. These large fused, multinucleated cells are called syncytia [55]. However, syncytia formation following infection with oncolytic NDV is cell line dependent and the determinant cellular factors are still subjects of investigations. Oncolytic strains are shown to be cytotoxic to human tumor cell lines of ectodermal, endodermal and mesodermal origin. It has been suggested that oncolysis is exerted by activation of intrinsic as well as extrinsic caspase-dependent apoptosis pathways [58, 59]. In contrast, non-lytic strains kill infected cells more slowly by interfering with cell metabolism [60].

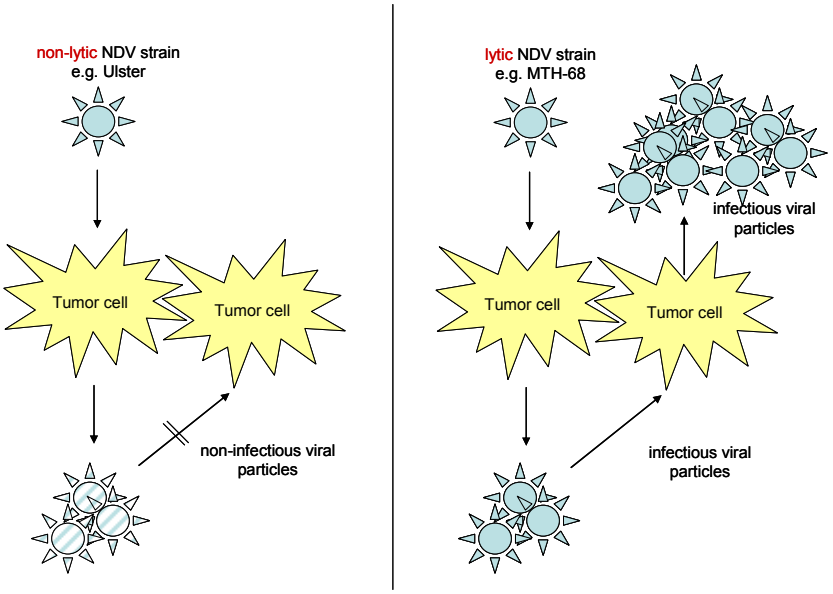

Figure 1-4: **Monocyclic or multicyclic replication pattern of NDV in tumor cells**

Non-lytic NDV strains e.g. Ulster infects tumor cells and produce non-infectious viral particles which lead to an abortion of further viral replication (left). In contrast, infection of tumor cells by lytic NDV strains e.g. More than hope 1968 (MTH-68) lead to a multicyclic replication as infectious viral particles are produced that can infect other tumor cells thereby amplifying the viral load [36].

In this thesis a recombinant oncolytic NDV strain was utilized. This strain is derived from the mesogenic NDV strain "More than hope 1968" (MTH-68) obtained from Laszlo Csatary [61]. It was originally used as an attenuated veterinary NDV vaccine for protection of poultry against fowl plague [62].

1.5 Antiviral interferon response upon NDV infection in mammalian cells

1.5.1 Interferon type I

Interferons (IFNs) are cytokines which were first described by Isaacs and Lindemann in 1957 as secreted factors which interfere with viral replication [63]. To date, there are 3 types of interferons described with potent antiviral, antiproliferative and immunomodulatory activities [64]. NDV is known to strongly induce the expression of the key antiviral type I IFNs α and β in mammalian cells, especially when added to human peripheral blood cells [65, 66]. In contrast to IFNα which comprises of 13 isotypes in humans, there is only a single IFNβ gene known [67]. Almost all nucleated cells produce IFNα/β following viral infection but plasmacytoid dendritic cells (pDCs) are 10–100 -fold more efficient in producing IFNα/β then other cell types (reviewed in [68]).

1.5.2 IFN induction in normal cell

Following cell entry, viral replication including generation of single- and double-stranded viral RNA exclusively takes place in the cytosol. Viral RNAs constitute pathogen associated molecular patterns (PAMPs) which initiate an innate IFN-mediated antiviral response in a cell type and pathogen type-specific manner. These PAMPs are recognized by either cytosolic RIG-1-like receptors (RLRs) including the RNA helicases retinoic acid inducible gene-1 (RIG-1) and melanoma-differentiation-associated gene 5 (MDA-5) or by Toll-like receptors (TLR) expressed on the cell surface of membranes or on endosomes in a cell type-specific manner. In pDCs, the antiviral response following NDV infection seems to be mainly replication-independent and relies on the recognition of single-stranded RNA (ssRNA) by the TLR system probably due to endosomal uptake of virions [69, 70].

In conventional DCs, macrophages and fibroblasts the induction of an IFN response is replication-dependent and is mediated via cytosolic RLRs [71]. In the early phase of interferon response it has recently been shown that the cytosolic RNA helicase RIG-1 is mainly activated following NDV infection by detection of the viral dsRNA intermediates [69, 72, 73]. RIG-1 consists of a C-terminal RNA helicase domain which interacts with dsRNA or virus specific 5`-triphosphate ssRNA and two N-terminal caspase recruiting and activation domains (CARDs) [74]. The adenosine triphosphate (ATP)-dependent unwinding of RNA induces a conformational change of RIG-1 which activates the CARD-mediated downstream signaling cascade. It results in the activation of the interferon-beta promoter stimulating factor 1 adaptor protein, IPS-1 (also known as MAVS, CARDIF or VISA) located on the mitochondrial membrane [75-77]. Subsequently, IPS-1 interacts with several signaling proteins. The interaction with TRAF3 (Tumor necrosis factor receptor-associated factor 3) leads to the activation of the Tank binding kinase-1 (TBK1) and the inhibitor of kappa light polypeptide gene enhancer in B-cells, kinase epsilon (IKKi), also known as IKKε. They, in turn, activate the transcription factor interferon-regulatory factor (IRF) 3 and in a second positive feedback loop of IFN response IRF7 by phosphorylation. IRF3 is ubiquitously and constitutively expressed. In contrast, IRF7 is either absent or present in low levels in most cell types (apart from pDCs where it is constitutively expressed) and is therefore mainly activated in a later phase of infection [78]. Upon activation of IRFs, they form homo-or heterodimers and translocate to the nucleus to mediate transcription of IFN type I cytokines. Early in infection, IRF3 induces the transcription of IFNβ and IFN4α. Upon secretion, they bind in a paracrine and autocrine manner to the cell surface transmembrane IFN-α/β receptor (IFNAR) comprising of two subunits (IFNAR 1 and 2). After ligand induced dimerization of the

intracellular domains of the subunits, the Janus-activated kinase 1 (JAK1) and the tyrosine kinase 2 (TYK2) are activated. These subunit-associated kinases in turn tyrosine-phosphorylate the signal transducers and activators of transcription 1 and 2 (STAT1 and 2). Following activation, STAT1 and 2 form a trimeric complex with IRF9 termed interferon-stimulated gene factor 3 (ISGF3). The complex translocates to the nucleus to bind DNA regulatory sequences-containing IFN-stimulated response elements (ISREs). The ISRE stimulation leads to transcription of numerous IFN-stimulated genes (ISGs). These gene products generate an antiviral state within the cell. In addition, STAT1 and 2 as well as IRF7, IRF9 and TLRs are transcribed in order to amplify the immune response. In contrast to IRF3, IRF7 can activate not only IFNβ but a broader range of IFNα isoforms. This process is important for a strong IFN response and allows for a rapid and comprehensive response to danger signals in pDCs [79]. The induction of the IFN-signaling pathway following NDV infection (e.g. in fibroblasts) is depicted in Figure 1-5.

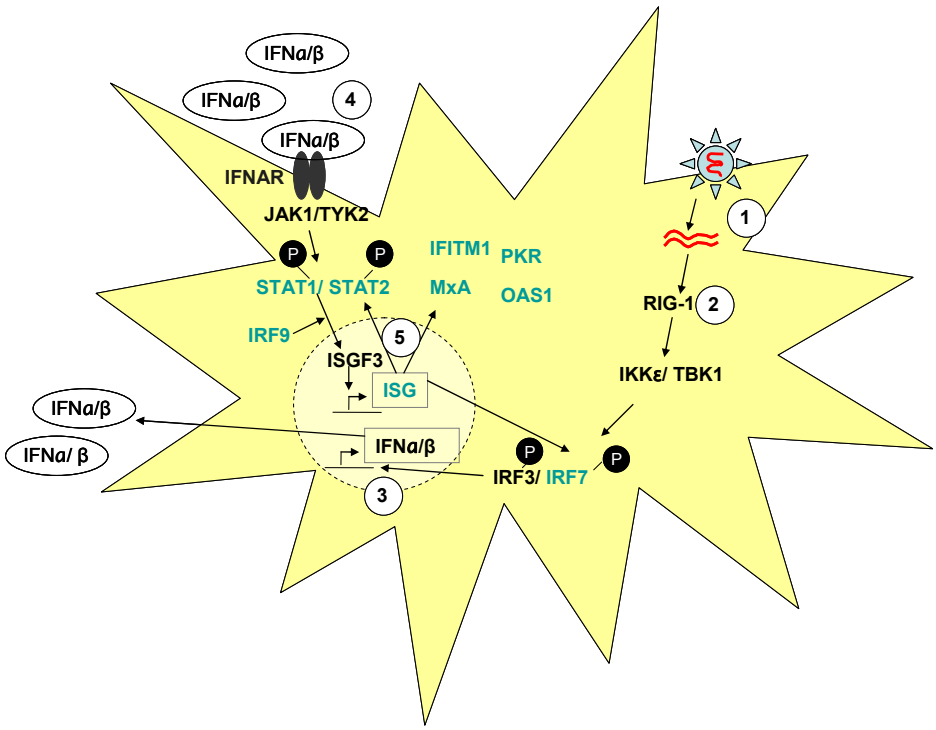

Figure 1-5: **Induction of IFN type I-signaling pathway following NDV infection**
Following NDV infection (1) and start of viral transcription and replication in the cytosol, viral dsRNA intermediate products activate a RIG-I induced signaling cascade (2) mediating IFN type I expression and secretion (3). Secreted IFN binds to the cognate IFN receptor in an autocrine and paracrine manner (4) thereby activating the JAK/STAT pathway. Activation leads to transcription of antiviral genes (5) and upregulation of STATs and IRF7/9 as a positive feedback loop mechanism (indicated in green).

1.5.3 Antiviral effector proteins

IFN-stimulated proteins generate an antiviral state in infected and neighboring cells due to a paracrine action of IFN preventing viral replication and spread. Well known ISG-products with direct antiviral functions are, for example, the cytosolic protein kinase R (PKR), the 2´-5´-oligoadenylate synthetases (OAS) or the myxovirus resistance proteins (Mx proteins) which are shown to be activated following NDV infection [36].

Mx proteins are IFN-inducible GTPases of the dynamin superfamily. In humans, the cytosolic MxA enzyme exhibits a wide (cell type-specific) antiviral spectrum against different types of viruses, irrespective of their intracellular replication site. The mechanism of action has been studied for a few viruses but is still incompletely understood. In the case of viruses replicating in the cytoplasm, such as the RNA virus VSV, MxA may direct nucleocapsids to alternative sites in the cytoplasm. As a consequence, they are not functional for viral RNA synthesis, but are likely to be immobilized and subsequently degraded [80]. Unlike Mx proteins, OAS and PKR are constitutively expressed at a basal level. They are activated by recognition of dsRNA which constitutes a replication intermediate in the viral life cycle of RNA viruses. Upon activation of OAS proteins, they catalyze the polymerization of ATP into 2`-5`linked-oligoadenylates (2`-5`-A) of different lengths [81]. These molecules are known to activate the endoribonuclease RNAse L by inducing its homodimerisation leading to viral and cellular single-stranded RNA destruction [82]. Following dsRNA recognition of PKR, it undergoes autophosphorylation and phosphorylates the alpha subunit of the eukaryotic initiation factor eIF-2 leading to a blockage of viral and most cellular protein translations [83].

Proposed antiviral actions of these ISG-proteins are depicted in Figure 1-6.

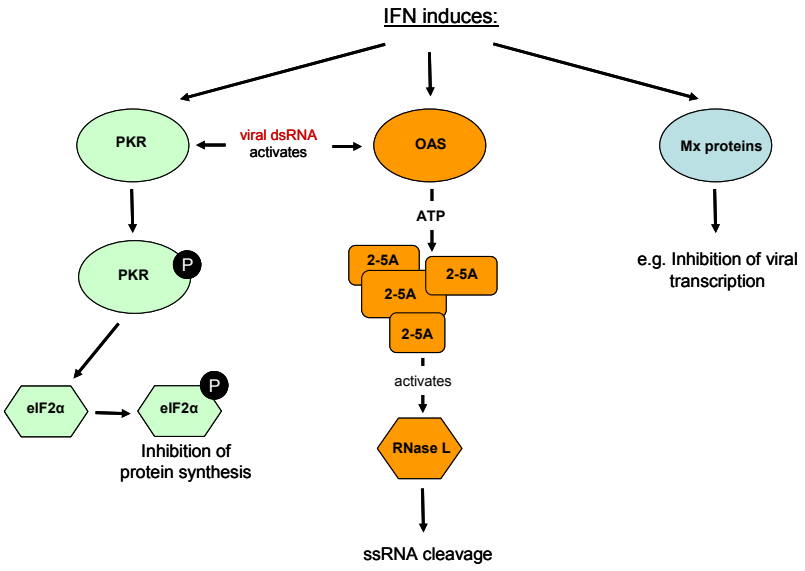

Figure 1-6: Antiviral mechanisms of IFN-inducible gene products
The best characterized IFN-induced antiviral pathways leading to inhibition of translation, RNA cleavage or inhibition of viral transcription, comprise the dsRNA dependent PKR and OAS system as well as the Mx proteins. Adapted from: [82]

Many IFN-induced proteins are poorly characterized. However, some of these are very likely to possess antiviral activity. For instance, the IFN type I and II inducible interferon-induced transmembrane protein 1 (IFITM1 also known as Leu-13 or 9-27) was originally shown to be expressed as a cell surface molecule on lymphocytes [84]. Recently, it was found to be located on endoplasmatic reticulum [85]in human liver cells. It is supposed to play a role in anti-proliferative action mediated by IFNs. Expression of IFITM1 was demonstrated to partially inhibit VSV replication when overexpressed in VSV-susceptible mouse cells. Although, when tested in parallel, IFITM1 was found to have less powerful antiviral activity toward VSV than the MxA protein [86].
Besides syngergistic effects of interferon-induced antiviral protein activities, they can further limit viral spread by inducing cellular apoptosis as it has been implicated for PKR and RNase L [87, 88].

1.5.4 Defects in the interferon response in tumor cells

NDV selectively replicates in tumor cells [55]. Replication of only one infectious NDV particle can lead to the death of approximately 10,000 cell culture cancer cells in two or three days [36]. However, precise mechanism rendering cancer cells permissive for NDV replication are not entirely understood. Acquired defects in the IFN response, most likely leading to increased proliferation and resistance to apoptosis, are thought to be responsible for

the tumor-selective replication [89] (Figure 1-7). In 2006, Krishnamurthy and colleagues [90] showed that highly NDV-susceptible HT-1080 cells are insensitive to both secreted IFN and exogenous IFNβ treatment. A remarked reduction in the levels of phosphorylated STAT1 and 2 resulted in impaired direct antiviral effects of IFN. Fiola and colleagues [91] then analyzed the induction of antiviral enzymes following infection of several human tumor cell lines and non-tumorigenic cells with a lentogenic NDV strain. Tumor cells infected with NDV showed a delayed expression of antiviral proteins like MxA and PKR in comparison with normal cells. Furthermore, whilst viral replication stopped in non-tumorigenic cells after the production of positive-strand RNA, replication of NDV continued in tumor cells. These results indicate that an early and efficient antiviral response is essential to inhibit NDV replication [91]. In 2009, Wilden and colleagues [92] investigated a variety of murine tumor and normal cells with respect to their constitutive expression of antiviral IFN-related genes and IFN type I secretion. They showed a strong inverse correlation between NDV replication and the level of the basal expression like RIG-1, IRF3 and IFNß. In addition, tumor cell-specific reduced basal levels of the antiviral effectors like PKR and OAS1 could also be observed. They stated that the amount of constitutively expressed gene product at the time of infection is more important than the amount generated after infection. Reduced basal expressions could therefore allow for an efficient progression of viral replication which can not be blocked later on [92].

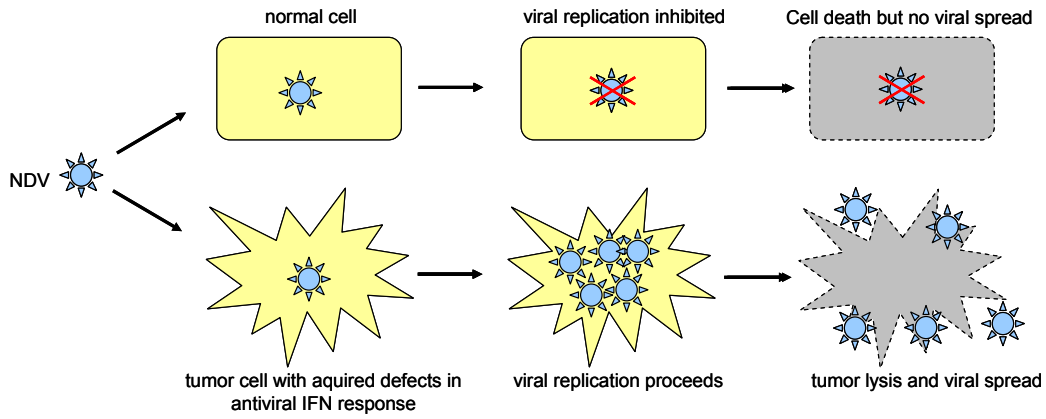

Figure 1-7: Tumor cell-specific replication of NDV
Viral replication, cell killing, viral release and spread in tumor cells is not inhibited in contrast to normal cells. It is supposed that cancer cells acquire defects in the IFN pathway during the process of tumorigenesis leading to a lack of antiviral defence. Adapted from: [22]

1.6 Further mechanisms in tumor cells leading to oncolytic virus susceptibility

It has been stated that oncogenic Ras activity or an activated Ras-pathway can mediate oncolytic virus susceptibility by interfering with factors involved in mediating antiviral responses. An activated Ras pathway has been hypothesized to promote reovirus translation by disruption of the PKR-eIF-2α checkpoint [93, 94]. However, a recent study showed that Ras transformation does not affect reovirus translation but rather promote efficient uncoating, production of infectious progeny viruses and release [95]. An activated Ras/Raf/MEK/Erk-pathway was recently shown to enhance oncolytic replication of VSV by negatively effecting IFNα-mediated antiviral responses. This was shown to be due to downregulated IFN-inducible factor MxA, which is known to block VSV RNA synthesis [96]. In addition, efficient translation of VSV was demonstrated to depend on increased expressions of the epsilon subunit of the eukaryotic initiation factor-2B (eIF-2Bε) in a variety of VSV-susceptible mammalian tumor cells. These elevated levels lead to an aberrant guanine nucleotide exchange activity of eIF-2B which most likely mediates a partial overcome of the PKR-eIF-2α checkpoint [97] as it is depicted in Figure 1-8.

.

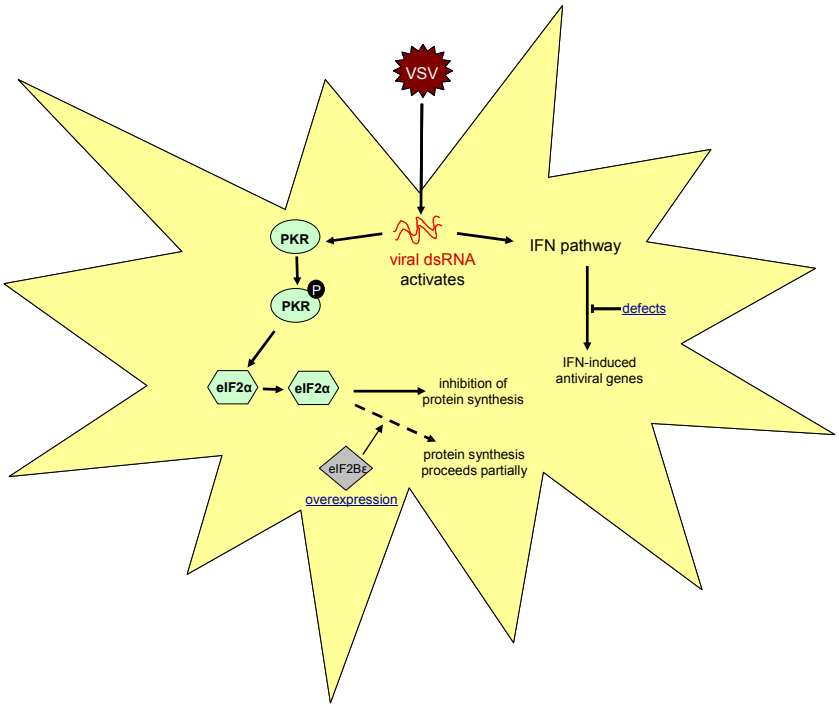

Figure 1-8: Molecular determinants of VSV oncolysis
Following VSV entry, viral dsRNA intermediates produced during viral replication can activate an antiviral IFN response (IFN synthesis, secretion and receptor binding as well as activation of the JAK/STAT pathway) leading to the transcription of antiviral genes. Furthermore, cytosolic dsRNA activates PKR which in turn leads to eIF-2α phosphorylation preventing the eIF-2B-mediated exchange of GDP for GTP. This process blocks the initiation of translation. Tumor cell-specific susceptibility of VSV is supposed to depend on defects in IFN-triggered signal transduction in combination with defects in translational control downstream of eIF-2α phosphorylation. Adapted from [97].

So far, there have been no investigations with respect to a correlation of eIF-2Bε overexpression and NDV susceptibility. In contrast, Lorence and colleagues in 1994 showed that N-Ras transformation of human fibroblasts rendered cells 1000-fold more sensitive to NDV mediated cytoxicity than normal fibroblasts. It was then hypothesized that it could be due to Ras-mediated altered expressions of sialic acids on the cell membrane. Ubiquitously expressed sialylated cellular receptors are necessary for virus attachment [98]. However, the molecular basis for Ras-induced NDV susceptibility in tumor cells was not further investigated.

1.7 Application of NDV in virotherapy

Due to its antineoplastic activity, NDV is among other oncolytic viruses in the focus of virotherapy. First antineoplastic effects of NDV in patients have been reported in 1964 when myelogenous leukemia was treated by intravenous administration of NDV [99]. NDV is considered as a safe agent as it is human apathogenic (and the general human population is seronegative), selectively replicates in tumor cells and shows no signs of recombination. As its replication is restricted to the cytosol and lacks a DNA phase, it makes it very unlikely that it can promote malignant transformation of infected normal cells (reviewed in [36]).

Lytic as well as nonlytic strains have been investigated in clinical trials for their anti-cancer potential. Strains that have been most widely tested for the treatment of human cancer are MTH-68, PV-701, 73-T, HUJ and Ulster.

There are two basic approaches for the utilization of NDV for cancer therapy. The first approach utilizes oncolytic strains for tumor selective cytolysis [100]. NDV has been tested as an oncolytic agent using the intratumoral, systemic or nasal approach. The systemic route has been developed by three groups utilizing different virus strains. Three phase I clinical trials with the mesogenic PV701 strain have been performed which demonstrated partial tumor regression in some patients or transient stable diseases [101-103]. When patients were desensitized by an initial treatment with a lower dose ($12x10^9$ plaque forming units (PFU)/ m^2), the maximum tolerated dose was increased tenfold ($120x10^9$ PFU/ m^2) [103]. In a phase I/II trial in patients with recurrent glioblastoma multiforme utilizing the replication-defective, lentogenic NDV strain HUJ, intravenous administration was well tolerated and in one patient a complete response was achieved lasting three months [104]. Csatary and colleagues reported in a phase I case study about the administration of mesogenic MTH-68/H to four patients with

glioblastoma multiforme after the conventional modalities of anti-neoplastic therapies had failed. The treatment resulted in survival rates of 5-9 years [105].

MTH-68 was also tested in an open phase II/B placebo-controlled study in cancer patients with advanced cancers by inhalation. Patients receiving virus therapy had a higher rate of survival at one to two years. After two years, out of 33 patients receiving virus therapy seven patients had survived [106]. However, the patients in this clinical trial were not randomized and also received other treatments.

The second approach is the use of NDV as a tumor vaccine. Immune stimulation is caused by the expression of tumor-specific antigens as well as viral antigens on the cell surface of infected, inactivated tumor cells (whole cell vaccines) or by plasma membrane fragments from NDV-infected cancer cells (oncolysates) [36, 107, 108].

Altogether, clinical phase I trials have proven the safety of NDV in human cancer patients. Nevertheless, the clinical proof of concept is not reached, yet. Randomized controlled phase II and III studies and the enrollment of a larger number of patients are needed to confirm the results of studies done so far.

In order to further improve the efficacy of NDV in cancer treatment, there is a strong need to investigate the biology behind the tumor-specific replication of this natural oncolytic virus in more detail.

Subsequently, the process of tumorigenic transformation of human cells is described as the development of *in vitro* models of carcinogenesis is based on it. Genetic defined *in vitro* models can also be utilized to further reveal tumor cell-specific replication of NDV.

1.8 Tumorigenic transformation of human cells

Normal human somatic cells possess a limited potential to proliferate (*in vivo* and *in vitro)*. It depends on the proper maintenance of telomeres and responses to certain cell-physiological stresses. Cells undergo a permanent growth arrest after a finite replicative lifespan [109]. This process is termed replicative senescence resulting in the activation of p53- and retinoblastoma (Rb)-tumor suppressor pathways due to a loss of structural integrity of the telomere nucleoprotein [110, 111]. Furthermore, cells can pass to a senescent state when exposed to a number of stress conditions. It can be induced, for example, by low serum or growth factor concentrations, high oxidative stress and high levels of DNA damage e.g. caused by UV-irradiation. Senescent cells remain metabolically active but do not divide any longer. As damaged telomeres are potent inducers of senescence, this process is supposed to function as

an important tumor suppressor mechanism by preventing the development of neoplastic cells [111-113].

Cell populations which succeed in inactivating the Rb- and p53-signaling pathways can bypass sensescence and continue to divide until critical telomere shortening appears. Chromosome ends are no longer protected from the cell machinery which normally detects and repairs DNA breaks [114]. Cells then enter a second proliferative block, termed crisis, which is characterized not only by short telomers but also by massive genomic instability and apoptosis. However, a rare number of cells (one in 10^7 human cells) can emerge from crisis and are invariably immortal [109, 111]. It is proposed that the escape from crisis and the entrance into an immortal growth state depends on the activation of telomere maintenance functions. Telomerase activation or in rare cases a poorly understood mechanism of alternative lengthening of telomeres (ALT), probably based on recombination between telomeres, is responsible for telomere maintenance. Telomerase is a cellular enzyme with reverse transcriptase activity. It adds telomeric repeats to the ends of telomeres, thereby extending them and providing telomere homeostasis [109, 115]. Activation of telomerase after the accumulation of diverse mutations results in unstable genomes. These cells are predisposed to oncogenic transformation [115]. The process of tumorigenesis and its relation to telomere length is depicted in Figure 1-9.

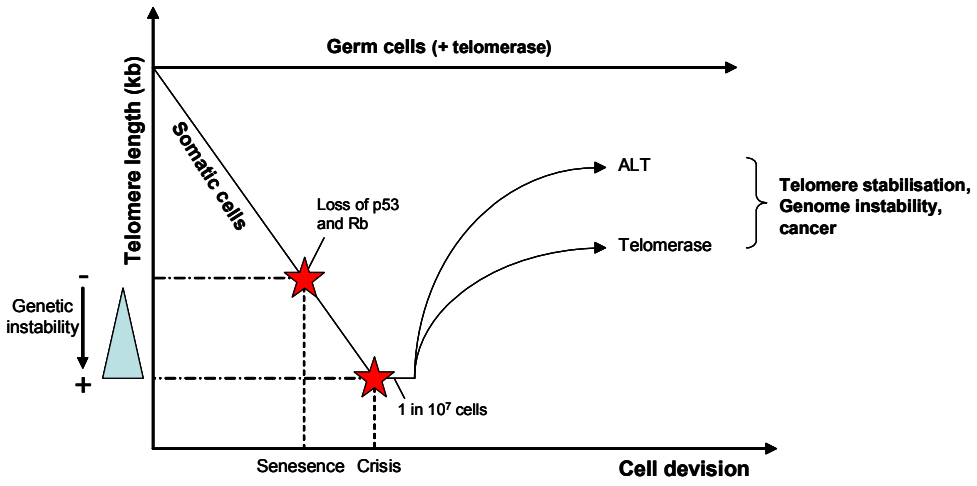

Figure 1-9: Telomere shortening, senescence and cancer
Telomere length (ordinate) is progressively lost during ongoing rounds of cell devision (abscissa) in telomerase negative somatic cells. It eventually leads to p53- and Rb-dependent growth arrest (senescence). Inactivation of these tumor suppressor pathways bypasses senescence and mediates further cell division and telomere shortening. Cells then enter a state termed crisis as telomeres eventually erode to a length at which no protection of chromosome ends is possible, accompanied by end-to-end chromosome fusion and apoptosis. Rare clones can escape crisis and maintain stable telomere lengths by activating telomere maintenance mechanism (telomerase activation or ALT mechanism). Germline cells are telomerase positive and therefore maintain their telomere lengths. Adapted from:[109]

Normal cultured human cells can systematically be converted to a tumorigenic state by introduction of defined genetic elements. Hahn and colleagues first demonstrated that at least four to six distinct pathways have to be altered to render human epithelial or fibroblast cells tumorigenic [116, 117].

In the following chapter, an *in vitro* model for multiple stages of skin carcinogenesis is described as it was chosen to be validated as a model for viral oncolysis in this thesis.

1.9 The HaCaT-derived cell line model for skin carcinogenesis

HaCaT cells are spontaneously immortalized aneuploid but non-tumorigenic human keratinocytes with largely preserved differentiation capacity. These epithelial cells were originally isolated from sun-exposed adult skin and propagated under low Ca^{2+} conditions and elevated temperature [118]. It is likely that immortalization of cells was promoted by UV-induced p53 mutations *in situ* and prolonged stressful culture conditions which led to increased genetic alterations (loss of senescence genes, see Figure 1-9). In addition, HaCaT cells are characterized by elevated telomerase activity. Although, it is not clear whether it caused immortalization or was acquired during this process [119]. Transformation of HaCaT cells with oncogenic *H-RasV12* induced tumorigenic growth *in vivo* in some but not all HaCaT-Ras clones. Oncogenic H-Ras clones could be classified with respect to their benign or malignant phenotype after subcutaneous injection into nude mice. Benign clones grew slowly and formed nodules while malignant clones e.g II4 cells were characterized by a progressive and infiltrating growth of highly differentiated squamous cell carcinomas *in vivo*. The different tumorigenic potential of HaCaT-Ras clones could not be explained by increased levels of H-Ras expression or the integration site. It was therefore assumed that the additional chromosomal and genetic aberrations detected in malignant Ras-clones compared to benign clones lead back to the genetic background of the recipient cells. [119, 120]. Cells re-cultured from several rounds of *in vivo* passaging of a benign Ras clone exhibited no growth advantage *in vitro* but increased malignant phenotypes *in vivo*. Furthermore, they showed a reduced differentiation potential as a consequence of selective pressure. The RT3 cell line established by three rounds of tumor passaging was characterized by enhanced, highly invasive and metastatic squamous cell carcinoma tumor growth *in vivo* with poor differentiation. This more aggressive cell line showed distinct chromosomal alterations and an autocrine growth control by *de novo* expression of hematopoietic growth factors granulocyte-colony stimulating factor (G-CSF) and granulocyte macrophage-colony-stimulating-factor (GM-CSF). In RT3 cells a

H-Ras oncogene amplification was detected compared to the parental benign cell line which hinted to a role of activated Ras during the process of tumor progression [121]. The generation of this model is schematically depicted in Figure 1-10.

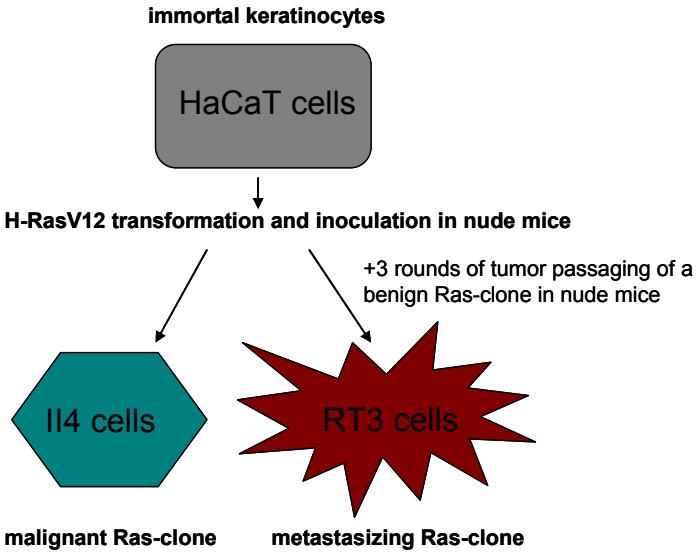

Figure 1-10: Generation of a HaCaT-derived multistage model for skin carcinogenesis
Immortalized HaCaT cells (grey) with acquired genetic alterations during immortalisation were transferred into a tumorigenic state by activated *H-Ras* transfection. A malignant HaCaT-Ras clone (II4 cells) could be isolated following one round of *in vivo* passaging and a metastasizing HaCaT-Ras clone was recultivated following 3 rounds of *in vivo* passaging of a benign HaCaT-Ras clone. Adapted from: [119].

Non-tumorigenic HaCaT cells and a HaCaT-derived tumorigenic counterpart cell line e.g. II4 or RT3 could provide a valid tool to further investigate the process of tumorigenic transformation. In order to identify novel tumor cell-specific genes or pathways, the tumor cell-selective replication of NDV could be exploited e.g. in a cell-based screening by means of RNA interference (RNAi).

1.10 RNAi and its application in virus-based screenings

RNAi comprises a naturally occuring, evolutionary conserved sequence-specific RNA-directed process for silencing gene expression at the post-transcriptional level (Figure 1-11). This mechanism probably evolved as a means of defense against viral invaders or genomic parasites (transposons) [122]. Although there have been earlier reports about this phenomenom (reviewed in [123]), RNAi gained attention when Fire, Mello and colleagues described the mechanism in Caenorhabditis elegans in 1998 [124]. In cells of many low and high organisms short dsRNA triggers the inhibition of gene expression. They are typically expressed in the nucleus in form of long primary micro-RNAs (miRNAs). These are processed by the nuclear RNAse III-like endoribonuclease Drosha and partners into shorter

precursor or pre-miRNAs. These are subsequently exported into the cytoplasm by Exportin-5. Subsequently, they are further cleaved by the ribonuclease Dicer into approximately 22 nt long miRNAs with characteristic two nt long 3`-overhangs. The antisense strand of the miRNA is then incorporated into a RNA-induced silencing complex (RISC) to allow binding of the 3`untranslated region (UTR) of its mRNA target to inhibit mRNA translation. This target binding is imperfect since its specificity is primarily determined by nucleotides two to eight from the 5`-end of the antisense strand, termed seed-region. Consequently, a single miRNA is probably capable of regulating several cellular targets and vice versa it is likely that expression of a single gene is controlled by diverse miRNAs (reviewed in [125]). In 2001, Tuschl and colleagues first reported about the feasibility to trigger efficient gene silencing in mammalian cells by introducing short, only ~21 nt long dsRNAs, termed small interfering RNAs (siRNAs) [126, 127]. Due to the reduced length of siRNAs, they circumvent the recognition by the typical cellular dsRNA sensors PKR, RIG-I or TLRs (reviewed in [125]). In contrast to the imperfect matching miRNAs, siRNAs are designed to be perfectly and specifically complementary to a sequence in the target mRNA [128]. SiRNAs induce site-specific cleavage of the latter by a particular component (Slicer) of the RISC complex, termed Argonaute-2 protein (Ago-2). Out of the four human Ago proteins which have been found to interact with the RISC complex, only Ago-2 is capable to nick bound mRNA. It results in the subsequent degradation of these mRNAs by cellular RNAses (reviewed in [125]). However, transcripts being less than 100 % complementary with an siRNA have been shown to be also targeted for knockdown by the RNAi pathway. This phenomenon is generally referred to as “off-targeting”. It depends on the concentration of siRNA, can induce up to threefold suppression of dozens of genes, and is mediated by either the sense or antisense strand of the siRNA (reviewed in [129]). In order to avoid false positive results, an siRNA-mediated phenotype should ideally be reproducible with at least two or three individual siRNAs targeting different areas of the target-mRNA.

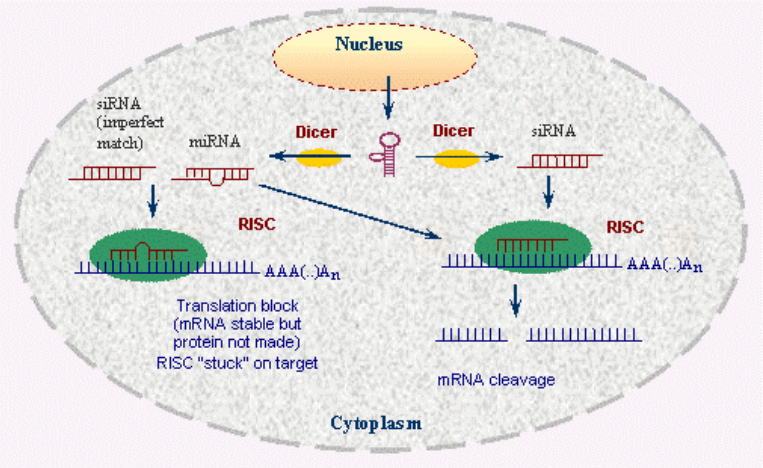

Figure 1-11: A simplified model for the RNAi pathway
In the first step of RNAi, the trigger RNA (dsRNA, miRNA primary transcript or shRNA) is processed into miRNA or siRNA by the ribonuclease Drosha (in the nucleus) and cytolosic Dicer. In a second step, siRNAs or miRNAs are incorporated into the RISC complex and unwound. Antisense RNA then hybridizes with the (specific) mRNA target. Gene silencing is either induced by degradation of targeted mRNA by the RNAse H enzyme Argonaute (Slicer) or in case of mismatches induced by translational inhibition.
Source: http://www.ncbi.nlm.nih.gov/projects/genome/probe/doc/TechRnai.shtml

Since it was demonstrated that RNAi was effective in mammalian cells, and efficient siRNA design algorithms were developed, RNAi mediated loss-of-function screens were initiated to reveal the biological functions of genes and their products. Application of the RNAi technology in high-throughput screens has been proven to be a fast and powerful tool to identify a broad range of genes which play important roles in many diseases including cancer. These genes can be potential new targets for therapeutics. Multiple types of RNAi libraries are available which can be divided into two categories, RNA-based or DNA- based. The former are composed of synthetic siRNAs that are transfected directly into cells. It results in a transient knockdown of proteins for several days. Maximal knockdown and duration is dependent on the individual turnover rate of the targeted mRNA and resultant protein and the growth rate of the cells. In contrast, DNA-based libraries utilize plasmids or viral vectors to express short hairpin RNAs (shRNAs) which are processed into siRNAs intracellularly. When stably expressed, they can lead to a permanent knockdown of target genes (reviewed in [130]).

In the past, several functional siRNA-based screens were performed in order to understand host-pathogen interactions during the life cycle of viruses causing severe human diseases e.g. the human immunodeficiency virus (HIV) [131-133], hepatitis C virus [134], respiratory syncytial virus [135] or West Nile virus [136] or to exploit virus-specific pathways to better understand the normal function of the implicated cellular system [137]. The former could eventually lead to the development of improved therapeutic antiviral strategies or to overcome the emergence of drug resistances against these pathogens.

Until now, there have been no attempts to indirectly uncover genes connected with tumorigenesis by screening for genes which are essential for tumor-selective replication of oncolytic viruses. By utilizing a model for viral oncolysis in combination with the RNAi technology it allows to screen for virus-sensitizing genes in the tumorigenic cell line and subsequently to verify the NDV-sensitizing feature of any confirmed gene in the non-susceptible counterpart cell line.

1.11 Aims of the PhD thesis

The exact mechanism underlying the tumor-selective replication of NDV is currently not well understood. In order to improve the anti-tumor efficacy, oncolytic replication has to be analyzed in more detail. Currently, defects in the IFN-signaling pathway, acquired during the process of tumorigenic transformation, are proposed to support NDV replication in tumor cells. However, for other naturally occurring oncolytic viruses e.g. VSV it has been demonstrated, that additional tumor cell-specific deregulated pathways can contribute to enhanced oncolytic virus replication. Therefore, this study aimed to develop and validate a screening approach, based on a cellular model for oncolysis, to identify and further investigate NDV-sensitizing pathways in human tumor cells.

As a first step, a genetically defined and closely related *in vitro* tumor cell line model had to be established or validated which could also be utilized as a model for NDV oncolysis. This model should comprise a non-tumorigenic, non-NDV-susceptible cell line and a derived tumorigenic, NDV-susceptible counterpart cell line. As a second step, this cell panel with opposing NDV-susceptibilities should be analyzed with respect to known oncolytic virus sensitizing factors or pathways. In a third step, the tumorigenic, NDV-susceptible cell line should be utilized to systematically screen for novel genes or pathways which play a pivotal role in oncolytic virus replication but are not directly connected with the IFN pathway. To do so, an siRNA-based non-automated screening approach had to be established and validated to indirectly uncover genes connected with tumorigenesis by screening for genes which are essential for tumor-selective replication of oncolytic viruses. As a last step, one siRNA-validated NDV-sensitizing gene should then be analyzed in more detail with respect to its NDV-sensitizing property and its potential connection with tumorigenesis thereby validating the screening strategy.

Such tumor cell -specific, NDV-sensitizing genes constitute potential targets for anti-cancer treatment or biomarkers for efficient oncolytic NDV replication.

2 MATERIALS

2.1 Equipment

AMAXA nucleofector	AMAXA, Cologne, Germany
Automatic Pipettes	Eppendorf, Hamburg, Germany
Cell culture incubator	Labotec, Goettingen, Germany
Centrifuge	Eppendorf
Fast Real-Time PCR System	Applied Biosystems, Foster City, CA, USA
Freezer -20 °C	Liebherr, Biberach an der Riss, Germany
Freezer -80 °C	ThermoFisher Scientific, Karlsruhe, Germany
Glassware	Fortuna, Schott Duran, Mainz, Germany
Gel imaging system Gel Doc 2000	Bio-Rad, Hercules, CA, USA
Gel electrophoresis chamber	Biometra, Goettingen, Germany
Heatable magnetic stirrer	Heidolph Instruments,Schwabach, Germany
Inverse optical microscope	Zeiss, Jena, Germany
Laminar flow hood Hera Safe	ThermoFisher Scientific
Microwave oven	Bosch, Heidelberg, Germany
Nanodrop 2000 spectrophotometer	ThermoFisher Scientific
Odyssey Infrared Imaging System	LI-COR, Bad Homburg, Germany
Orbital shaker	Heidolph Instruments
PCR thermocycler	Biometra
pH meter	Hanna Instruments, N. Highlands, CA, USA
Pipettes (0.5-1000 µl)	Eppendorf
Pipetting aid *Pipetboy acu*	Integra Biosciences, Fernwald, Germany
Power supply for electrophoresis	Pharmacia, Stockholm, Sweden
Refrigerator	Bosch
SDS-PAGE electrophoresis equipment	Invitrogen, Karsruhe, Germany
Shaker	Heidolph
Sunrise photometer	TECAN, Crailsheim, Germany
Table centrifuge	Eppendorf
Thermomixer comfort	Eppendorf
VICTOR microtiter well plate reader	PerkinElmer Life Sciences, Waltham, MA, USA
Water bath	Grant Instruments, Cambridge, UK
Western Blot equipment	Invitrogen

2.2 Software

Axiovision Release 4.7.9.0	Carl Zeiss Imaging Solution
EndNote 9.0	Thomson Reuters, San Fransisco, CA, USA
Irfan View 3.98	Irfan Skiljan, Wiener Neustadt, Austria
Office 2003	Microsoft Corporation, Redmond, WA, USA
Paintshop Pro 9.0	Corel, Unterschleißheim, Germany
Vector NTI Advance 10	Invitrogen

2.3 Consumables

Aluminium foil	Forti Folien, Neuruppin, Germany
Cell scraper	Renner, Dannstadt, Germany
Cell culture flasks (25, 75, 125, 225 cm^2)	Corning, New York, USA
Cell culture plates (6, 12, 24, 96 well)	Corning
Centrifuge tubes (15 and 50 ml)	Corning
Cover slips	R. Langenbrinck, Teningen, Germany
Cryo vials	Carl Roth, Karlsruhe, Germany
FAST-READ 102 NEW GRID counting chamber	Immune Systems Limited, UK
Laboratory gloves	Kimberly-Clark, Koblenz-Rheinhafen, Germany
Micro test tubes (0.5 -2.0 ml)	Eppendorf
Novex Bis-Tris HCL polyacrylamide gel	Invitrogen
Optical adhesive film	Applied Biosystems
Parafilm	Pechinery plastic packing, Chicago, IL, USA
Pasteur pipettes	WU Mainz, Mainz, Germany
Petri dishes	Corning
Pipette filter tips (0.5-1000 µl)	Eppendorf
Pipette tips (0.5-1000 µl)	Eppendorf
PVDF membrane filter pater sandwich (0.2 µm pore size)	Invitrogen
Realtime PCR plates, 96 well	Applied Biosystems
Syringe-driven filter units, 2 µm pore size	Corning
Syringes	CODAN, Lensahn, Germany

2.4 Chemicals

Agarose	Invitrogen
Ampicillin	Sigma-Aldrich, Schnelldorf, Germany
Crystal violet	Sigma-Aldrich
DMSO	Merck, Darmstadt, Germany
EDTA	Merck
Ethanol	Merck
Ethidium bromide solution (10 mg/ ml)	Merck
Formaldehyde	Carl Roth
Glycerol	Merck
Isopropanol	Merck
Kanamycin	Sigma-Aldrich
Methanol	Merck
Milk powder	Carl Roth
Paraformaldehyde	ThermoFisher Scientific
Seaplaque agarose	Cambrex Bio Science, Rockland, ME, USA
Sodium Chloride	Merck
Tris-acetate	Sigma-Aldrich
Tris-HCL	Sigma-Aldrich
Triton X 100	Sigma-Aldrich
Tween 20	Sigma-Aldrich

2.5 Small molecule inhibitors

Table 2-1: Small molecule inhibitors

Chemical name	Commercial name	Inhibitor for:	Provider
N6-[2-[[4-(Diethylamino)-1-methylbutyl]amino]-6-methyl- 4-pyrimidinyl]-2-methyl-4,6-quinolinediamine trihydrochloride	NSC 23766	Rac1 [138]	Merck
2-(4-morpholinyl)-8-phenyl-4H-1-benzopyran-4-one]	LY294002	PI3K [139]	Invitrogen

2.6 Commercial kits and assays

alamarBlue® assay	Invitrogen
AMAXA Nucleofector™ Kit V	AMAXA
BCA protein assay Kit	ThermoFisher Scientific
BLOCK-IT™ Lentiviral RNAi Gateway® Vector Kit	Invitrogen
BLOCK-IT™ U6 RNAi Entry Vector Kit	Invitrogen
Cells-to-cDNA™ II Kit	Ambion, Austin, TX, USA
CellTiter-Glo® Luminescent cell viability assay	Promega, Madison, WI, USA
iLite AlphaBeta human Type I activity detection Kit	Neutekbio, Galway, Ireland
QIAquick Gel Extraction Kit	Qiagen, Hilden, Germany
QuikChange II XL Site-directed Mutagenesis Kit	Stratagene, La Jolla, CA, USA
QIAprep Spin Miniprep Kit	Qiagen
QIAfilter Plasmid Maxi Kit	Qiagen
Steady- Glo® Luciferase Assay system	Promega

2.7 Taqman assays

Table 2-2:Taqman assay obtained from Applied Biosystems

Gene name	TaqMan® Endogenous Controls (Aplied Biosystems)
18s	4333762F
GAPDH	4333764F
	TaqMan® Gene Expression Assays (Applied Biosystems)
IFITM1	Hs_01652522_g1
MxA	Hs_00182073_m1
PKR	Hs_00169345_m1
OAS1	Hs_00242943_m1
Rac1	Hs_01588892_g1

2.8 Antibodies and immunofluorescence reagents

Table 2-3: Antibodies

Primary antibodies/ antisera	Source	Provider
Actin	polyclonal; rabbit	Sigma-Aldrich
AP1ß (A-5)	monoclonal; mouse	Santa Cruz, Santa Cruz, CA, USA
AP2α	monoclonal; mouse	Santa Cruz
CLTA	monoclonal; mouse	Santa Cruz
eIF-2Bε (H-290)	polyclonal; rabbit	Santa Cruz
GAPDH	monoclonal, mouse	Chemicon International, Temecula, CA, USA
H-Ras (C-20)	polyclonal; rabbit	Santa Cruz
IFITM1 (P17)	polyclonal; goat	Santa Cruz
MxA	polyclonal; rabbit	Proteintech Group Inc, Chicago, IL, USA
NDV clone 30	serum; rabbit	Friedrich-Löffler Institute, Island Riems, Germany
OAS1	polyclonal; goat	Santa Cruz
Pak1	polyclonal; rabbit	Santa Cruz
PKR	polyclonal; rabbit	Cell Signaling, Beverly, MA, USA
Rac1 (23A8)	monoclonal; mouse	Gene Tex Inc., San Antonio, TX, USA
RhoA	polyclonal; rabbit	Cell Signaling
STAT1 (9H2)	monoclonal; mouse	Cell Signaling
STAT2	monoclonal; mouse	BD Transduction laboratories, San Diego, CA, USA
TIAM-1	polyclonal; rabbit	Cell Signaling
Phospho-specific primary antibodies		
P(Y701)-STAT1	monoclonal; mouse	BD Transduction laboratories
P(Y690)-STAT2	polyclonal; rabbit	Cell Signaling
P(T451)-PKR	polyclonal; rabbit	Invitrogen
Secondary antibodies		
Anti-rabbit labelled with Alexa Fluor 680	goat	Invitrogen
Anti-mouse labelled with Alexa Fluor 680	goat	Invitrogen
Anti-goat labelled with Alexa Fluor 680	donkey	Invitrogen
Anti-mouse labelled with Cy3	goat	Jackson ImmunoResearch, West Grove, PA, USA
Anti-rabbit labelled with Cy2	goat	Jackson ImmunoResearch

Texas Red-X phalloidin	Invitrogen
Hoechst 33258	Merck
CellTracker™ orange	Invitrogen

2.9 Human cell lines

Table 2-4: Human cell lines

Cell line	Source
HaCaT; immortalized keratinocytes	Deutsches Krebsforschungsinstitut (DKFZ), Heidelberg, Germany
RT3; squamous cell carcinoma derived from HaCaT cells, H-Ras transformed	DKFZ
II4; squamous cell carcinoma derived from HaCaT cells, H-Ras transformed	DKFZ
HCT 116; colon carcinoma	American Type Culture Collection (ATCC), Rockville, IN, USA
HT-1080; fibrosarcoma	ATCC
HT-29; colorectal adenocarcinoma	ATCC
MDA-MB-231; breast adenocarcinoma	ATCC

2.10 Commercial buffers, solutions and reagents

High-Range Rainbow protein marker	Amersham Biosciences, Freiburg, Germany
Phosphate buffered saline (PBS) w/o $Ca^{2+,}$ Mg^{2+}	Biochrom AG, Berlin, Germany
RNase Zap	Ambion
TAE buffer, 50x	Invitrogen
Trypan blue solution	Sigma-Aldrich
Western Blot Nupage LDS sample buffer, 4x	Invitrogen
Western Blot Nupage Sample Reducing Agent, 10x	Invitrogen
TaqMan Fast universal PCR Mastermix, 2x	Applied Biosystems
Complete, EDTA-free; Protease Inhibitor Cocktail tablets	Roche, Basel, Switzerland
Halt Phosphatase Inhibitor Cocktail, 100x	ThermoFisher Scientific
Matrigel	BD Biosciences
1 kb DNA Ladder	NEB, Beverly, MA, USA

2.11 Buffers and solutions

Table 2-5: Buffers and solutions

Name	Composition	Application
TE buffer	10 mM Tris HCL, pH 8 1 mM Na_2EDTA, pH 8	Plasmid storage
Freezing medium	12 % (v/v) DMSO in sterile FCS	Freezing of cells
Crystal violet with formaldehyde	0.1 % (w/v) crystal violet in dH_2O, pH 4.5 with HCL 4 % (v/v) formaldehyde ≥ 37 %	Plaque assay
Blocking buffer	0.1 % (v/v) Triton X 100 5 % (v/v) FCS in PBS	Immunofluorescence
Antibody dilution buffer	0.05 % (v/v) Triton X 100 5 % (v/v) FCS in PBS	Immunofluorescence
Protein extraction buffer	M-PER® mammalian protein extraction reagent with 1 % (v/v) HALT™ Phosphatase Inhibitor cocktail (100x) 4 % Complete, EDTA-free, Protease Inhibitor Cocktail (25x)	Protein extraction
Running buffer	100 ml NuPAGE® MOPS or MES SDS Running buffer (20x) ad 2 l dH_2O	SDS-Page
Transfer buffer	100 ml NuPAGE® Transfer buffer (20x) 200 ml Methanol ad 2 l dH_2O	Tank Blotting
0.1 % TBS-T buffer, 10x	200 mM Tris HCL, pH 7.5 1.5 M NaCl 1 % Tween-20	Western Blot analysis
Blocking buffer	5 % powdered milk in 0.1 % TBS-T (1x)	Western Blot analysis

2.12 Cell culture reagents

2.12.1 Culture media

DMEM (stable glutamine and phenol red) Biochrom AG
DMEM/ HAM's F12 (stable glutamtine and phenol red) Biochrom AG

2.12.2 Culture media supplements and reagents

Fetale calf serum (FCS) Biochrom AG
Penicillin (100 IU/mL)/Streptomycin (100 µg/ mL) Biochrom AG

Hygromycin B (50 mg/ml)	Merck
Puromycin (5 mg/ml	Invitrogen
Trypsin-EDTA solution, sterile	Biochrom AG

2.13 Transfections reagents

DharmaFECT Cell Culture Reagent (DCCR)	Dharmacon, Chicago, IL, USA
DharmaFECT transfection reagent 1, 2, 3, 4	Dharmacon
siRNA buffer, 5x	Dharmacon

2.14 Plasmids

pcDNA3.1 (-)-hygromycin B expression vector	Invitrogen
Human Rac1cDNA in pCMV6-XL5 (clone AB3094-A01)	Origene Technologies Inc., Rockville, MD, USA

2.15 Primers for Rac1 mutagenesis

Table 2-6: Primers for Rac1 mutagenesis

Name	Sequence
Rac1T17N sense	5`- GGAGACGGAGCTGTAGGTAAAAATTGCCTACTGAT
Rac1T17N antisense	5`-ATCAGTAGGCAATTTTTACCTACAGCTCCGTCTCC

2.16 Lentiviruses

The lentivirus production based on the following destination vectors:

pLenti6 V5-DESTpuro-H-RasV12	provided by Ulrike Ulbricht; Bayer Schering Pharma AG, Berlin, Germany
pLenti6 V5-DESTpuro-JRED	provided by Ulrike Ulbricht, Bayer Schering Pharma AG

(see Appendix Figure 7-1 and Figure 7-2 for plasmid cards)

2.17 Enzymes

Alkaline phosphatase	NEB
T4 DNA Ligase	NEB
NotI	NEB
BSMB1	NEB

2.18 Cytokines

Type I IFNα	Peprotech, Hamburg, Germany
Type I IFNβ	Peprotech

2.19 Chemically competent *E.coli* strains

E.coli DH5α™	Invitrogen
One Shot® OmniMAX™-T1^{R}	Invitrogen
E.coli One Shot Stbl3	Invitrogen

2.20 Culture medium and agar for *E.coli* cultivation

(Luria-Bertani) LB-medium	Biological Quality Control, Bayer Schering Pharma
LB-agar	Biological Quality Control, Bayer Schering Pharma

2.21 SiRNA

2.21.1 Single siRNAs targeting endogenous mRNAs and non-silencing siRNAs

Single siRNAs were obtained from Dharmacon. Details for siRNAs of secondary screen hits as well as H-Ras, IFITM1 and non-silencing siRNAs see Appendix Table 7-4.

2.21.2 Single siRNAs targeting viral mRNAs

Viral siRNAs were synthesized at Dharmacon.

Table 2-7: siRNAs targeting viral P- and V-mRNA

Name	Target mRNA	Sequence
P+V#1	viral P and V mRNA	sense: 5`-CGACAAGCUUAGCAAUAAAUU antisense: 5`-PUUUAUUGCUAAGCUUGUCGUU
P+V#2	viral P and V mRNA	5`-GCGCAAUCCCACAAGGCAAUU 5`-UUGCCUUGUGGGAUUGCGCUU
P+V#3	viral P and V mRNA	5`-GGACAGAUCAGACAAACAAUU 5`-UUGUUUGUCUGAUCUGUCCUU

2.21.3 SiRNA optimization kit and siRNA libraries

The siARRAY RTF Optimization Kit 1 and human siRNA libraries were obtained from Dharmacon.

Table 2-8: SMARTpool and custom siRNA libraries

Screen	Library
Primary screen with siGENOME SMARTpool siRNAs	Human siARRAY RTF Membrane Trafficking library (112 target genes)
Primary screen with siGENOME SMARTpool siRNAs	Human siARRAY RTF Tyrosine kinase library (76 target genes)
Secondary screen with 4 single siGENOME siRNAs per target gene	Custom library (sets of 4; 4x 2nmoles per target)

2.22 Newcastle disease virus

MTH-68 (NDV): mesogenic, obtained from Laszlo Csatary [61]

Viral transgene expressing MTH-68:

- MTH-68 expressing EGFP (NDV-EGFP) [140]
- MTH-68 expressing Firefly luciferase (NDV-luciferase) provided by Puehler/Beier; Bayer Schering Pharma AG

2.23 Mouse strain

NMRI nude mice Taconic, Germantown, NY, USA

3 METHODS

3.1 Molecular biological methods

3.1.1 Preparation of agarose gels

For a 1 % (w/v) gel 1 g agarose was dissolved in 100 mL 1x Tris-acetate-EDTA (TAE) buffer and the agarose was melt in a microwave oven. After cooling down to about 50 °C 1 µL ethidium bromide stock solution (10 mg/mL) was added to the agarose solution, thoroughly mixed and agarose solution was poured into a tray and allowed to set.

3.1.2 Preparation of DNA from agarose gels

For the extraction of DNA from agarose gels the QIAquick Gel Extraction Kit from Qiagen was used according to the manufacturer's instruction (Qiagen, QIAquick® Spin Handbook, July 2002). Gel extraction was performed by using the 'vacuum manifold' protocol (pp.25-27).

3.1.3 Determination of nucleic acid concentration

The DNA or RNA concentration of a sample was photometrically determined at the NanoDrop spectrophotometer using 1 µl of (undiluted) sample.
c [ng/µL] = A_{260} x ε (ε_{DNA} = 50 or ε_{RNA} = 40).
The ratio of A_{260}/A_{280} was used as a measure of the purity of a sample.

3.1.4 Plasmid purification

Mini-plasmid purifications were performed by using a vacuum manifold and the QIAprep Spin Miniprep Kit from Quiagen (QIAprep® Miniprep Handbook, May 2004 pp. 25, 26). In step 10, plasmid-DNA was eluted with 30 µl ddH_2O.
Maxi-preparations were performed by using the QIAfilter Plasmid Maxi Kit from QIAgen according to the manufacturer's instruction (QIAgen® Plasmid Purification Handbook, August 2003, pp.17-20). In step 15, plasmid pellets were redissolved in 250 µl 1x TE buffer.

3.1.5 Rac1 cloning into the pcDNA3.1 (-) expression vector

The Rac1 wild type (wt) cDNA clone for which the sequence was confirmed at AGOWA, was provided in a pCMV6-XL5 vector and was cloned into the pcDNA3.1 (-)-hygromycin B expression vector using the Not I restriction sites (see Appendix Figure 7-3 for the plasmid card).

1x DNA-restriction digestion mix:

Plasmid-DNA	2 µg
10x buffer 3	2 µl
10x BSA	2 µl
Not I	1 µl
ddH_2O	**to 20 µl**

Digestion was performed for 1 h at 37 °C. Subsequently, samples were heat-inactivated for 20 min at 65 °C. Subsequently, pcDNA3.1 vector ends were dephosphorylated by adding 1.5 µl (10 U) alkaline phosphatase to the sample for 1h at 37 °C. Immediately after, samples (vector and insert) were loaded on a 1 % agarose gel for subsequent DNA gel extraction. Ligation of Rac1 insert and pcDNA3.1 vector as well as a vector control ligation was performed at 16 °C over night.

T4-ligase 5x buffer	2 µl
T4-ligase	1 µl
pcDNA3.1 vector gel extract	1 µl
Rac1 insert gel extract	5 µl
ddH_2O	1 µl
	10µl

On the following day, 1 µl of the ligation samples were transformed into *E.coli* DH5α™ (Invitrogen) according to the manufacturer's instruction (http://tools.invitrogen.com/ content/sfs/ manuals/ 18258012.pdf), plated on LB-agar plates with 100 µg/ ml Ampicillin as a selection marker and incubated at 37 °C overnight.

Afterwards, colonies were picked and inoculated into 4 ml of LB-medium with 100 µg/ ml Ampicillin and incubated overnight on an orbital shaker at 37 °C.

On the following day, plasmid purifications and determination of DNA concentrations was performed. For verification of Rac1 insertion and orientation, a restriction analysis was performed by Not I or BSMB1 digestion of the plasmids for 1 h at 37 °C and subsequent gel electrophoresis.

In order to gain high yields and high purity of the pcDNA3.1 vector (which was used as a vector control) and the pcDNA3.1-Rac1 expression vector a maxi-preparation of the plasmid-DNA was performed following retransformation of 1 ng DNA in *E.coli* DH5α™. Bacteria were cultivation in LB-medium with 100 µg/ ml Ampicillin overnight. On the next day, maxi-plasmid-preparations were performed. The plasmid purity was verified by BSMB1 and Not I digestions with subsequent agarose gel analysis (see Appendix Figure 7-4 for the plasmid card).

3.1.6 Mutagenesis of Rac1

In order to generate a dominant negative (DN) Rac1 mutant (Rac1T17N) [141], mutagenic primer were designed. Primer design was performed with the help of Stratagene's QuikChange® Primer Design Program (http://www.stratagene.com/tradeshows/feature.aspx?fpId=118). Primers were synthesized at MWG (see Table 2-6 for primer sequences). The site-directed mutagenesis of Rac1 and the Dpn I digestion was performed with the QuikChange II XL Site-directed Mutagenesis Kit (Stratagene) according to the manufacturers instructions (Instruction Manual Revision B, December 2005, pp. 9-11).
1x mutagenesis mix:

10x reaction buffer	5 µl
(10 ng) pcDNA3.1-Rac1	1 µl
(125 ng) Rac1_T17N fw primer	1 µl
(125 ng) Rac1_T17N rev primer	1 µl
dNTP mix	1 µl
Quick Solution	3 µl
ddH_2O	38 µl
	50 µl
PfuUltra HF DNA polymerase (2,5 U/ µl)	1 µl

As a negative control, a sample without pcDNA3.1-Rac1 was prepared.

The PCR thermocycler reaction was performed as following:

Table 3-1: PCR thermocycler reaction for Rac1 mutagenesis

Segment	Cycle	Temperature	Time
1	1	95°C	1 min
2	18	95°C	50 sec
		60°C	50 sec
		68°C	6 min 30 sec (1 min/ kb of plasmid length
3	1	68°C	7 min

Following PCR reaction and Dpn I mediated digestion of the template, 2 µl of the samples were transformed into One Shot® OmniMAX™-T1^R chemically competent *E.coli* according to the manufacturers instructions.
(http://tools.invitrogen.com/content/sfs/manuals/ oneshot_omnimax2_man.pdf)
Subsequently, transformed *E.coli* were spread on LB-agar plates with 100 µg/ ml Ampicillin and incubated overnight at 37 °C.
On the following days, mini-preparations of plasmids were performed. The mutagenesis was verified by sequence analysis at AGOWA. Finally, a verified clone was used for a maxi-plasmid preparation (see Appendix Figure 7-4 for the plasmid card).

3.1.7 Generation of NDV specific siRNAs

Viral NDV specific siRNAs targeting the ORF of the P and V mRNA (viral P+V siRNA 1-3) were designed with the help of Dharmacon's siDesign Center software tool (sequences are provided in the Table 2-7).
(http://www.dharmacon.com/DesignCenter/DesignCenterPage.aspx).
In order to minimize off target effects, siRNA sequences were blasted to exclude sequence homology with human genes.

3.1.8 CDNA synthesis

Cell lysis and subsequent complementay DNA (cDNA) synthesis without previous RNA isolation was performed with the Cells-to-cDNA™ II Kit from Ambion according to the manufacturer's instructions. $2x10^4$ cells were lysed in 50 µl lysis buffer provided in the kit.

3.1.9 Quantitative real-time PCR

Realtime PCR reactions were performed to relatively quantify expression levels of a specific target gene between different samples. In general, singleplex reactions (in triplicate) were performed using gene-specific pre-developed Taqman assays as well as pre-developed Taqman assays for the endogenous controls Glyceraldehyde 3-phosphate dehydrogenase (GAPDH) or 18s. Assays were run in a 7500 Fast Real-Time PCR System by ABI Prism®. Relative quantification of gene expression and standard deviation calculations were performed by using the "Relative Standard Curve Method" as described in the "Guide to Performing Relative Quantification of Gene Expression Using Real-Time Quantitative PCR" provided by Applied Biosystems.
(http://www3.appliedbiosystems.com/cms/groups/mcb_support/documents/generaldocuments/cms_042380.pdf; pages 35-43)
For standard curve preparations, cDNA samples of untreated cells in the experiment were used.

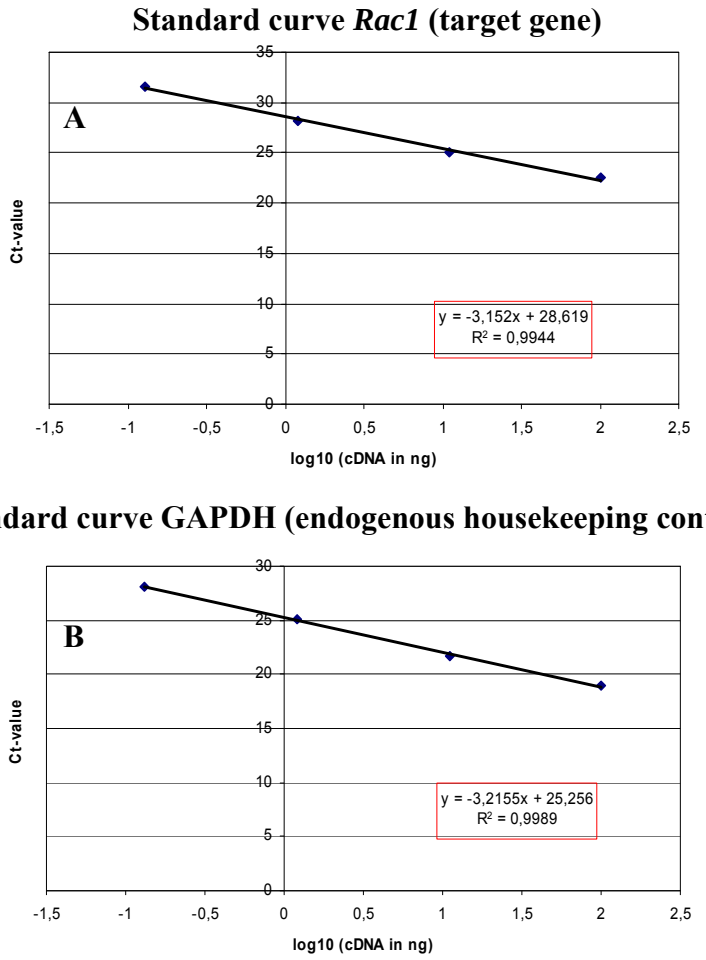

Figure 3-1: Typical Taqman real-time PCR Standard curve plots (log of input versus Ct value)
(A) for a target gene and
(B) for the endogenous control.

By utilizing the standard curves, target- and endogenous-control Ct-values could be interpolated into masses (ng). In order to calculate a normalized target value, the mass of the target had to be divided by the mass of the endogenous control.

Normalized target = target [ng]/ endogenous control [ng]

For determination of relative expression levels, the normalized target values of the test samples had to be divided by the normalized test sample which is used as a calibrator (e.g. non-silencing siRNA control or vector control).

Fold difference in target expression = Normalized target (test sample)/ normalized target (calibrator sample)

Results were expressed as average values ± standard deviation (SD). The standard deviation (of the quotient) was calculated as follows:
As a first step, the coefficient variation (cv) for the target gene and the endogenous control had to be calculated:

cv = SD (of the masses)/ mean value (of the masses)

Next, the cv of the quotient had to be calculated:

$$cv = [(cv_{\text{target gene}})^2 + (cv_{\text{endogenous control}})^2]^{1/2}$$

The standard deviation is finally calculated by:

SD = cv x mean value (of the normalized target)

3.2 Cell biological methods

3.2.1 Cell culture methods

All cells were grown at 37 °C in a cell incubator in a 5 % carbon dioxide / 100 % humidity (atmosphere). If not mentioned otherwise all cell culture media were not supplemented with antibiotics. The adherent cells were detached from the surface of the cell culture flasks with the help of a prewarmed Trypsin / EDTA solution. For cell detachment the growth medium was removed and cells were washed with PBS whereby the wash volume was adapted to the flask size. Then 13 µL prewarmed trypsin / EDTA solution per square centimetre surface was added and HaCaT-derived cells were subsequently incubated for 30 minutes, all other cell

lines 5 – 10 minutes at 37 °C in a cell incubator. When cells were detached an appropriate amount of fresh prewarmed cell culture medium was added to inactivate Trypsin before cells were used for further experiments. All cell culture materials used were sterile.

HaCaT, II4, RT3, RT3 K1 and HT-29 cells

The cell lines were cultured in DMEM Ham's F12 with phenol red and stable glutamine supplemented with 10 % FCS. Cells were split twice a week 1:10–1:15 when reaching 90 % confluency.

HCT 116 cells

The human colon carcinoma cell line was cultured in DMEM with phenol red and stable glutamine supplemented with 10 % FCS. Cells were split twice a week 1:7-1:10 when reaching 90 % confluency.

MDA-MB-231 cells

The human colon carcinoma cell line was cultured in DMEM Ham's F12 with phenol red and stable glutamine supplemented with 10 % FCS. Cells were split twice a week 1:15-1:20 when reaching 90 % confluency.

HT-1080 cells

The human fibrosarcoma cell line was cultured in DMEM with phenol red and stable glutamine supplemented with 10 % FCS. Cells were split twice a week 1:10-1:15 when reaching 90 % confluency.

3.2.2 Determination of cell number and cell viability

Cells were counted with the help of disposable urine sediment chambers (FAST-READ 102 NEW GRID) based on Neubauer's blood counting chamber with a volume of 0.1µl. In order to distinguish live and dead cells, death cells were stained by Trypan blue in a 1:10 dilution. 30 µl of the diluted cell suspension was transferred to the chamber for counting using an optical microscope. Cells suspensions which exceeded 100 cells per large square had to be diluted again. At least 4 large squares were counted. The cell titer was calculated with the following formula:

Cells/ ml = mean of cell count * dilution factor 10 * $1x10^4$

3.2.3 Freezing and thawing of cells

Freezing of cells was performed by adding 1 ml of ice-cold freezing medium to $1x10^6$ trypsinised, washed and pelleted cells by centrifugation at 145x g for 5 min. Cells were transferred to cryo-vials and stored in pre-cooled (4 °C) freezing boxes at -80 °C for 1-3 days. Subsequently, cryo-vials were transferred to liquid nitrogen containers and stored at -196 °C.

Frozen cells in a cryo-vial were thawed in a water bath at 37 °C and immediately after thawing, cell culture medium was added and cells transferred to a cell culture flask (75 cm^2) containing 15 ml of pre-warmed fresh culture medium. Within 24 h, cell culture medium had to be changed to remove DMSO and dead cells.

3.2.4 Unspecifically staining of cells for mixed cell culture experiments

For the mixed cell culture infection experiments of HT-29 and HaCaT cells, the HaCaT cell line was unspecifically fluorescently stained by CellTracker™ orange. $4x10^5$ HaCaT cells were seeded in a 6-well plate to reach a confluency of 60 % on the following day. The day after seeding, growth medium of cells was replaced by growth medium without FCS but 5 µM CellTracker™ orange (1:2000 dilution of stock solution). Staining was performed at 37 °C in the incubator for 45 min. Subsequently, cells were washed with 1x PBS and fresh growth medium was added. Cells were further incubated for 30 min at 37 °C. Cells were then washed again and provided with fresh growth medium with supplements. Fluorescence was checked by fluorescence microscopy. In the evening cells were trypsinised and 6-wells with stained cells were pooled and counted. Simultaneously, HT-29 cells were trypsinised and counted. Subsequent to counting, $4,8x10^6$ cells of both cell lines were transferred to a 15 ml centrifuge tube and centrifuged at 188x g for 5 min. Cell pellets were resolved in 8 ml growth medium. Cells were then mixed in a 1:1 ration and $6x10^5$ cells per ml were seeded in 12 well dishes and incubated overnight before further treated.

3.2.5 Cell viability assays

Measurement of cell vitality was performed by using alamarBlue® assay (Invitrogen) or CellTiter-Glo® Luminescent cell viability assay (Promega). The alamarblue® assay is based on a fluorometric/ colorimetric reduction-oxidation reaction (REDOX) indicator. Reduction due to metabolic activity of cells causes the indicator to change from an oxidized (non-

fluorescent, blue) state to a reduced (fluorescent, red) form. Cells were plated in a volume of 100 µl in opaque-black optical 96 well plates. 10 µl alamarBlue was added directly to the cells and incubated for 1 h in the incubator. Fluorescence was measured at 530 nm excitation and 590 nm emission wave length.

The CellTiter-Glo® Luminescent cell viability assay measures the presence of ATP in metabolically active cells. The assay is based on the principle that luciferine is mono-oxigenated by luciferase in the presence of MG^{2+}, ATP and molecular oxygen causing a luminescent signal. The assay was performed according to manufacturer`s instructions (Promega, Technical Bulletin No. 288, Februar 2004, page 5) For luminescent assays, cells had to be plated in opaque-white optical 96-well plates.

Fluorescence or luminescence signals were measured at the VICTOR microtiter well plate ready.

3.2.6 Proliferation assay

$2x10^3$ cells per 100 µl were seeded in 96 wells in sextuple. 24, 48, 72 and 96 h post seeding cell metabolism was measured by adding 10 µl alamarBlue® (Invitrogen). 1 h post incubation at 37 °C in an incubator, fluorescence signals were measured at the VICTOR microtiter well plate reader. Fluorescence signals 24 h after seeding were used for normalization.

3.2.7 Crystal violet staining of cells

In order to detect cell lysis following NDV infection, DNA of cells was unspecifically stained with Crystal Violet. As a first step, cells were washed with PBS. Subsequently, cells were fixed and stained with 0.1 % Crystal Violet/ 4 % formaldehyde for 30 min (with simultaneous UV-irradiation for NDV inactivation). Finally, cells were washed 4 times with dH_2O to remove excess staining and let dry.

3.2.8 Colony Formation assay in soft agar

Colony Formation assay in soft agar. Cells grown in monolayer cell culture were trypsinized and $1x10^4$ cells were resuspended in 2 ml of growth medium containing 0.4 % Seaplaque-agarose and 10 % FCS. Cell suspensions were plated on previously solidified 0.6 % Seaplaque-agarose layers in 6 well plates and were incubated for 4 weeks before colony formations were monitored by inverse optical microscopy using a 2.5x plan neofluar objective.

3.2.9 Transfection of cells using DharmaFECT transfection reagents

For siRNA transfection experiments, lipid based DharmaFECT transfection reagents and predesigned siRNAs (Dharmacon) reconstituted in siRNA buffer were used. As there are 4 different DharmaFECT formulations offered, each cell line had to be tested for optimal transfection conditions with respect to transfection efficiency and cytotoxicity. SiRNA transfection experiments were generally performed in a 96-well format using the reverse transfection method or in a 6-well format by forward transfection. The final concentration of each siRNA or siRNA pool transfected was 50 nM.

Reverse tranfections were performed by aliquoting 25µl of siRNA/transfection reagent mix in DCCR into 96 wells (in triplicate or sextuple). Alternatively when using the Reverse transfection library plates, lyophilised siRNAs were reconstituted with 25 µl DCCR/ DharmaFECT 3 transfection reagent mix per 96 well. The mix was incubated for 30 min at room temperature. In the meantime, cells were harvested, counted and appropriately diluted in growth medium without antibiotics. Finally, 100 µl of cell solution was added to the transfection mix (final volume per 96 well: 125 µl). Cells were incubated in the incubator for 24 h before transfection medium was replaced by fresh growth medium containing antibiotics (100 IU/ mL Penicillin and 100 µg/ mL Streptomycin). 48 h post transfection knockdown efficiency was measured by Taqman realtime PCR or Western Blot analysis.

Forward transfections in a 6-well format were performed by following the manufacturer's instructions (Dharmacon, product insert siRNA transfection reagents).

The optimized transfection conditions for HaCaT, RT3 and HCT 116 cells are listed in the Table 3-2:

Table 3-2: Optimized transfection conditions

Cell line	Transfection format	Transfection method	DharmaFECT reagent	Volume of DharmaFECT reagent/ well [µl]	Cell number
HaCaT	96 well	reverse	2	0.5	$2x10^4$
RT3 K1	96 well	reverse	3	0.375	$2x10^4$
RT3 K1	6 well	forward	3	4	$3x10^5$
HCT 116	96 well	reverse	1	0.33	$3x10^4$

3.2.10 Electroporation of cells

Electroporation is a DNA transfer method based on electric pulses which induce transient cell membrane permeability. HaCaT and RT3 K1 cells are not efficiently transfected with

plasmid-DNA by lipid-based methods. Therefore, gene delivery was performed by electroporation using AMAXA`s nucleofection technology. HaCaT and RT3 K1 cells were nucleofected using the cell line Nucleofector™ Kit V according to AMAXA's optimized nucleofection protocol for HaCaT cells (March 2003; pp. 2-4). $5x10^6$ cells were nucleofected with 5 µg of plasmid-DNA and split in 3 6 wells for incubation.

3.2.11 Development of stable transfected or transduced cell lines

For stable selection of transfected or transduced cell lines, titration of the selection markers (antibiotics) had to be performed first. Cells were seeded in 24 well dishes to reach 30 % confluence the next day. Growth medium was then replaced by cell culture medium containing increasing concentrations of the antibiotic (in duplicate) which is used as a selection marker in subsequent transfection or transducing experiments. Every 3 days, cells had to be provided with fresh growth medium with antibiotics. For further experiments, the lowest concentration was nominated, which induced (efficient) cell death within approximately 1 week and did not allow for re-growth of cells within 2 weeks.
Stable selection started 48 h post electroporation or transduction of cells. Growth medium was replaced by growth medium containing the previously determined concentration of antibiotic which served as an selection marker. As a positive control for cell death and as an indicator for final selection, untreated cells were treated as well. In Table 3-3 concentrations of antibiotics are listed which were used for stable selection of cells in various experiments

Table 3-3: Concentration of antibiotics for stable selection

Cell line	Antibiotics	Concentration [µg/ml]	Experiment
HaCaT	Puromycin	0.5	H-RasV12 transduction
HaCaT	Hygromycin B	300	Rac1wt electroporation
RT3 K1	Hygromycin B	300	Rac1_T17N electroporation

3.2.12 Immunofluorescence (IF)

For immunofluorescently staining, cells were either seeded on cover slipes in 24 wells or in 96 wells of opaque-black optical plates. On the next day or following drug treatment or infection experiments, cells were washed with PBS and fixed with 3.7 % Paraformaldehyd in PBS for 15 min at room temperature. NDV-infected cells were UV-irradiated during the fixation step. Subsequently, cells were washed 3 times with PBS before further treated. For cells seeded on cover slipes all following steps were performed outside the dish in a humid

atmosphere. For permeabilization of cells and blockage, cells were incubated with blocking buffer for 45 min. Subsequently, cells were incubated with primary antibodies diluted in antibody dilution buffer for 2 h and washed 3 times with blocking buffer before incubated with the secondary antibody or Phalloidin for 1 h in the dark. Finally, cells were washed 3 times with PBS for 5 min. In the second washing step Hoechst 33258 (dilution 1:10000) was added. Cells stained on cover slipes were covered with 40 % Glycerin in PBS and transferred to object slides for subsequent fluorescence microscopy. Cells stained in a 96 well plate were kept in PBS and fluorescence analyzed by inverse optical microscopy.

3.2.13 Determination of biological active interferon secretion in cell culture supernatants

The quantitative determination of biologically active interferon I in cell culture supernatants of NDV-infected cells was measured by iLite AlphaBeta human Type I activity detection kit (Neutekbio). This method is based on a luciferase gene reporter assay by using interferon type I sensitive cell lines stably transfected with an interferon sensitive response element.
The assay was performed according to the manufacturer's instructions (Neutekbio, product information).

3.2.14 Measurement of viral luciferase activity of infected cells

Viral luciferase activity of NDV-luciferase infected cells was quantified using the Steady-Glo® Luciferase Assay system. The assay was performed according to the manufacturers instructions (Promega, Technical Manual Steady-Glo® Luciferase Assay system April 2006, page 5). Cells had to be plated in opaque-white optical 96-well plates. Luminescence signals were measured at the VICTOR microtiter well plate reader.

3.2.15 Cell survival experiment of IFN-stimulated and NDV-infected cells

Confluent RT3 K1 cells seeded in opaque-white optical plates 96 wells were pretreated with 100 µl growth medium containing increasing concentrations of IFNα or β overnight. Subsequently, cells were infected with NDV-luciferase at a multiplicity of infection (MOI) of 0.01 diluted in growth medium or mock infected in the absence of IFN type I. Unstimulated and uninfected cells were used as a cell viability control for IFN treated cells. Cell viability of stimulated infected and stimulated mock-infected cells was measured 72 h post infection using the CellTiter-Glo® Luminescent cell viability assay according to manufacturer`s

instructions. Cell survival of infected cells following IFN treatment was determined by dividing cell viability of IFN-stimulated infected cells by cell viability of stimulated mock infected cells.

3.3 Virological methods

All virological experiments were performed under S2 conditions.

3.3.1 Production of NDV stocks

EGFP-expressing NDV was propagated by infection of 80 % confluent HT-29 cells (30 ml growth medium) in a 162 cm^2 cell culture flask with a MOI of 0.01. 72 h p.i. when cells were efficiently infected (which could be controlled by fluorescence microscopy) and cell lysis progressed, cell culture supernatant was harvested. Subsequently, the supernatant was centrifuged by 1700 x g for 5 min at 4 °C to remove cell debris. Finally, the virus containing supernantant was aliquoted and frozen at -80 °C. 1 aliquot was used for determination of NDV-titer by Plaque formation assay.
Luciferase-expressing NDV and NDV without transgene were provided by the workgroup Puehler/Beier; Bayer Schering Pharma AG, Berlin. In short, the virus was propagated in embryonated chicken eggs. The harvested virus-containing alantoic fluid was cleared by tangential filtration flow, aliquoted and stored at -80 °C.

3.3.2 Determination of virus yield in supernatants

Virus titers were determined by plaque assay using confluent HT-1080 cells in a 24-well format. After one-hour attachment of the virus to the cells, the inoculum was removed and replaced with 0.7 % SeaPlaque-agarose-containing medium (Cambrex Bio Science). Plaques were counted 24 h after the infection following fixation and staining with 0.1 % crystal violet/ 4 % formaldehyde for 4 h. The NDV-titer was calculated as following:

NDV titer [PFU /ml] = counted plaques * dilution factor*4

3.3.3 NDV infection of cells

In general, if not otherwise stated, infection of adherent cells was performed when cells reached a confluency of (nearly) 100 %. Before infection, cells were washed with PBS. Virus dilutions were performed in serum-free medium for infection experiments in 6 wells. Growth

medium with supplements was used for virus dilutions when cells grown in 96 wells were infected. Cells were incubated with infectious medium (100 µl per 96 well, 1 ml per 6 well) for 1 h on a shaker in the 37 °C incubator. Following infection of 6 wells infectious medium was replaced by serum-containing fresh medium and further incubated.

3.3.4 UV-treatment of NDV

Infected cells were exposed to UV-light of a cell culture bench for 30 min when NDV inactivation was necessary.

3.3.5 Infection studies following drug treatment of cells

Cells were seeded in opaque 96 well optical plates. On the following day, cells were pre-treated with 100 µl of small molecule inhibitors with increasing concentrations diluted in growth medium with supplements for 1 h. Afterwards, cells were infected with NDV-luciferase at an MOI of 0.01 in the presence or absence of inhibitor diluted in growth medium with supplements. Infected untreated cells and solvent only treated cells were used as controls for cytotoxicity. 24 h p.i. the luciferase based readout and a cell viability assay was performed.

For immunofluorescence experiments following drug treatment and infection, cells were seeded on cover slips in a 24 well dish. On the next day, cells were pre-treated with 500 µl 50 µM Rac1 inhibitor NSC 23766 for 1h before cells were infected with an MOI of 1 in the presence of inhibitor. Three hours p.i. cells were fixed with 3.7 % paraformaldehyde and UV-irradiated.

3.3.6 Lentiviral transduction of HaCaT cells

The day before lentiviral H-rasV12 transduction of HaCaT cells, $8x10^5$ cells were seeded in a 6 well plate to reach 90 % confluence on the following day. Cells were transduced with 1 µg (p24) pLenti6-HrasV12 or pLenti6-JRED (as a control) (provided by Ulrike Ulbricht, Bayer Schering Pharma AG, Berlin) in 500 µl growth medium in the presence of polybrene with a final concentration of 6 µg/ ml. Five hours post infection cells were washed 4 times with growth medium before growth medium with antibiotics was added. 48 h post transduction, selection of transduced cells started with Puromycin as a selection marker.

3.4 Protein chemical methods

3.4.1 Generation of cell lysates

If not stated otherwise, confluent adherent cells in a 6 well dish were directly lysed with M-PER® mammalian protein extraction reagent following the manufacturer's instruction (product insert; instructions; 2007). 70 µl lysis buffer (containing protease and phosphatase inhibitor cocktails) per 6 well (~$1x10^6$ cells) was added. Cells were scraped and collected in ice-cold microcentrifuge tubes. Cells grown in 96 well plates were directly lysed with 25 µl lysis buffer per 96 well. To support lysis, 96 well plates were gently shaken on an orbital shaker for 5 min before cell lysates were collected in PCR tubes and replicates pooled. Following centrifugation for 10 min at 14000x g and 4 °C, supernatants were transferred to new tubes and protein concentrations were determined by BCA protein assay. Finally, samples were shock-frozen in liquid nitrogen and stored by -80 °C until further analysis.

3.4.2 BCA protein assay

The BCA protein assay is a common colorimetric method for protein quantification of a sample. Its detergent-compatible formulation is based on bicinchoninic acid (BCA). Proteins in the sample mediate Cu^{+2}-reduction to Cu^{+1} in an alkaline medium. This causes a purple-colored reaction product formed by chelation of 2 molecules of BCA with 1 cuprous ion (Cu^{+1}). The chelat complex exhibits a strong extinction at 562 nm and is nearly linear between 20 and 2000 µg/ ml protein). The BSA standard, provided in the BCA™ protein assay was used to prepare protein standards in a range between 20 and 1,25 µg/ 50 µl. 50µl of the standards and 5 µl of test samples in 45 µl dH_2O (1:10 dilution) were transferred onto a 96 well flat bottom plate in triplicate. Following incubation at 37 °C for 30 min, absorbance was measured at the Tecan Sunrise microplate spectrophotometer. The standard curve was used for interpolation of sample protein concentrations.

3.4.3 SDS-polyacrylamid gel electrophoresis

Sodium dodecyl sulfate polyacrylamide gel electrophoresis (SDS-PAGE) was performed to separate proteins according to their molecular weight by applying an electric field. The anionic detergent SDS was used for protein denaturation and negative charging of the

proteins. Therefore, migration speed in the electric field only depends on protein size when treated with SDS. Protein samples were mixed with 4x NuPAGE® LDS (Lithium dodecyl sulfate) sample buffer and 10x NuPAGE® sample reducing agent and heated for 5 min at 95 °C in a thermoblock for complete reduction. Subsequently, samples were loaded onto a pre-cast 4-12 % NuPAGE® Novex Bis-Tris-HCl buffered (pH 6.4) polyacrylamide gel with a stacking acrylamide concentration of 4 % and a separation acrylamide concentration of 4-12 %. As a molecular weight marker, the full range Rainbow molecular weight marker was added. For separation of small proteins the NuPAGE® MES SDS buffer was used and for resolving medium to large size proteins the gel was run with NuPAGE® MOPS SDS buffer. The electrophoresis was run in a XCell SureLock™ Mini-Cell with a constant current of 75 mA until the bromophenol blue of the sample buffer had run out of the gel. Electrophoresis was stopped, the gel cassette was cut open and the acrylamide gel was transferred into transfer buffer for subsequent protein transfer.

3.4.4 Western Blot analysis

Proteins, separated by SDS-Page, were transferred onto PVDF membranes by tank-blotting with the XCell II™ Blot Module according to the manufacturers instructions (Invitrogen, instruction manual XCell II Blot Module, December 2003 version 1, pp.12-14 and 17). For protein immobilisation, precast PVDV membranes and filter paper and the NuPAGE® transfer buffer was used. The blot was run for 75 min at 400 mA. Subsequently, the bands of the molelular weight marker were marked using a pencil. Subsequently, the blot was blocked with 5 % powdered milk in 0.1 % TBS-T buffer for 2 h and incubated with the primary antibodies overnight at 4 °C. After incubation with the appropriate secondary antibody labelled with Alexa Fluor 680 for 1 h, visualization of bound antibodies was performed by using the Odyssey® Infrared Imaging System.

3.5 In vivo experiment

3.5.1 Xenograft experiment

The tumor growth of HaCaT, RT3 and RT3 K1 cells was determined by subcutaneous inoculation of $5x10^6$ cells (previously grown to 70 % confluency in cell culture flasks) in 100 µl culture medium 1:1 mixed with Matrigel™ into the right flank of female NMRI nude mice (n=10/ group; body weight 18-20 g). The measurement of tumor area was performed

using caliper and was started 5 days post inoculation. Measurements were repeated on day 8 and 12 (after inoculation). Mice were sacrificed on day 12 by cervical dislocation. Animal studies were conducted in accordance with the guiding principles in the care and use of animals htpp://www.the-aps.org/about/opguide/appendix.htm#care.

3.6 Microscopy

Fluorescence and phase contrast images were captured using an inverse optical microscope (Axiovert 25) and the Axio Vision Release 4.7.2.0 software.

3.7 Statistics

Statistical significance of the differences in the subcutaneous tumor growth of RT3 and RT3 K1 cells in nude mice was calculated using a paired Student's t-test. P-values ≤ 0.05 were considered statistically significant

4 RESULTS

4.1 Characterization of a HaCaT-derived cell transformation model concerning NDV susceptibility and applicability in a NDV-sensitizing siRNA-based screen

4.1.1 NDV selectively replicated in tumor cells in a mixed cell culture infection experiment

The naturally occurring oncolytic Newcastle disease virus is known to replicate in a variety of tumor cells but not in non-tumorigenic cells [55]. In the first experiment tumor selective NDV replication in a mixed cell culture experiment comprising of human non-tumorigenic HaCaT keratinocyte cells and human tumorigenic HT-29 colon carcinoma cells should be confirmed. In order to distinguish between the two cell types, HaCaT cells were unspecifically stained with the CellTrackerOrange fluorescent dye. HaCaT and HT-29 cells were mixed, co-cultured as a confluent monolayer and infected with EGFP-expressing NDV at an MOI of 0.01 (Figure 4-1). In contrast to HaCaT cells which did not show viral replication, efficient NDV replication with subsequent oncolysis of cells could be detected in the tumorigenic HT-29 cell line. It was indicated by viral EGFP expression and cell lysis of infected cells.

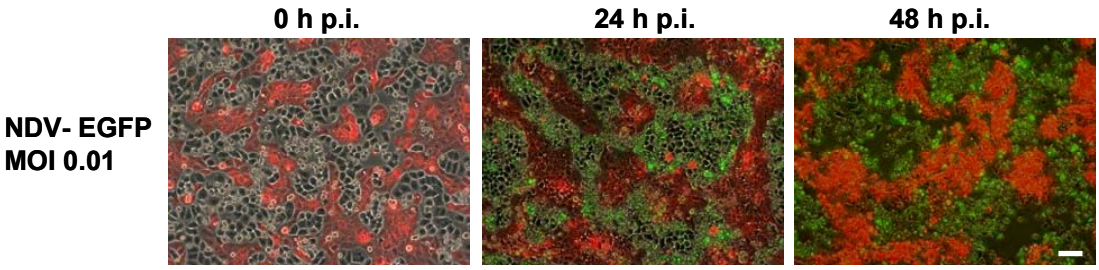

Figure 4-1: Tumor cell-specific replication of NDV in a mixed cell culture experiment
HaCaT cells were labeled with CellTrackerOrange and 1:1 mixed with unlabeled HT-29 colon carcinoma cells. The confluent co-culture monolayer was subsequently infected with NDV-EGFP at an MOI (multiplicity of infection) of 0.01. At the indicated time points picture were captured for phase contrast (cells, gray), CellTrackerOrange (HaCaT cells, red) and enhanced green fluorescent protein (EGFP; NDV-EGFP infected cells, green). The images show an overlay of all three channels. Infected HaCaT cells appear yellow. Infected HT-29 cells appear green (scale bar = 100 µm).

Tumor-selective replication of NDV could be shown in this co-culture experiment of HaCaT and HT-29 cells. However, for the identification of NDV-sensitizing factors which are simultaneously linked to tumorigenesis a cell line model for transformation with similar genetic backgrounds was more appropriate. In the following section, the HaCaT-derived *in vitro* model for skin carcinogenesis comprising of cell lines which constitute different stages of transformation [119] was evaluated for its applicability as a model for oncolysis.

4.1.2 Tumorigenic RT3 cells showed transient NDV susceptibility

In order to evaluate whether Ras transformation and subsequent single or repeated *in vivo* passaging rendered non-susceptible HaCaT cells susceptible to NDV, the tumorigenic HaCaT-Ras clonal cell line II4 and the metastasizing cell line A5-RT3 (RT3) derived following 3 rounds of *in vivo* passaging of the formerly non-tumorigenic HaCaT-Ras clone A5, were analyzed and compared with respect to NDV susceptibility. Cells were infected with EGFP-expressing NDV using a low MOI. NDV replication indicated by viral EGFP expression was assessed by fluorescence microscopy. As it is depicted in Figure 4-2, NDV did not replicate in HaCaT and II4 cells. Only single EGFP-expressing cells could be detected during the monitored time period. In contrast, infection of RT3 cells was characterized by a transient NDV replication. Approximately 40 % of the cells showed viral EGFP expression. However, EGFP expression did not dramatically increase 48 h p.i. indicating that there was no progression of NDV infection.

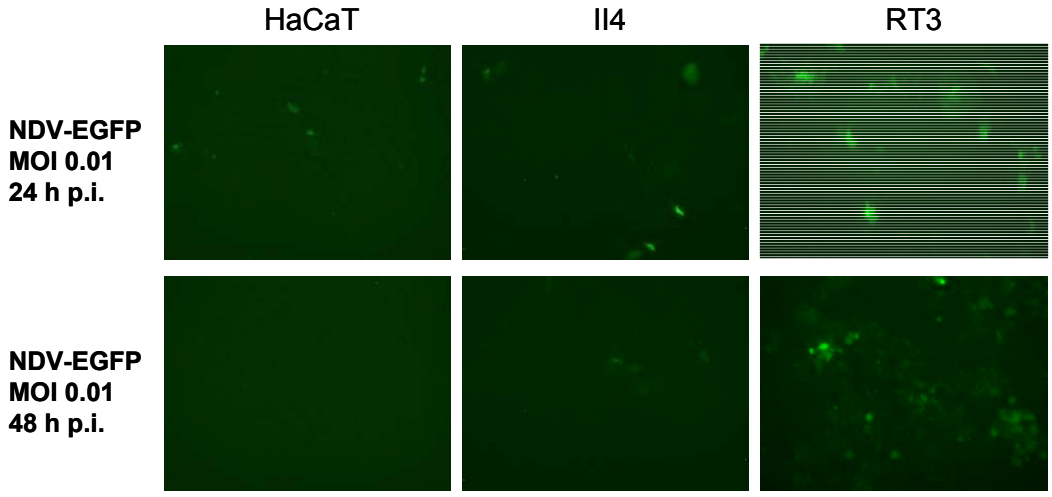

Figure 4-2: Representive fluorescence pictures showing that RT3 cells were more susceptible to NDV replication than HaCaT and II4 cells
Confluent tumorigenic II4 and RT3 cells were infected with EGFP-expressing NDV (MOI 0.01). Twenty-four hours p.i. and 48 h p.i viral EGFP expression was monitored by fluorescence microscopy (scale bar= 100 µm).

Malignant transformation of HaCaT cells did not generally lead to NDV susceptibility as indicated by the non-susceptible II4 cell line. However, the RT3 cell line was at least partially NDV sensitive. In the following experiment, it was tested, whether RT3 subclones with increased NDV susceptibility could be isolated.

4.1.3 RT3 subclone 1 formed larger anchorage-independent colonies *in vitro* and tumors *in vivo*

Subcloning of RT3 cells was performed by exploiting the tumor cell-specific feature to form colonies in soft agar due to their ability of anchorage-independent growth. Several soft agar colonies could be isolated and re-cultivated. The RT3 subclone 1 (RT3 K1) excelled by forming colony sizes above average compared to RT3 cells when colony formation assay in soft agar was repeated (Figure 4-3). HaCaT cells were used as a negative control for colony formation in soft agar.

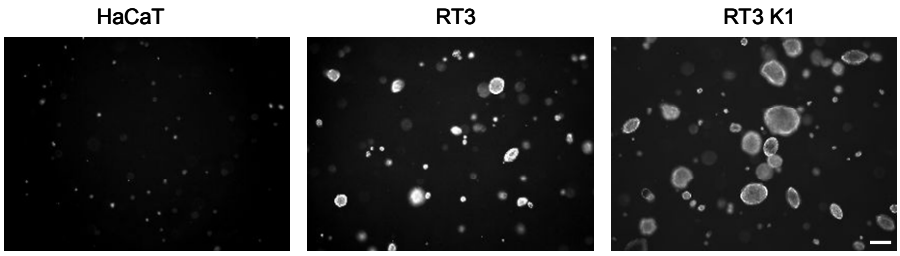

Figure 4-3: RT3 K1 cells formed larger colonies in soft agar compared to RT3 cells
Cells were seeded in soft agar and incubated for 4 weeks before pictures of colony formation were taken (scale bar= 500 µm).

Oncogenic Ras is known to induce anchorage-independent growth of cells [142, 143]. For Ras-transformed sequentially tumor-passaged and re-cultivated cell lines such as RT3, a correlation between enhanced Ras expression and progression of malignancy was demonstrated [121]. As RT3 K1 cells were characterized by increased colony formation in soft agar compared to the parental RT3 cells, the following experiment was performed to compare H-Ras expressions of both cell lines on protein level. Therefore, cell lysates of RT3 and RT3 K1 cells were tested in a Western Blot analysis experiment. HaCaT cell lysate was used as a control for endogenous H-Ras expression (Figure 4-4).

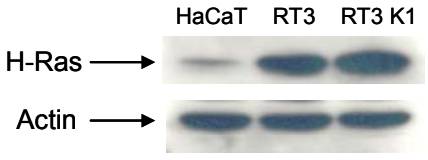

Figure 4-4: H-Ras expression in RT3 K1 cells was not enhanced compared to RT3 cells
Protein samples were subjected to SDS page and subsequent Western Blot analysis of H-Ras expression in HaCaT, RT3 and RT3 K1 cells using a polyclonal H-Ras anti-rabbit antibody. Actin expression served as an endogenous control.

In RT3 K1 cells no enhanced H-Ras expression compared to the parental RT3 cells was detectable. Nevertheless, the ability of increased anchorage-independent growth indicated malignant progression.

In order to investigate whether enhanced growth of RT3 K1 cells in soft agar correlated with an increased tumorigenic potential *in vivo*, tumor growth of the parental HaCaT cells, the RT3 tumor cells and the derived RT3 K1 cells was compared after subcutaneous inoculation of equal numbers of cells into nude mice (Figure 4-5 B).

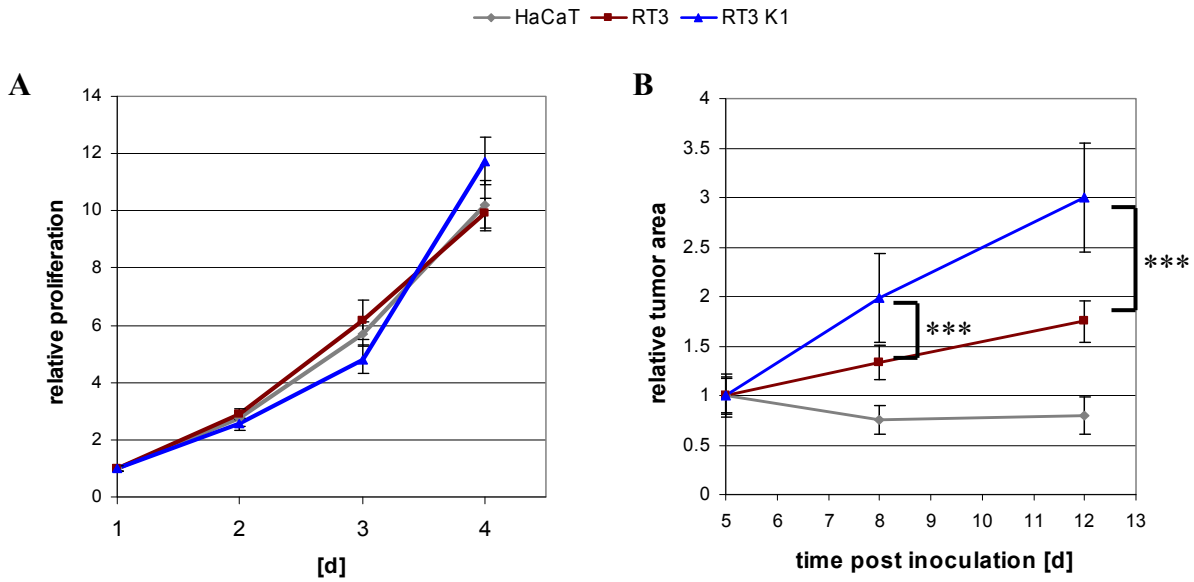

Figure 4-5: RT3 K1 cells showed no enhanced *in vitro* growth but increased *in vivo* growth compared to parental RT3 cells
(A) HaCaT, RT3 and RT3 K1 cells were seeded at low density and and metabolic activity was measured at the indicated time points by alamarBlue assay. Measurement at day 1 after seeding was used for normalization. Error bars represent ±SD of quadruples.
(B) Cells were subcutaneously inoculated in nude mice. Tumor size measurement started 5 days post inoculation and was repeated on day 8 and 12. Tumor sizes on day 5 were used for normalization. Error bars represent ±SD (n=10/ group). The difference in tumor growth of RT3 and RT3 K1 cells on day 8 and 12 were statistically highly significant (p= 0.000523 and p= 0.000125) according to the Student's t-test.

While the parental HaCaT cells remained non-tumorigenic and thus served as a negative control, the RT3 cells formed rapidly growing tumors. The RT3 K1 subclone grew even faster than their parental cell line. Within one week the tumor size tripled, while the original RT3 cells showed only a twofold increase in tumor size within the same period.

Therefore, RT3 K1 cells not only featured an enhanced anchorage-independent growth but also an increased malignancy *in vivo* compared to the parental RT3 cell line.

Enhanced tumor growth of RT3 K1 cells could not be explained by a faster growth *in vitro* compared to RT3 cells (Figure 4-5 A).

4.1.4 Malignant tumor progression of RT3 K1 cells correlated with increased NDV susceptibility

RT3 K1 cells differed from their parental RT3 cells by enhanced colony growth in soft agar and tumor growth in nude mice. Malignant progression is a consequence of additional or increased aberrant functions of tumor associated factors or deregulated signaling pathways. Therefore, it was tested, whether this increased malignant phenotype of RT3 K1 cells favoured oncolytic NDV replication.

In order to address this issue, RT3 and RT3 K1 cells were infected with the same amount of recombinant NDV-expressing EGFP or firefly luciferase using a low multiplicity of infection (MOI 0.01). These viral transgenes allow for visualization or quantification of NDV replication in the infected cells. Non-susceptible HaCaT cells were used as a negative control for viral replication. NDV replication in NDV-EGFP infected cells was determined by fluorescence microscopy 24 h after infection. HaCaT cells did not show NDV replication as there were only single EGFP expressing cells detectable. As seen in previous infection studies, RT3 cells showed partially NDV replication indicated by islets of EGFP expressing cells. In contrast, RT3 K1 cells were highly infected as approximately 90 % of the cells expressed viral EGFP (Figure 4-6).

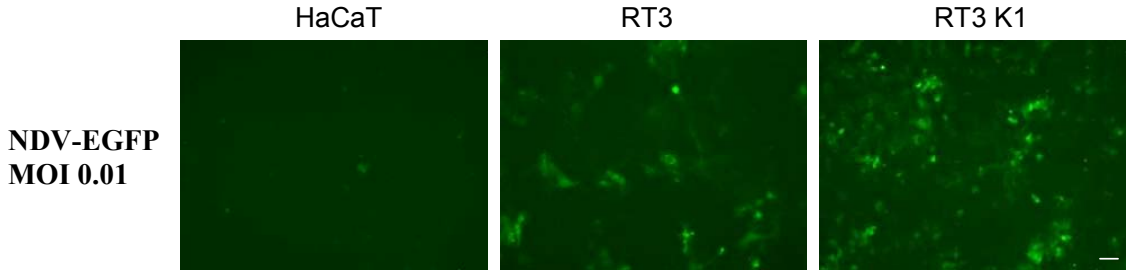

Figure 4-6: Representive fluorescence pictures showing that RT3 K1 cells were more susceptible to NDV replication than their parental RT3 cells
Confluent HaCaT, RT3 and RT3 K1 cells were infected with EGFP-expressing NDV (MOI 0.01). Viral EGFP expression was monitored by fluorescence microscopy (scale bar = 100 µm).

Increased replication of NDV in RT3 K1 cells could be confirmed by quantification of viral transgene activity when cells were infected with luciferase expressing NDV for 24 h. Viral luciferase activity in RT3 cells was five times as high as in non-susceptible HaCaT cells whereas viral transgene activitiy in RT3 K1 cells was approximately nine times as high (Figure 4-7).

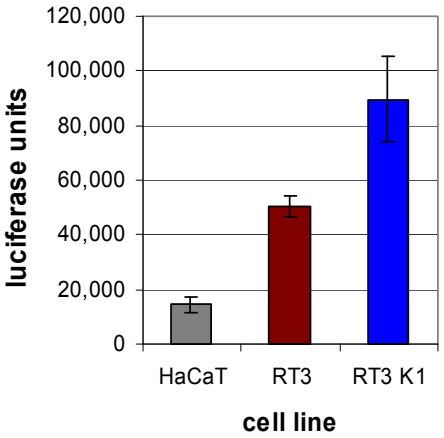

Figure 4-7: NDV replication in RT3 K1 cells was increased compared to RT3 cells
HaCaT, RT3 and RT3 K1 cells were infected with luciferase-expressing NDV (MOI 0.01). Viral luciferase activity was measured 24 h p.i.. Error bars represent ±SD of sextuples.

NDV replication in tumor cells is accompanied by cell lysis (oncolysis) when lytic strains are utilized (e.g. MTH-68). Therefore, enhanced replication of NDV in RT3 K1 cells should lead to increased oncolysis compared to RT3 cells. To proof this, cells were infected with increasing MOIs and time dependent cytopathic effects were determined by measuring cell viability using HaCaT cells as a non-susceptible control (Figure 4-8).

Twenty-four hours post infection there was no loss of cell viability detectable in any of the tested cell lines. Major differences were measured at 48 h p.i.. Whereas more than 80 % of HaCaT cells were still viable at an MOI of 0.1, the majority of the RT3 K1 cells were killed at MOIs as low as 0.01 after 48 h. The RT3 cells showed an intermediate phenotype. In summary, this data demonstrated that RT3 K1 cells were clearly more susceptible to NDV induced oncolysis than their parental cell line RT3.

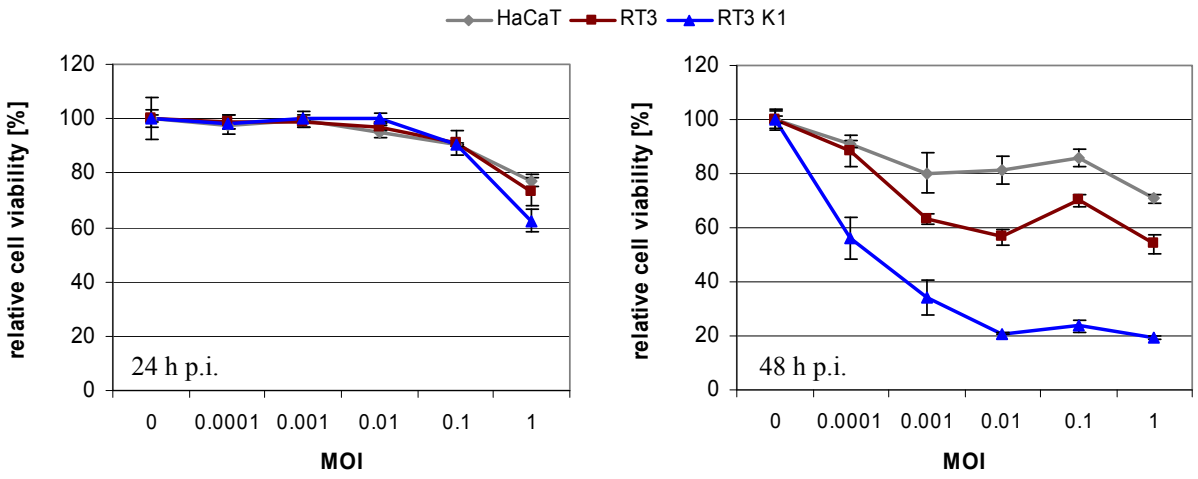

Figure 4-8: RT3 K1 cells were more sensitive to NDV-mediated cell death than their parental RT3 cells
HaCaT, RT3 and RT3 K1 cells were infected with luciferase-expressing NDV with increasing MOIs. Cell viability was measured at 24, 48 h p.i. and normalized to mock infected cells. Error bars represent ±SD of sextuples.

4.1.5 NDV could enter HaCaT cells but replication was limited compared to RT3 and RT3 K1 cells

In order to proof the ability of NDV to productively infect all three cell lines and to correlate the results of viral transgene infection experiments with virus production, NDV-protein expression and release of progeny infectious viruses were monitored in a time course infection experiment. At various time points (0–48 h) post infection at an MOI of 0.01 cell supernatants were collected for determination of released progeny virus by plaque assay. In addition, cells were harvested and lysed for determination of NDV protein expression by Western Blot analysis (0-24 h p.i.).

In Figure 4-9 it is shown that in general, all cell lines could be infected and produced NDV-specific proteins detectable at 16 h p.i. but to varying extents. In RT3 K1 cells, viral protein expression was increased compared to the parental RT3 cells. In HaCaT cells the lowest amount of viral proteins was detectable. Furthermore, it did not increase at 24 h p.i.. In contrast, in RT3 and RT3 K1 cells viral protein production continued and reached a similar protein level. The minor increase in protein expression in RT3 K1 cells could be due to pixel saturation. However, RT3 and RT3 K1 cells showed a similar time course of protein production.

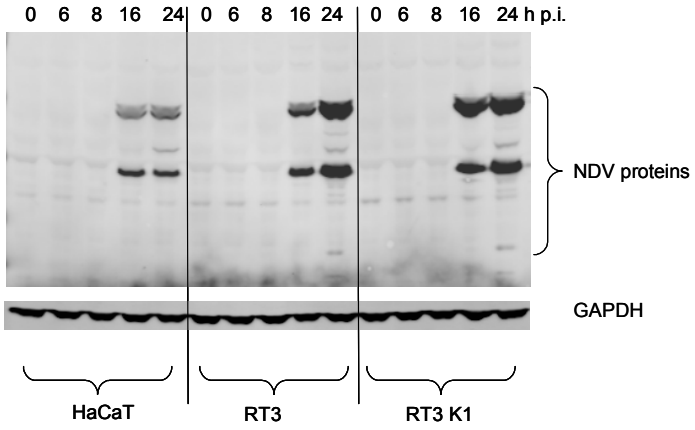

Figure 4-9: Increased viral protein production in tumorigenic HaCaT cells compared to non-tumorigenic HaCaT cells
HaCaT, RT3 and RT3 K1 cells were infected with NDV at an MOI of 0.01. At the indicated time points, cells were harvested and lysed for protein extraction. Protein samples were subjected to SDS page and subsequent Western Blot analysis of NDV protein expression using a polyclonal anti-NDV sera. GAPDH expression served as an endogenous control.

When measuring released progeny virus in the supernatants no significant differences were detected at 16 h after infection of the three cell lines (Figure 4-10). However, after multiple viral replication cycles (24 h), the viral titer in the supernatant of RT3 K1 cells was about

thousandfold increased compared to HaCaT cells. RT3 cells exhibited an intermediate phenotype. The saturation in virus production in the RT3 K1 cells was based on the cytotoxicity of the virus and the death of the virus-producing cells.

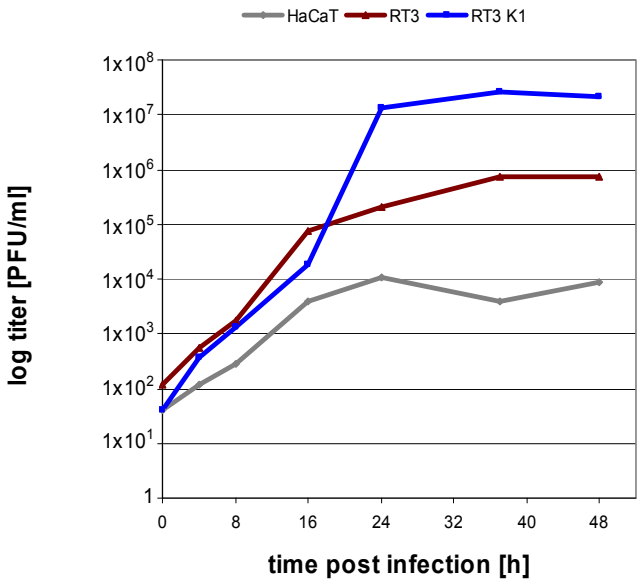

Figure 4-10: Virus production and release in RT3 K1 cells was increased compared to RT3 cells
HaCaT, RT3 and RT3 K1 cells were infected with an MOI of 0.01 and supernatants were harvested at the indicated time points. NDV production and release in supernatants was measured by plaque-assay.

In summary, in all 3 cell lines infection, viral protein expression, production and release of progeny infectious virus was detectable. However, opposed to tumorigenic HaCaT cells viral protein expression and virus production/ release were reduced in non-tumorigenic HaCaT cells.

4.1.6 NDV replication in the tumorigenic HaCaT cells was not caused by elevated eIF-2Bε expression levels

It is likely that tumor-selective replication of oncolytic viruses is not only mediated by defects in the IFN response. As it was shown for the oncolytic RNA virus VSV, its tumor cell-specific replication could be supported by deregulated translational control. Deregulation was demonstrated to be a result of tumor cell-specific overexpression of the eukaryotic initiation factor eIF-2Bε [97]. For this reason we tested the expression of eIF-2Bε in various NDV-susceptible and non-susceptible HaCaT-derived tumor cell lines by Western Blot analysis (Figure 4-11). Non-susceptible HaCaT cells were used as a non-tumorigenic control for eIF-2Bε expression.

Overexpression of eIF-2Bε was not detected in any of the tumorigenic HaCaT cell lines thereby ruling out the possibility of elevated elF-2B activity as a cause for the selective replication of NDV in RT3 K1 cells.

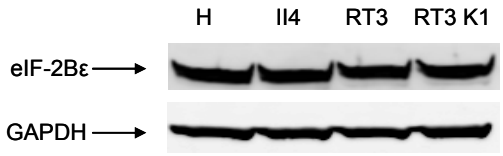

Figure 4-11: Expression of eIF-2Bε did not differ in susceptible and non-susceptible tumorigenic HaCaT cell lines
HaCaT (H), II4, RT3 and RT3 K1 cells were harvested and lysed for protein extraction. Equal amounts of protein samples were subjected to SDS page and subsequent Western Blot analysis of NDV protein expression using a polyclonal anti-rabbit eIF-2Bε antibody. GAPDH expression served as an endogenous control.

4.1.7 IFN type I production and secretion following NDV infection was not impaired and IFN stimulation still induced an antiviral state in tumorigenic HaCaT cells

For NDV, as a strong IFN type I inducer, it is proposed that susceptibility of tumor cells is mediated by defects in the IFN pathway [66, 90-92]. These defects are a common feature of tumorigenic cells as it is connected with increased and uninhibited proliferation and tumor cell survival [89]. In the following experiments it was tested whether IFN type I production and secretion was still intact in the tumorigenic RT3 and RT3 K1 cells compared to the non-tumorigenic HaCaT cells. At various time points after NDV infection at an MOI of 1, cell supernatants were collected and analyzed for biological active IFNα and β. The time course experiment was stopped at 16 h p.i.. Cell vitality of RT3 K1 cells started to decrease afterwards due to NDV-mediated cytotoxicity at an MOI of 1. All three cell lines reacted to the NDV infection with a clear secretion of interferon. The induction of IFN type I appeared to be even stronger in RT3 and RT3 K1 cells as compared to the non-tumorigenic HaCaT cells (Figure 4-12 A). To determine whether type I IFN can still act antivirally on the cells, an indirect assay was used. RT3 K1 cells but not HaCaT cells (as they do not show severe virus-induced cell death) were pre-treated with recombinant human IFN type I. Subsequently, cells were challenged with NDV at a low MOI and monitored for cell survival after 48 h
(Figure 4-12 B). Cell survival indicates that interferon was able to prevent viral cytotoxicity. Both IFNα and IFNβ mediated protection in the RT3 K1 cells.
In summary, there were no gross defects in IFN type I secretion and IFN mediated induction of an antiviral state in the tumorigenic HaCaT cells.

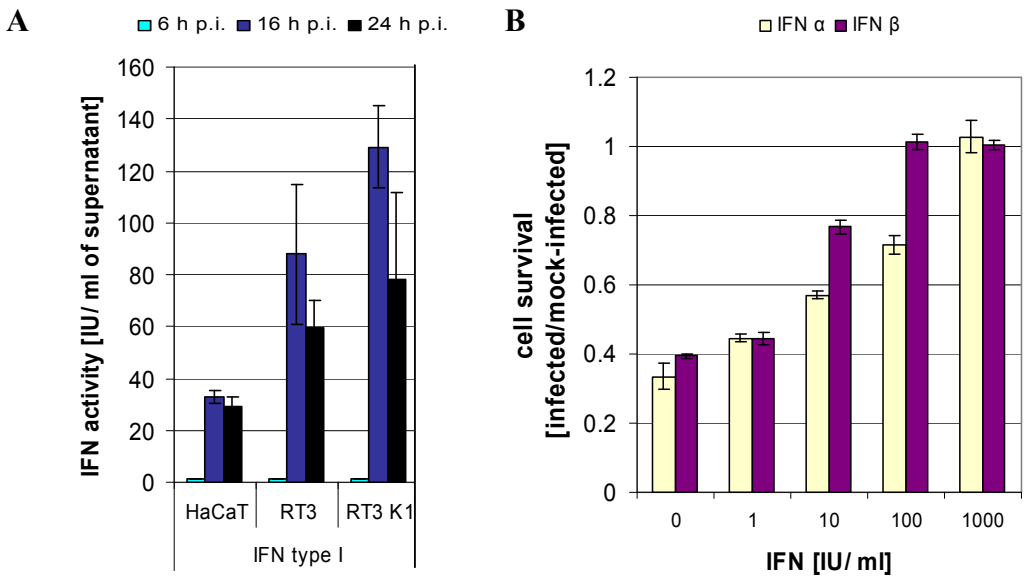

Figure 4-12: Secretion of IFN type I in tumorigenic HaCaT cells was enhanced compared to HaCat cells and IFN type I stimulation reduced NDV-mediated oncolyis of RT3 K1 cells
(A) Detection of biological active type I IFN protein secretion following infection of HaCaT, RT3 and RT3 K1 cells with NDV (MOI 1) in a time course experiment. Error bars represent ±SD of triplicate values.
(B) Cell survival of RT3 K1 cells following stimulation with increasing concentrations IFNα/ β and infection with NDV at an MOI of 0.01. Cell viability was measured 48 h p.i.. Cell viabilities of uninfected but IFN-stimulated cells were used for normalization. Cell vitality of uninfected but IFN-stimulated cells was >80 % compared to untreated cells. Error bars represent ±SD of triplicate values.

4.1.8 STAT1/2 activation and induction was decreased in the tumorigenic HaCaT cells

In the previous experiment it was shown, that IFN type I production and secretion following NDV infection was not impaired in the tumorigenic HaCaT cells. Following secretion, IFNα and β bind to IFN-specific receptors on the cell surface of infected and neighboring cells. Binding induces activation of the JAK-STAT signaling pathway. In that context, STAT1 and 2 are activated by specific phosporylations. Activation induces heterodimer formation and nucleus translocation in conjunction with IRF9, termed as ISGF3 complex.

The accessory NDV protein V is an important virulence factor as it is known to antagonize the interferon type I mediated antiviral defence by inactivating and degrading STAT1 in the natural host the bird [43]. This mechanism is host restricted and human STAT1 is resistant to V-protein mediated blockage.

However, in several human melanomas and squamous-cell carcinomas STAT1 has been found to be down-regulated [144, 145]. This lack of expression is hypothesized to promote cancer cell proliferation and survival. In normal cells interferon-induced STAT1 activity can cause growth arrest and apoptosis. It is suggested that this transcription factor functions as a tumor suppressor [146].

In the following time course infection experiment, activation and induction of STAT1 and 2 were analyzed as defects could be connected with NDV susceptibility. Therefore, HaCaT, RT3 and RT3 K1 cells were infected with NDV at an MOI of 1. Cellular protein extracts at various time points after infection were tested in a Western Blot analysis for STAT protein expression, activation and induction (Figure 4-13).

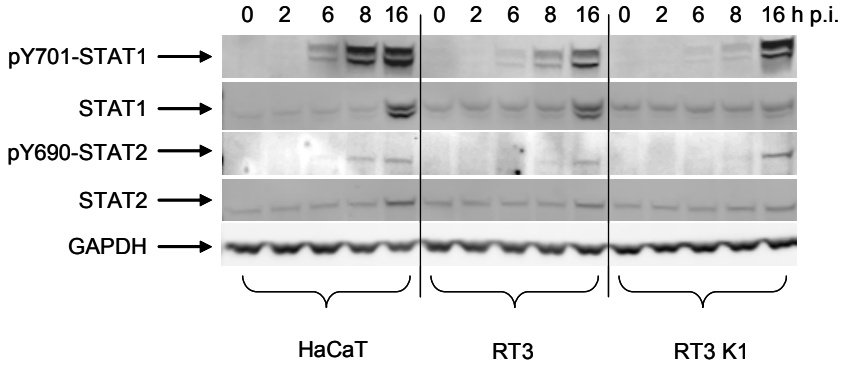

Figure 4-13: Impaired STAT1 and 2 activation and induction in the HaCaT-derived cell transformation model
HaCaT, RT3 and RT3 K1 cells were infected with NDV (MOI 1). At the indicated time points, cells were harvested and lysed for protein extraction. Equal amounts of protein samples were subjected to SDS page and subsequent Western Blot analysis of STAT1 and 2 activation and induction using phospho-specific antibodies for STAT1 and STAT2 activation and monoclonal anti-mouse antibodies for STAT1 and 2 expression. GAPDH expression served as an endogenous control.

Six hours after infection STAT1α /β activation by phosphorylation of tyrosine 701 could be detected in all three cell lines but to a higher extend in HaCaT cells. Activation increased afterwards. In RT3 cells, activation was not as strong and in RT3 K1 cells and delayed compared to HaCaT. Following activation, STAT1 induction was traceable at 16 h p.i. in HaCaT and RT3 cells. Although, induction of STAT1 was reduced in RT3 cells compared to HaCaT cells. In contrast, there was no STAT1 induction in RT3 K1 cells detectable. The same activation and induction pattern could be observed for STAT2. In HaCaT cells detection of STAT2 activation started at 8 h p.i. and induction at 16 h p.i. For RT3 cells signaling was decreased as it was seen for STAT1 before. In RT3 K1 cells NDV infection led to a delayed but strong STAT2 activation and no induction. STAT1 and 2 expression and activation could be observed in HaCaT cells as well as tumorigenic HaCaT cells. However, STAT activation and induction in the tumorigenic HaCaT cells was impaired. It could negatively affect antiviral gene induction which was investigated in the following experiment.

4.1.9 Tumorigenic HaCaT cells showed defects in antiviral gene induction

PKR, OAS1 and MxA are proteins which exhibit direct antiviral activity against RNA viruses. They are induced following NDV infection and activation of the IFN-signaling pathway. Reduced basal expression and induction of any of these proteins have been correlated with increased NDV susceptibility of tumor cells [91, 92]. In the previous experiment it could be shown that the tumorigenic HaCaT cell lines exhibited impaired STAT activation and/ or induction. Reduced activation of these antiviral genes following NDV infection could be a consequence of it. Therefore, not only basal expressions but also inductions of these three genes after infection with high MOIs of NDV were measured. Basal mRNA expression levels of the monitored genes did not severely differ between the three cell lines. Furthermore, following NDV infection, induction of all genes as early as 6 h p.i. could be detected (Figure 4-14). However, mRNA induction levels of *OAS1* and *MxA* were found to be reduced compared to HaCaT cells.

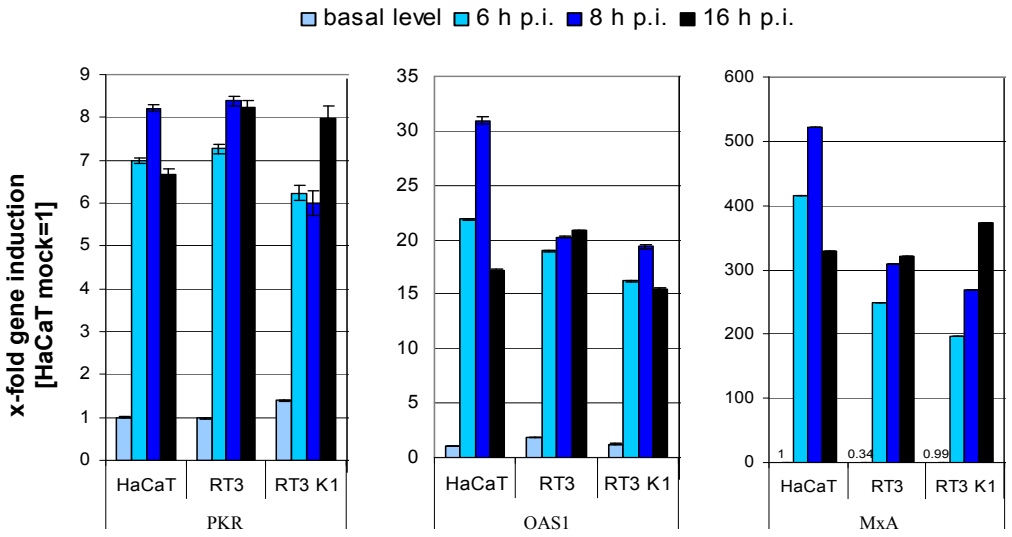

Figure 4-14: Detection of antiviral gene induction in infected HaCaT cellsas well as in RT3 and RT3 K1 cells
HaCaT, RT3 and RT3 K1 cells were infected with NDV (MOI 1). At the indicated time points cells were harvested for cDNA synthesis. *PKR*, *OAS1* and *MxA* transcription was measured by Taqman realtime PCR. Basal level of *PKR, OAS1* and *MxA* expression in HaCaT cells was used for normalization. Error bars represent ±SD of triplicate values.

These observations were confirmed when protein expression levels of both were compared. OAS1 induction was found to be slightly reduced whereas MxA protein expression was clearly reduced and delayed in the tumorigenic cell lines compared to HaCaT cells. The differences were more severe in RT3 K1 cells (Figure 4-15).

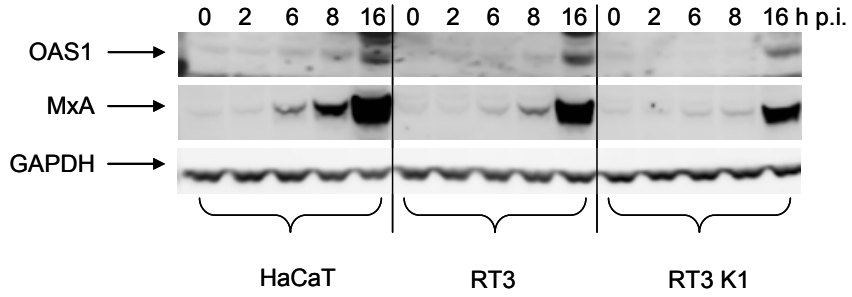

Figure 4-15: Slightly decreased OAS1 and strong impaired MxA induction in RT3 and RT3 K1 cells following infection
HaCaT, RT3 and RT3 K1 cells were infected with NDV at an MOI of 1. At the indicated time points, cells were harvested and lysed for protein extraction. Equal amounts of protein samples were subjected to SDS page and subsequent Western Blot analysis of NDV protein expression using an MxA-specific polyclonal anti-rabbit antibody and an OAS1-specific polyclonal anti-goat antibody. GAPDH expression served as an endogenous control.

In general, despite defects in STAT1/2 activation and induction in RT3 and RT3 K1 cells following NDV infection, induction of the direct antiviral factors PKR, OAS1 and MxA was still present in the tumorigenic cell lines. However, it was most obvious for MxA that the induction was tumor cell-specifically decreased. RT3 K1 cells displayed even stronger defects than RT3 cells.

4.1.10 PKR activity was not inhibited in Ras-transformed HaCaT cells

Activation of PKR is mediated by autophosphorylation following detection of (viral) dsRNA intermediates. It results in the phosphorylation of the translation initiation factor eIF-2α subunit. Consequently, a translation of most viral and cellular mRNAs is blocked.
Oncogenic Ras is known to produce an inhibitor of PKR which can render Ras-transformed cells permissive for viral infection [93, 147].
In the following time course infection experiment, activation and induction of PKR was investigated. RT3 and RT3 K1 cells were initially Ras-transformed and could therefore feature an impaired PKR activation following NDV infection promoting NDV permissiveness (Figure 4-16). A strong and comparable PKR activation as a consequence of NDV infection/ replication could be shown in all three cell lines at 16 h p.i.. Basal PKR phosphorylation could already be detected in mock infected tumorigenic HaCaT cells. Along with PKR mRNA induction shown in the previous experiment for all three cell lines, induction of PKR production could also clearly be detected on protein level in HaCaT and Ras-transformed RT3 cells at 16 h p.i. but not in RT3 K1 cells as it was shown for STAT1 and 2 before.

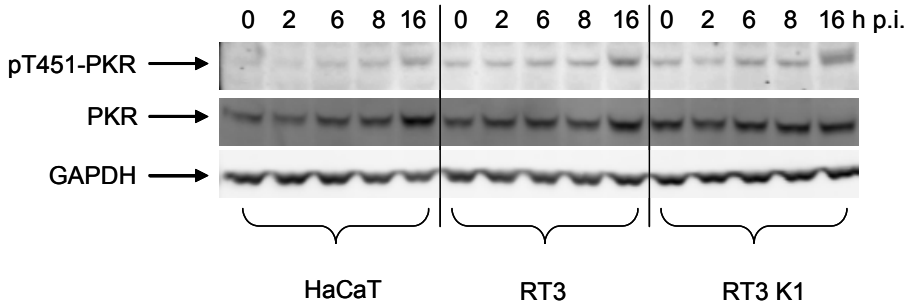

Figure 4-16: PKR activation following NDV infection was detected in all three cell lines
HaCaT, RT3 and RT3 K1 cells were infected with NDV (MOI 1). At the indicated time points, cells were harvested and lysed for protein extraction. Equal amounts of protein samples were subjected to SDS page and subsequent Western Blot analysis of NDV protein expression using a phospo-specific anti-rabbit antibody for PKR activation and a polyclonal anti-rabbit antibody for PKR expression. GAPDH expression served as an endogenous control.

4.1.11 Impaired antiviral IFITM1 induction in infected tumorigenic HaCaT cells

Beside the major intracellular mediators of antiviral defence like MxA, PKR and OAS1, there are several IFN-inducible proteins with currently unexplored antiviral features. IFITM1 is a cellular transmembrane protein known to be activated following IFN type I and II stimulation of cells. For the oncolytic RNA virus VSV it could be shown that IFITM1 exhibits partially inhibitory activity although the mode of action was not clear [86].

In the following time course infection experiment, IFITM1 transcription and protein expression was monitored in order to detect differences in the activation pattern which could contribute to the NDV susceptibility in the tumorigenic HacaT cells (Figure 4-17 A). In addition to a slightly increased basal expression of IFITM1 in HaCaT cells, a strong induction following NDV infection could only be observed in HaCaT cells. IFITM1 induction was tumor specifically decreased at any of the measured time points after infection.

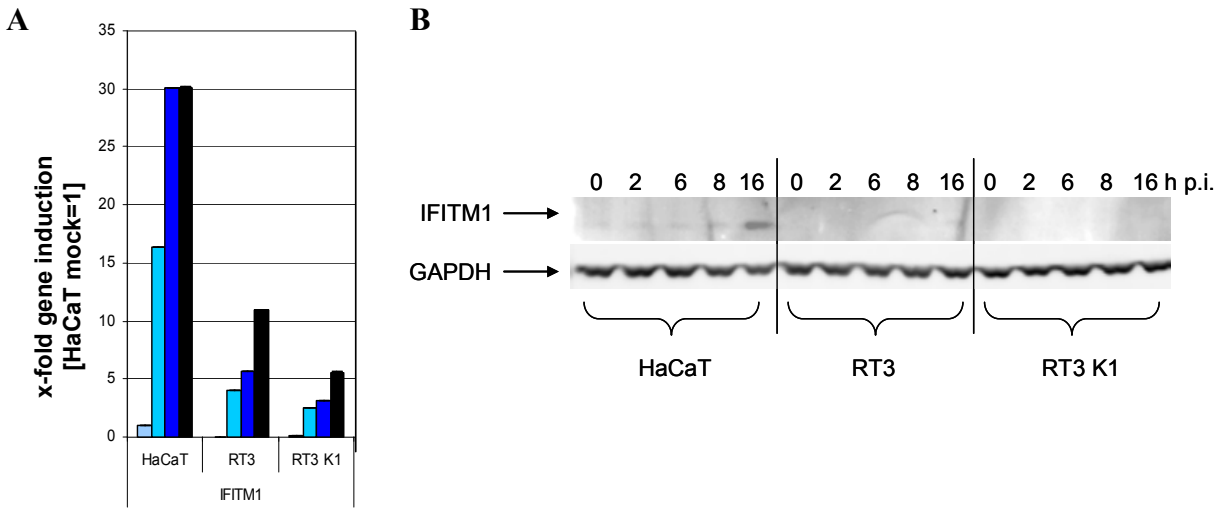

Figure 4-17: IFITM1 induction was tumor cell-specifically decreased
HaCaT, RT3 and RT3 K1 cells were infected with NDV at an MOI of 1. At the indicated time points cells were harvested for:
(A) cDNA synthesis. IFITM1 transcription was measured by Taqman realtime PCR. Basal level of IFITM1 expression in HaCaT cells was used for normalization. Error bars represent ±SD of triplicate values.
(B) protein extraction. Equal amounts of protein samples were subjected to SDS page and subsequent Western Blot analysis of NDV protein expression using a polyclonal anti-goat antibody for IFITM1 detection. GAPDH expression served as an endogenous control.

Results were confirmed on protein level (Figure 4-17 B). In HaCaT cells, IFITM1 protein expression could be detected at 16 h p.i. when cells were infected with NDV at an MOI of 1 in a time course infection experiment. In contrast, no IFITM1 protein expression in RT3 and RT3 K1 cells was shown up to the last measurement at 16 h p.i..
In summary, tumorigenic HaCaT cells lacked the ability for IFN-induced IFITM1 induction following NDV infection.

4.1.12 SiRNA-induced IFITM1 knockdown did not increase NDV susceptibility in HaCaT cells

IFITM1 antiviral activity has not been extensively investigated and induction was severely impaired as shown in Figure 4-17. Therefore, it was of interest if IFITM1 activity features NDV-repressing activity or whether it is dispensable. An IFITM1 siRNA knockdown experiment was performed in non-susceptible HaCaT cells in order to investigate if IFITM1 knockdown could render non-transformed HaCaT cells (at least partially) NDV susceptible.
Fourty eight hours after transfection with four single siRNAs, cells were infected with NDV-luciferase at an MOI of 0.01 or mock infected for 24 h. Subsequently, cells were harvested and the IFITM1 knockdown on protein level was confirmed by Western Blot analysis (Figure 4-18). Efficient IFITM1 knockdown was indicated by a severely decreased or total loss of IFITM1 induction following NDV infection. In HaCaT cells, the specific siRNAs 1, 2 and 3

led to a strong reduction of IFITM1 induction whilst siRNA knockdown mediated by siRNA 4 was not as potent.

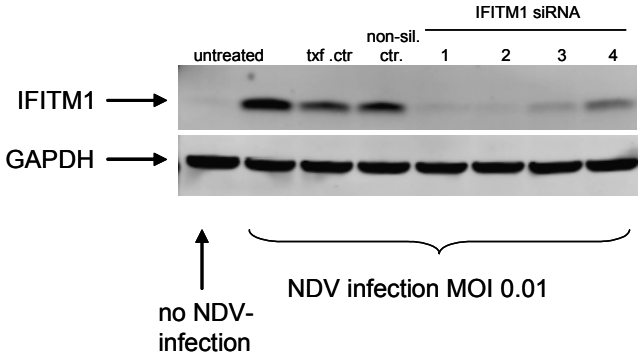

Figure 4-18: Transfection with IFITM1 specific siRNAs mediated reduced IFITM1 induction following NDV infection in HaCaT
HaCaT cells were reverse transfected using four specific siRNAs (siRNA 1-4). A non-silencing siRNA pool (non-sil. ctr) as well as untreated cells and a transfection reagent only control (txf.ctr.) were used as negative controls. Fourty-eight hours post transfection cells were infected with NDV-luciferase (MOI 0.01). Cell were harvested at 24 h p.i. and equal amounts of protein samples were used for SDS-Page and subsequent Western Blot analysis for detection of IFITM1 protein expression using an IFITM1-specific polyclonal anti-goat antibody.

In parallel, the same siRNA transfection and infection procedure was performed to determine viral luciferase activity as an indicator for NDV replication in these cells.

As it is shown in Figure 4-19, viral luciferase activity was very low (which resulted in high SD). Viral transgene expression was neither significantly increased nor decreased in cells transfected with the highly potent siRNAs 1 and 3 compared to the non-silencing control or the not as potent siRNA 4. In contrast, knockdown with siRNA 2 led to a drastic reduction of viral luciferase activity compared to the controls.

IFITM1 knockdown in HaCaT cells did therefore not increase NDV susceptibility compared to the non-silencing control indicated by similar viral transgene expressions.

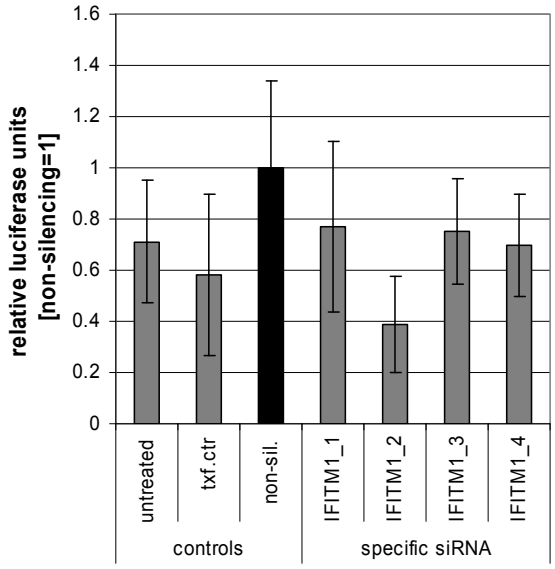

Figure 4-19: IFITM1 knockdown in HaCaT did not render cells susceptible to NDV
HaCaT cells were reverse transfected using four specific siRNAs (siRNA 1-4). A non-silencing siRNA pool (non-sil. ctr.) as well as untreated cells and a transfection reagent only control (txf.ctr.) were used as negative controls. Cells were infected with NDV-luciferase (MOI 0.01) at 48 h post transfection and viral luciferase activitiy was measured 24 h p.i.. Results are presented as relative viral luciferase activity normalized to the non-silencing siRNA control. Error bars represent ±SD of sextuple values.

4.1.13 Ras activity was required for oncolytic NDV susceptibility in RT3 K1 cells

Previous experiments have shown that the Ras-transformed cell lines RT3 and RT3 K1 are characterized by partial defects in antiviral gene induction which could contribute to their NDV susceptibility.

As it was demonstrated for PKR (with respect to reovirus infection) and for MxA in connection with VSV replication, oncogenic Ras transformation is supposed to mediate sensitivity to oncolytic virus replication by negatively influencing antiviral activity [93, 96, 148].

In the following experiment, the question should be answered, whether Ras activity also contributed to the NDV susceptibility of RT3 K1 cells.

RT3 K1 cells were transfected with H-Ras-specific siRNAs and knockdown efficacy was determined 48 h post transfection by Western Blot analysis. In Figure 4-20, the H-Ras knockdown is depicted. All specific siRNAs induced a strong H-Ras knockdown in RT3 K1 cells compared to the controls.

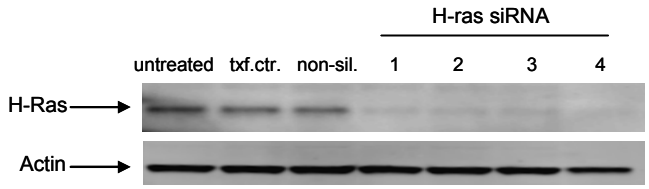

Figure 4-20: Specific siRNAs mediated knockdown of H-Ras in RT3 K1 cells
RT3 K1 cells were reverse transfected using four single H-Ras-specific siRNAs (siRNA 1-4). A non-silencing siRNA pool (non-sil.ctr) as well as untreated cells and a transfection reagent only control (txf.ctr.) were used as negative controls for H-Ras knockdown. Fourty-eight hours post transfection, cells were harvested and lysed for protein extraction. Subsequently, equal amounts of protein samples were subjected to SDS-Page and Western Blot analysis. SiRNA-mediated H-Ras knockdown was detected by using an H-Ras specific polyclonal anti-rabbit antibody. Actin expression served as an endogenous control.

Simultaneously, transfected cells were infected with NDV-luciferase or NDV-EGFP to evaluate NDV replication by means of viral transgene expression 24h p.i.. As shown in Figure 4-21 A and B, H-Ras knockdown led to a dramatic decrease in viral transgene expressions at 24 h p.i.. It was mediated by all specific siRNAs compared to the non-silencing controls.

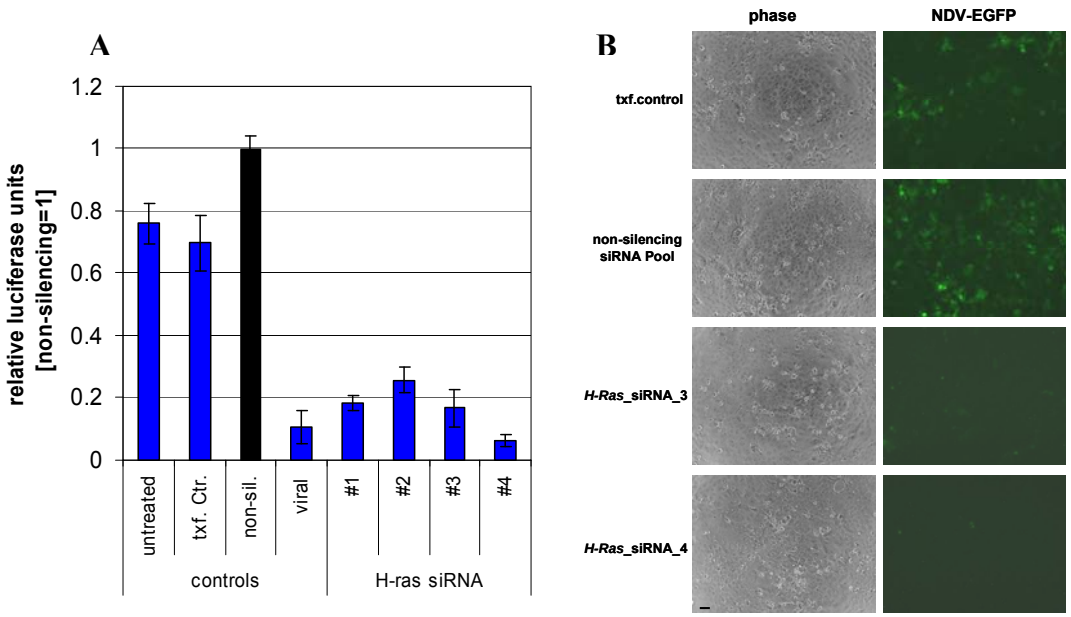

Figure 4-21: Viral transgene activity or expression was reduced following siRNA-mediated H-Ras knockdown in RT3 K1 cells
RT3 K1 cells were reverse transfected using four single H-Ras-specific siRNAs (siRNA 1-4). A non-silencing siRNA pool (non-sil.) as well as untreated cells and a transfection reagent only control (txf.ctr.) were used as negative controls for H-Ras knockdown. Fourty-eight hours post transfection, cells were infected with NDV-luciferase or NDV-EGFP at an MOI of 0.01. Viral luciferase activitiy was measured at 24 h p.i..
(A)Results are presented as relative viral luciferase activity normalized to the non-silencing siRNA control. Error bars represent ±SD of sextuples.
(B)Viral EGFP expression was measured by fluorescence microscopy and representive fluorescence pictures are shown (scale bar= 100 µm).

In summary, it could be clearly demonstrated that Ras activity contributed to the NDV susceptibility of RT3 K1 cells as siRNA-mediated knockdown of Ras led to a severe reduction of viral replication indicated by decreased viral transgene activity or expression.

4.1.14 Subclones of Ras-transformed HaCaT cells showed oncogenic Ras activity but opposing NDV susceptibilities

The following experiments were performed in order to investigate whether Ras transformation of HaCaT cells directly mediate NDV susceptibility. As it was shown in the beginning, the malignant Ras clone II4 is non-susceptible to NDV. In contrast Ras-transformed RT3 and RT3 K1 cells are permissive for NDV infection and replication. The II4 and RT3 cell lines were originally isolated following *in vivo* tumor growth or repeated *in vivo* passaging, respectively. It could not be ruled out that the different phenotypes with respect to NDV susceptibility were gained as a consequence of selective pressure during *in vivo* growth. Therefore, the initial Ras transformation experiment performed by Boukamp and colleagues in 1990 was repeated [120]. HaCaT cells were H-RasV12 transduced. Subsequently, cells were subcloned by limiting dilution to identify clones with H-Ras levels comparable to those in the highly NDV susceptible RT3 K1 cells and the non-susceptible II4 cells. Three HaCaT-Ras subclones (C5, H5 and H6) with H-Ras expression levels nearly as high as in RT3 K1 and II4 cells could be isolated (Figure 4-22).

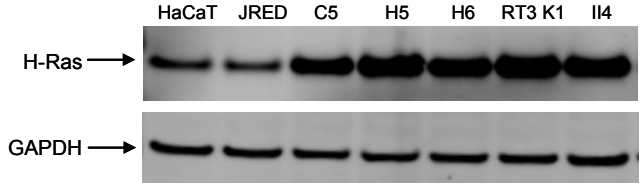

Figure 4-22: HaCaT-Ras clones with high H-Ras expression levels
Cells were harvested and lysed for protein extraction. Equal amounts of protein samples were subjected to SDS page and subsequent Western Blot analysis of H-Ras protein expression in HaCaT, HaCaT-JRED transduction control, HaCaT H-Ras clones C5, H5 and H6, RT3 K1 and II4 cells using a polyclonal anti-rabbit antibody. GAPDH expression served as an endogenous control.

In order to prove oncogenic Ras activity in these HaCaT-Ras clones a colony formation assay in soft agar was chosen as it is known that oncogenic Ras mediates anchorage-independent growth of transformed cells [142]. Four weeks after seeding in soft agar, HaCaT cells and the transduction control cells expressing the fluorescence protein JRED did not show any colony formation. RT3 K1 cells were characterized by growth of big colonies. In contrast to the HaCaT-Ras clone C5, which did not show anchorage-independent growth, the HaCaT-Ras clones H5 and H6 featured colony formation. However, colonies were smaller than RT3 K1 colonies (Figure 4-23).

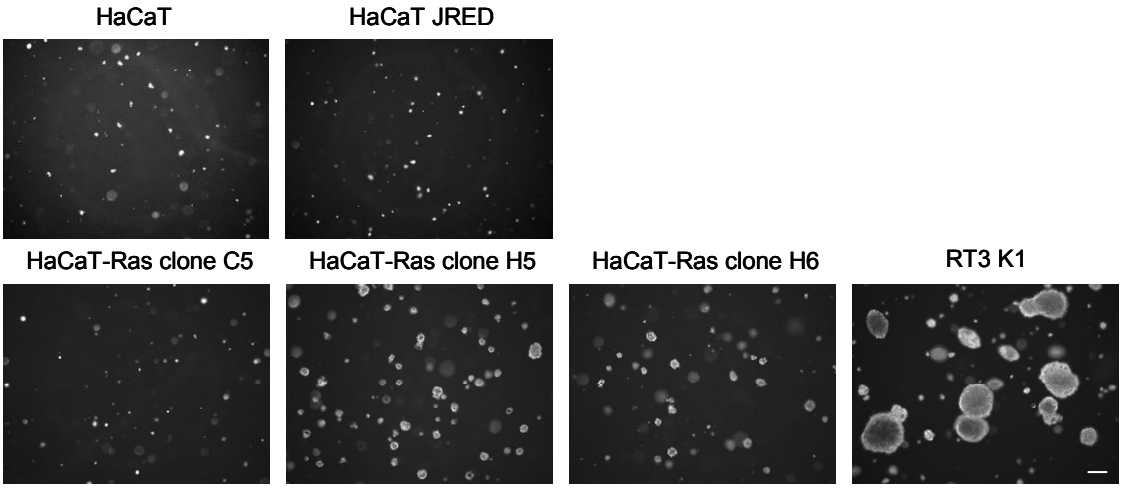

Figure 4-23: Differences in the ability of anchorage-independent growth of HaCaT-Ras clones
HaCaT-Ras clones C5, H5 and H6 were seeded in soft agar and incubated for 4 weeks before pictures of colony formation were taken. Non-tumorigenic HaCaT cells and the HaCaT transduction control (HaCaT JRED) were used as negative controls for colony growth and RT3 K1 cells as a positive control (scale bar= 500 µm).

Generally, transfection of HaCaT cells with the H-Ras oncogene and subsequent subcloning led to the isolation of HaCaT-Ras subclones with similar degrees of H-Ras expression compared to RT3 K1 and II4 cells. Oncogenic Ras activity was confirmed by anchorage-independent growth.

In the following infection experiment it was tested, whether Ras transformation of non-susceptible HaCaT cells directly mediated NDV susceptibility. Therefore, the isolated HaCaT-Ras subclones with varying Ras activities such as clone C5 (which did not show oncogenic Ras induced anchorage-independent growth and was used as a negative control in the next experiment) and clones H5 and H6 (Ras activity was demonstrated by anchorage-independent growth) were infected with NDV-luciferase at an MOI of 0.01. Twenty-four hours after infection, viral luciferase activity was measured to determine NDV replication. As shown in Figure 4-24, HaCaT-Ras clones C5 and H6 were not characterized by enhanced NDV replication compared to the non-susceptible HaCaT cells and the HaCaT-JRED transduction control. In contrast to that, NDV replication in the HaCaT-Ras clone H5 was stronger than in the highly susceptible RT3 K1 cells.

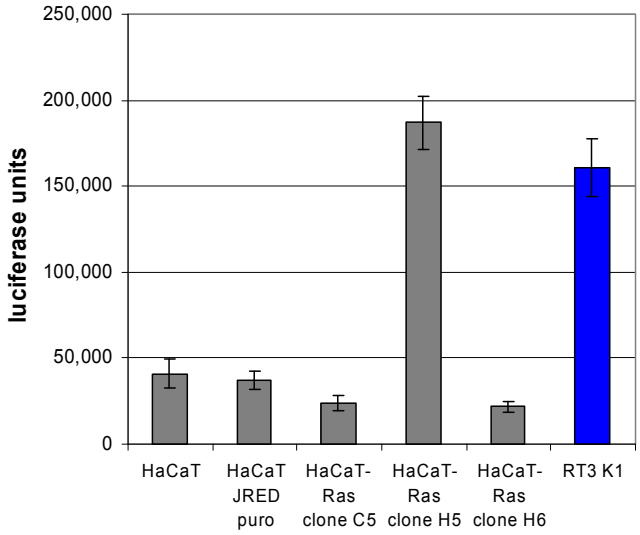

Figure 4-24: HaCaT-Ras subclones showed different NDV-susceptibilities
HaCaT and HaCaT-JRED transduction control (negative controls for NDV susceptibility and oncolysis), HaCaT-Ras subclones C5, H5 and H6 and RT3 K1 cells (positive control for NDV susceptibility and oncolysis) were infected with luciferase-expressing NDV (MOI 0.01) or mock infected.
Viral luciferase activity was measured 24 h p.i.. Error bars represent ±SD of sextuple values.

In summary, overexpression of activated H-Ras in HaCaT cells led to the isolation of HaCaT-Ras subclones with proven Ras activity (clone H5 and H6). However, these subclonal cells did not show a unique phenotype with respect to NDV susceptibility. It indicated that there are cellular factors beside Ras, which support susceptibility.

4.2 SiRNA-based screening for NDV-sensitizing genes and candidate validation

4.2.1 SiRNA based screening strategy

So far, tumor selective replication of NDV is known to depend on tumor cell-specific defects in the IFN-mediated antiviral defense of RNA viruses such as NDV. The aim of the siRNA-based screening was to identify genes which are not directly related to the innate immune response but essential for NDV replication and simultaneously connected with tumorigenesis of cells. These NDV-sensitizing genes could be potential new therapeutic targets for cancer treatment as well as biomarkers for virotherapy. For this siRNA-based screening approach, the RT3 K1 cells were most appropriate as they are strongly susceptible to NDV infection and replication. Furthermore, the non-tumorigenic and non-susceptible parental cell line HaCaT could be used for further analysis of confirmed virus-sensitizing hits.

In the first part of the thesis it was shown, that in non-transformed HaCaT cells NDV replication and spread was inhibited so that there was almost no virus-mediated luciferase activity measurable 24 h post infection with a luciferase expressing NDV. In contrast, tumorigenic RT3 K1 cells were characterized by efficient NDV replication leading to increased virus-mediated measurable luciferase activity in these cells (Figure 4-25).

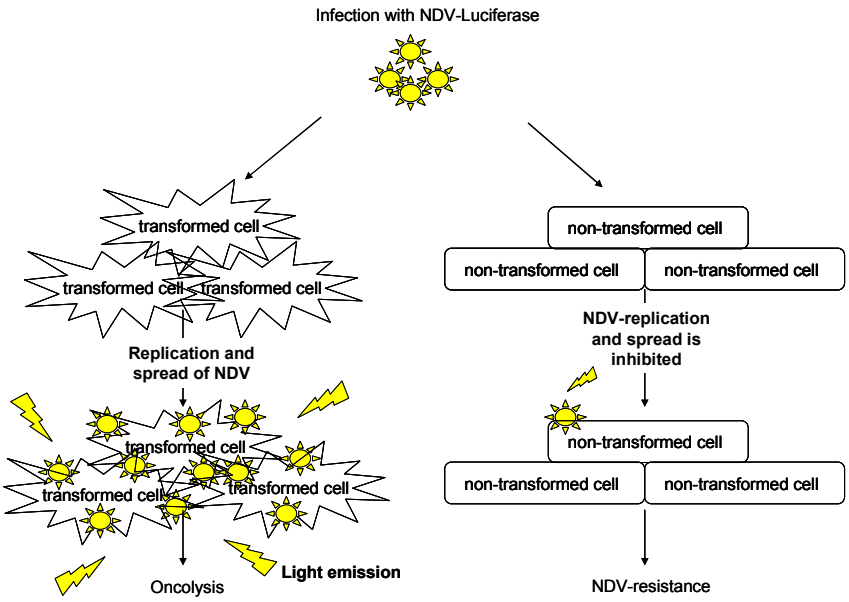

Figure 4-25: Schematic depiction of viral replication in tumor cells or non-transformed cells indicated by viral luciferase activity

The screen was based on the principle that whenever an endogenous gene, that is involved in the NDV replication is knocked down via its corresponding siRNAs, this could be detected by a reduced viral luciferase signal. In contrast to that, genes that inhibit viral replication could be identified by enhanced signals following knockdown (Figure 4-26).

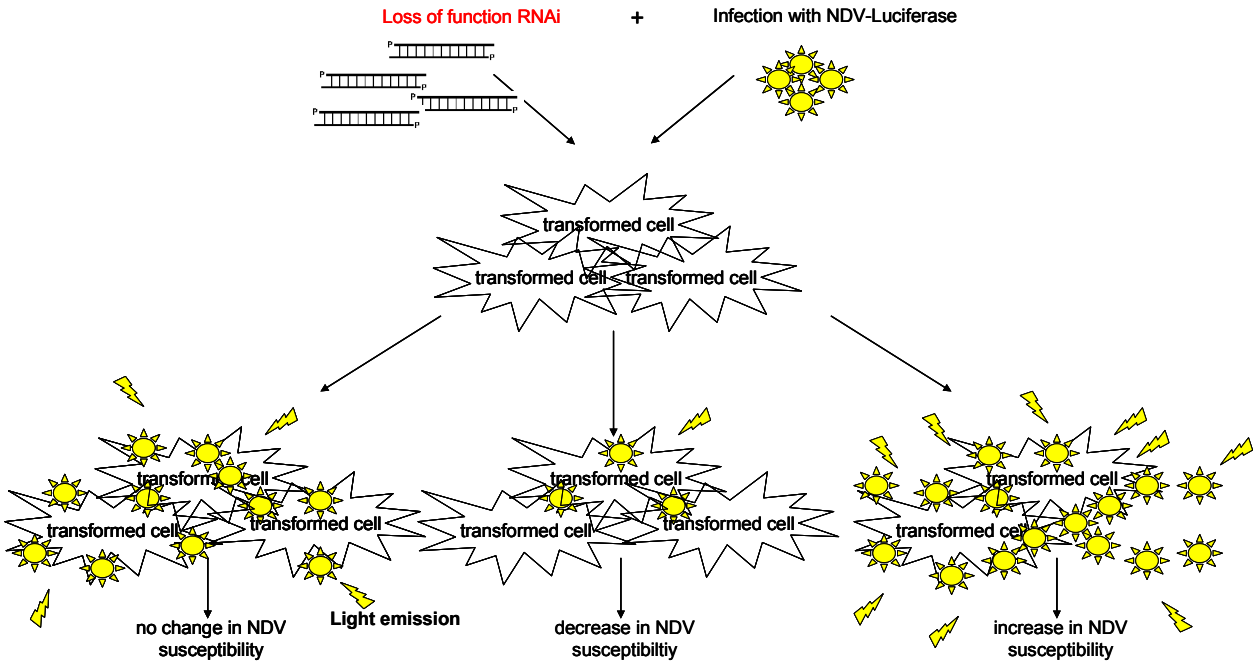

Figure 4-26: Schematic depiction of viral replication and luciferase expression and activity (light emission) in tumor cells transfected with specific siRNAs targeting endogenous genes which are essential or non-essential for the oncolytic NDV life cycle.

In general, genome-wide human siRNA libraries as well as focused siRNA libraries comprising specific gene families or genes which participate in specific cellular functions are commercially available. Genome-wide libraries can only be screened in an automated approach as they comprise of approximately 18,000 genes (e.g. Dharmacon's siGENOME library). Focussed siRNA libraries are smaller so that they can either be applied in an automated or non-automated screen.

As a non-automated screening approach was planned, two small reverse transfection (RTF) siRNA libraries in a 96-well format were chosen. Specific siRNA-SMARTpools (four pooled individual siRNAs per target gene transcript) are pre-aliquoted and lyophilised in 96-well plates for single use. In order to repeat the screening, four 96-well plates with the same configuration are delivered. The screening plates can be equipped with custom-made controls (e.g. internal positive controls) as well as standard siRNA controls (negative controls). To start the screening, lyophilized siRNAs have to be resuspended in presence of the transfection

reagent before cells are added (reverse transfection) and incubated for at least 24 hours. Subsequently, transfected cells can be further treated before the readout is performed.

The first library chosen comprised of 112 siRNAs targeting proteins known or predicted to participate in membrane trafficking/remodelling e.g. important for endocytosis, vesicular trafficking or protein degradation. This membrane trafficking library was chosen, as the viral life cycle of NDV is not completely investigated so far. There are no hints concerning (tumor cell-specific, deregulated) cellular factors or functions which are hijacked for viral RNA/ protein trafficking within the infected cells. Furthermore, a tyrosine kinase library was chosen comprising of 76 specific siRNAs. Tyrosine kinases are important enzymes that catalyze the phosporylation of tyrosine residues of various targets involved in cell cycle, migration, metabolism, proliferation, differentiation and survival [149]. Tyrosine kinases which can be devided into transmembrane receptor- and cytoplasmatic non-receptor tyrosine kinases are often aberrantly expressed or deregulated in transformed cells [150].

4.2.2 Assay development for the screening of RT3 K1 cells with Dharmacon's RTF human library

To establish a screening assay based on Dharmacon's RTF siRNA libraries to screen for NDV-sensitizing cellular factors in RT3 K1 cells optimal transfection parameters had to be determined first. The optimal transfection reagent and volume as well as the adaption of cell number for reverse transfection in a 96-well format was tested using Dharmacon's siARRAY RTF Optimization Kit (Figure 4-27).

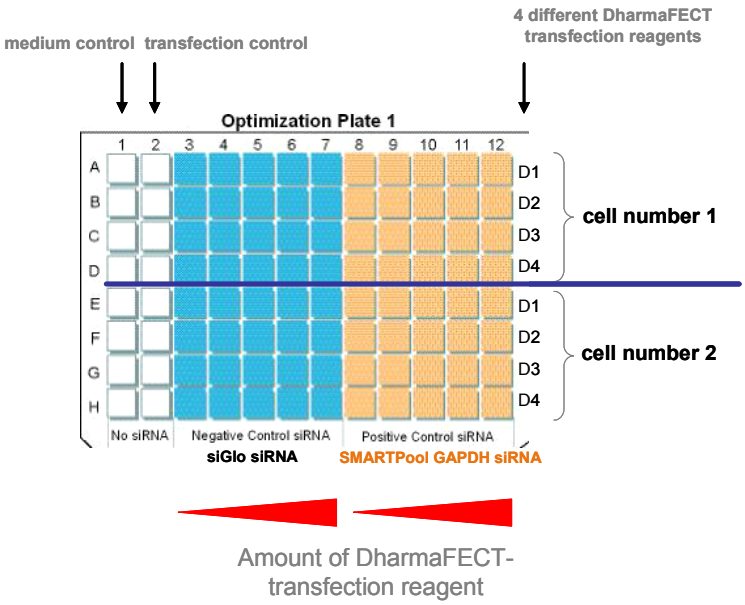

Figure 4-27: Depiction of Dharmacon's siARRAY RTF Optimization Kit 1

It allows to visually check for transfection efficacy by transfecting a fluorescently labeled siRNA which is not incorporated into the RISC complex (RISC-free siGLO siRNA with Cy-3-labeling) and to quantify knockdown efficacy by Taqman realtime PCR using GAPDH-SMARTpool siRNAs as a positive control.

As a first step, detection of cytotoxicity following transfection of four different transfection reagents DharmaFECT 1, 2, 3 and 4 at various concentrations were tested. Usually, confluent cells are used for NDV infection experiments. As many cellular target protein levels show an optimal knockdown at 48 h post transfection or later, cells had to be nearly 100 % confluent to start infection experiment at this time point. Therefore, different cell numbers ($1x10^4$ or $2x10^4$ cells/ 96-well) were reverse transfected with siGLO RISC-free siRNA in the optimization plate and incubated. The day after transfection, transfection medium was exchanged with normal growth medium and cells were further incubated. Fourty-eight hours post transfection cell viability was tested. The mock transfection samples served as controls (Figure 4-28).

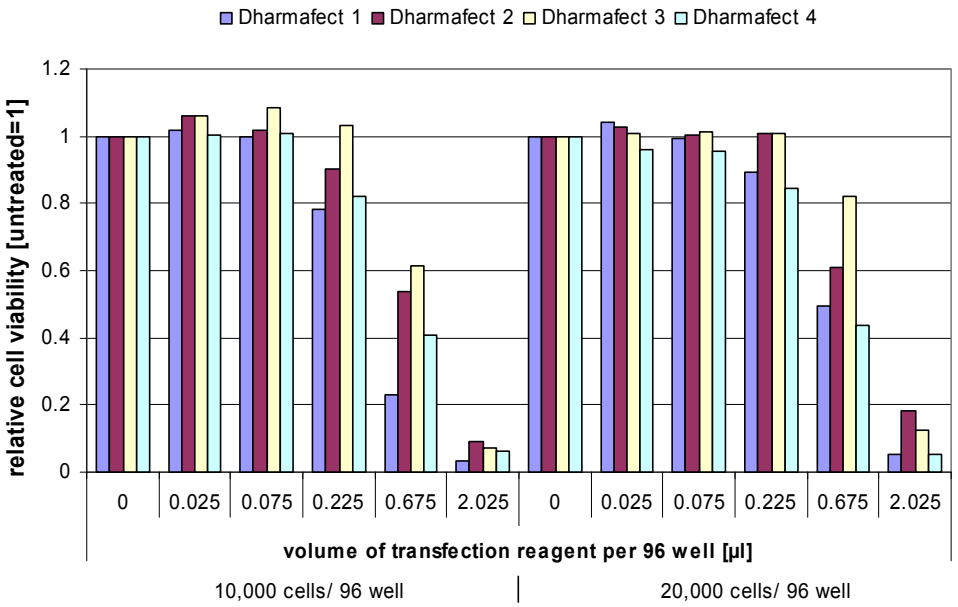

Figure 4-28: Induction of cytotoxicity following reverse tranfection of different RT3 K1 cell numbers with increasing volumes of DharmaFECT transfection reagents
$1x10^4$ or $2x10^4$ RT3 K1 cells were reverse transfected with different volumes of DharmaFECT 1-4 and 50 nM of siGlo risc free siRNA per 96-well. Mock transfected cells were used as negative controls and for normalization of cell viability. Fourty-eight hours post transfection, cell viability was measured using the CellTiter-Glo luminescent lell viability assay.

All DharmaFECT reagents tested showed a loss of cell viability with increasing amounts of transfection reagent, although cytotoxic effects strongly depended on cell number. DharmaFECT transfection reagents 1 and 4 showed a decrease in cell viability even at low transfection volumes (0.225 µl). Transfection with DharmaFECT 2 was severely cytotoxic at

0.675 µl of transfection reagent but DharmaFECT 3 excelled by low cytotoxic effects with increasing transfection volumes up to 0.675µl/ 96-well) of $2x10^4$ cells. Furthermore, when reverse transfection was performed using $2x10^4$ cells per 96 well, cells were almost complete confluent at 48 h post transfection when no cytotoxicity occurred.

Besides testing cytotoxic effects following transfection of siGLO siRNA with different transfection reagents, qualitative determination of siRNA delivery was performed.

When comparing the Cy-3 fluorescence intensities 24 h and 48 h post transfection of RT3 K1 cells with siGLO siRNA and a non-toxic volume of all tested DharmaFECT reagents, differences in fluorescence intensities and number of transfected cells were observed.

Transfection by DharmaFECT 3 and 4 led to a higher percentage of transfected cells and to a stronger fluorescence signal compared to DharmaFECT 1 and 2 (Figure 4-29).

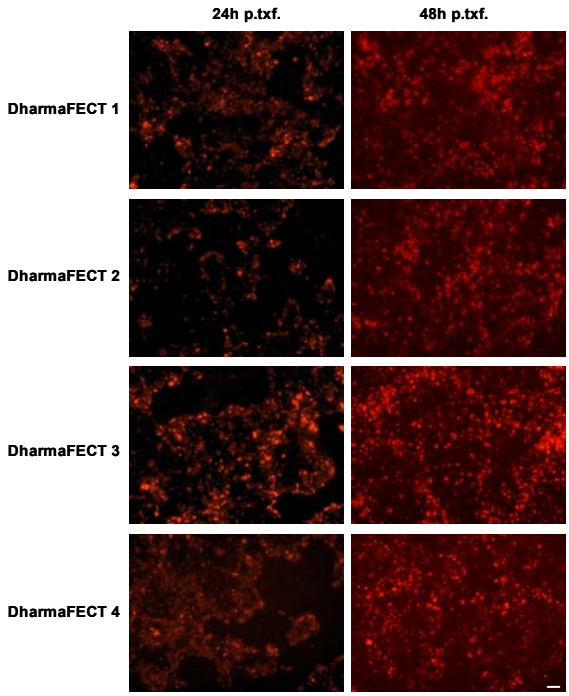

Figure 4-29: Transfection with different DharmaFECT reagents resulted in varying siRNA delivery efficacies
$2x10^4$ RT3 K1 cells were reverse transfected with 0.3 µl of DharmaFECT 1, 2, 3 or 4 and 50 nM of siGLO RISC-free siRNA per 96-well. Twenty-four and 48 h post transfection, cell viability was determined by detection of Cy-3 fluorescence using a fluorescence microscope (scale bar= 100 µm).

Dharmafect 3 was non-toxic up to a volume of approximately 0.7µl/ 96-well and qualitative determination of siRNA delivery showed a high transfection efficacy even at low volumes. Therefore, DharmaFECT 3 was chosen for quantitative determination of transfection efficacy using GAPDH siRNA as a positive knockdown control in RT3 K1 cells. $2x10^4$ cells were transfected with 50 nM GAPDH SMARTPool siRNA and increasing volumes of transfection

reagent. Cell viability and knockdown efficacies on RNA level using Taqman realtime PCR were determined 48 h post transfection (Figure 4-30).

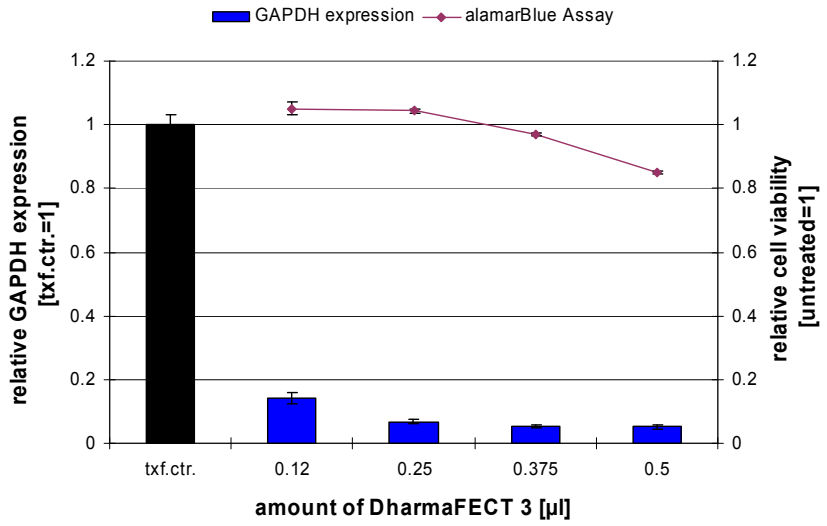

Figure 4-30: Knockdown efficacies elevated with increasing DharmaFECT 3 volumes
$2x10^4$ RT3 K1 cells were reverse transfected (in sextuple) using DharmaFECT 3 and 50 nM of GAPDH siRNA per 96-well. Untreated cells and a transfection reagent only control for each volume (txf.ctr.) were used as negative controls. Fourty-eight hours post transfection cells were harvested and used for cDNA synthesis. GAPDH expression of pooled triplicates was determined by Taqman realtime PCR using the transfection controls for normalization. In parallel a cell viability assay was performed by measuring triplicates using the alamarBlue assay. Metabolic activity of untreated cells was used for normalization. Error bars represent ±SD of triplicate values.

All volumes tested induced a GAPDH knockdown of more than 80 % at 48 h post transfection. With increasing volumes of DharmaFECT 3, GAPDH knockdowns were even more efficient. However, 0.375µl DharmaFECT 3 led to a knockdown greater than 90 % with no decrease in cell viability and was therefore chosen for the subsequent experiments. In Table 4-1 the optimal reverse transfection parameters are summarized.

Table 4-1: Summary of the optimal reverse transfection parameters for RT3 K1 cells

Reverse transfection parameter [96 well]	
Cell number per well	$2x10^4$ cells/ 100 µl growth medium
Final concentration of siRNA	50 nM
Transfection reagent and volume	0.375 µl DharmaFECT 3/ 25 µl DCCR (1.5 % DharmaFECT 3 in DCCR)

4.2.3 Design of a positive siRNA control targeting viral mRNAs

In order to evaluate the individual performance of a siRNA screen and to compare performances of repeated siRNA experiments, internal positive controls had to be designed and validated. In this particular screening setting, the positive control could either target endogenous cellular mRNA or viral RNA/ mRNA. The design of a siRNA targeting NDV specific genomic RNA/ mRNA was favored as it was expected to induce the maximal possible inhibition of viral replication. It is known for RNA viruses, that siRNA-mediated knockdowns of their viral genomes are generally unsuccessful as the genome is tightly protected by viral nucleocapsids. In contrast, targeting viral P- or L-mRNA seemed to be more effective as they are components of the RNA-dependent RNA polymerase complex, necessary for viral RNA synthesis and not protected by a capsid [151].

By using Dharmacon's siDesign Center which is an online software tool to design custom siRNAs, three individual siRNAs targeting the ORF of P- as well as RNA-edited V-mRNAs were designed and subsequently synthesized at Dharmacon.

Viral knockdown performances of the individual siRNAs were evaluated by measuring viral transgene activity following infection with NDV-luciferase and by detection of virus-induced oncolysis using a Crystal violet assay which stains intact remaining cells. In addition, cell culture supernatants of infected cells were collected and NDV titers of the individual samples were determined by plaque assay.

As it is shown in Figure 4-31 A, all viral P+V siRNAs tested severly reduced viral replication as indicated by decreased luciferase activity at 24 h p.i. compared to the controls. At this time point, neither cells transfected with controls nor with specific siRNA showed virus induced oncolysis. Fourty-eight hours p.i. cells transfected with a non-silencing siRNA or transfection reagent only were completely lysed as shown by Crystal violet assay (Figure 4-31 B). In contrast, all transfected viral siRNAs protected infected cells against virus induced cytolysis.

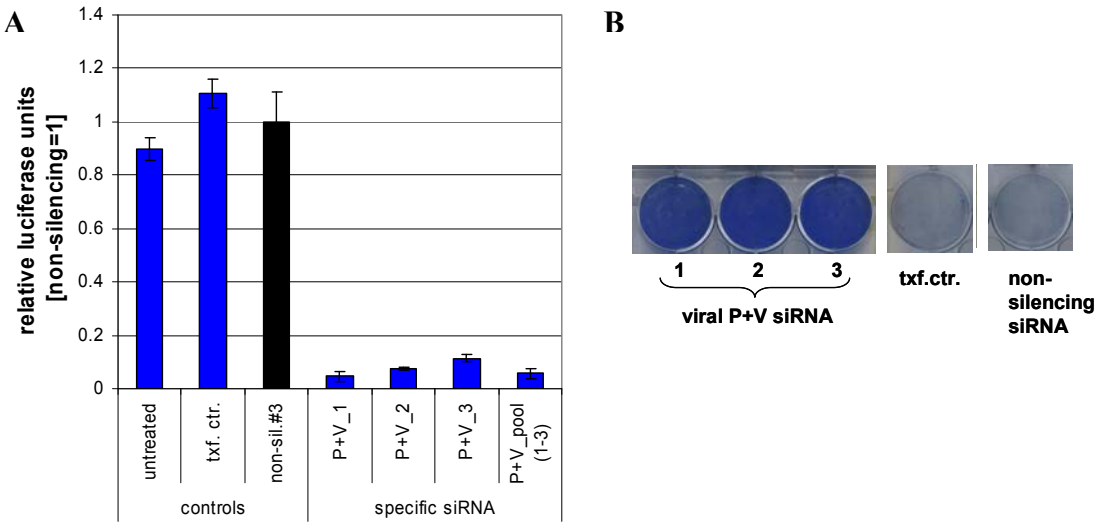

Figure 4-31: Viral replication and oncolysis was reduced following viral siRNA transfection
(A) RT3 K1 cells were reverse transfected using viral P+V siRNAs (siRNA 1-3). A non-silencing siRNA (non-sil. #3) as well as untreated cells and a transfection reagent only control (txf.ctr.) were used as negative controls. Fourty-eight hours post transfection, cells were infected with NDV-luciferase at an MOI of 0.01 and 24 h p.i. viral luciferase activitiy was measured. Results are presented as relative viral luciferase activity normalized to the non-silencing siRNA control. Error bars represent ±SD of sextuple values.
(B) RT3 K1 cells were transfected with viral siRNA (P+V siRNA 1-3). A non-silencing siRNA and a transfection reagent only control served as a positive control for NDV oncolysis. Twenty-four hours post transfection cells were infected with NDV at an MOI of 0.01 and 48 h p.i. viable cells were stained by a Crystal violett assay.

Results could be confirmed by measuring the NDV titer of cell culture supernatants 24 h p.i. by plaque assay. NDV titers of viral siRNA transfected and infected cells were reduced to ≥ 85 % compared to the non-silencing control (Figure 4-32).

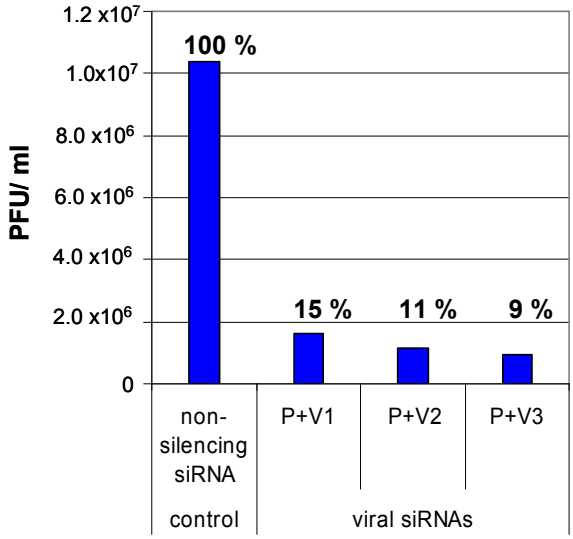

Figure 4-32: Reduced virus production/ release following viral siRNA transfection
RT3 K1 cells were transfected with viral siRNA (P+V siRNA 1-3). A non-silencing siRNA and a transfection reagent only control served as a positive control for NDV oncolysis. Twenty-four hours post transfection, cells were infected with NDV-EGFP (MOI 0.01) and 24 h p.i. cell culture supernatants were collected and NDV titers were measured by plaque assay.

Altogether, all viral siRNAs tested induced a strong viral knockdown and could be applied as internal positive controls in the siRNA-based screen.

4.2.4 Experimental procedure of the siRNA-based screen

Following determination of optimal transfection conditions as well as the design and validation of an internal positive control for the screening approach, the assay performance had to be defined.Transfection parameters were optimized to start NDV infection 48 h post transfection when cells have reached a confluent monolayer. Cells were then infected with NDV-luciferase as it allowed for highly sensitive quantification of viral replication. However, luciferase activity strongly depends on viable cells. Previous infection experiments of RT3 K1 cells at an MOI of 0.01 resulted in high viral luciferase signals but no oncolyis at 24 h p.i. (see Figure 4-7 and Figure 4-8). Proceeding replication in RT3 K1 cells was accompanied by cell destruction (oncolysis) so that the correlation between NDV-replication and luciferase activity is lost. Therefore, 48 h post transfection RT3 K1 cells were infected with NDV-luciferase at an MOI of 0.01 and the luciferase activity was measured 24 h p.i. when the viral transgene expressions still correlated with NDV-replication. For detection of cytotoxic effects following siRNA-treatment alone, mock infected duplicate RTF plates were used to perform cell viability assays 72 h post transfection. By this method, false positive screening candidates for reduction of viral replication could be excluded on the corresponding RTF plates used for siRNA treatment and viral infection. Each siRNA RTF library plate contained specific siRNA pools (comprising of four individual target-specific siRNAs per well), a pool of viral P+V siRNAs 1-3 (used as an internal positive control for assay performance and viral inhibition) as well as negative controls. Untreated cells determined the baseline phenotype. The transfection control (cells treated with transfection reagent only but no siRNA) and the RISC-free siRNA negative control used to distinguish between sequence-specific effects and non-specific silencing. Cell viabilities and luciferase signals on every RTF screening plate were normalized to the RISC-free siRNA control. In general, the screen allowed the observation of three relevant categories of siRNA-induced effects. Candidate genes could be detected which cause a reduction or induction of viral replication as well as cellular toxicity when knocked down in the tumorigenic RT3 K1 cells. As four identical siRNA RTF library plates were delivered, the screening of 188 genes in total (112 genes in the Membrane trafficking and 76 genes in the Tyrosine kinase library) could be performed twice. Subsequently, hit validation was performed in a secondary screen using individual siRNAs instead of SMARTpool siRNAs. The screening strategy is schematically depicted (Figure 4-33).

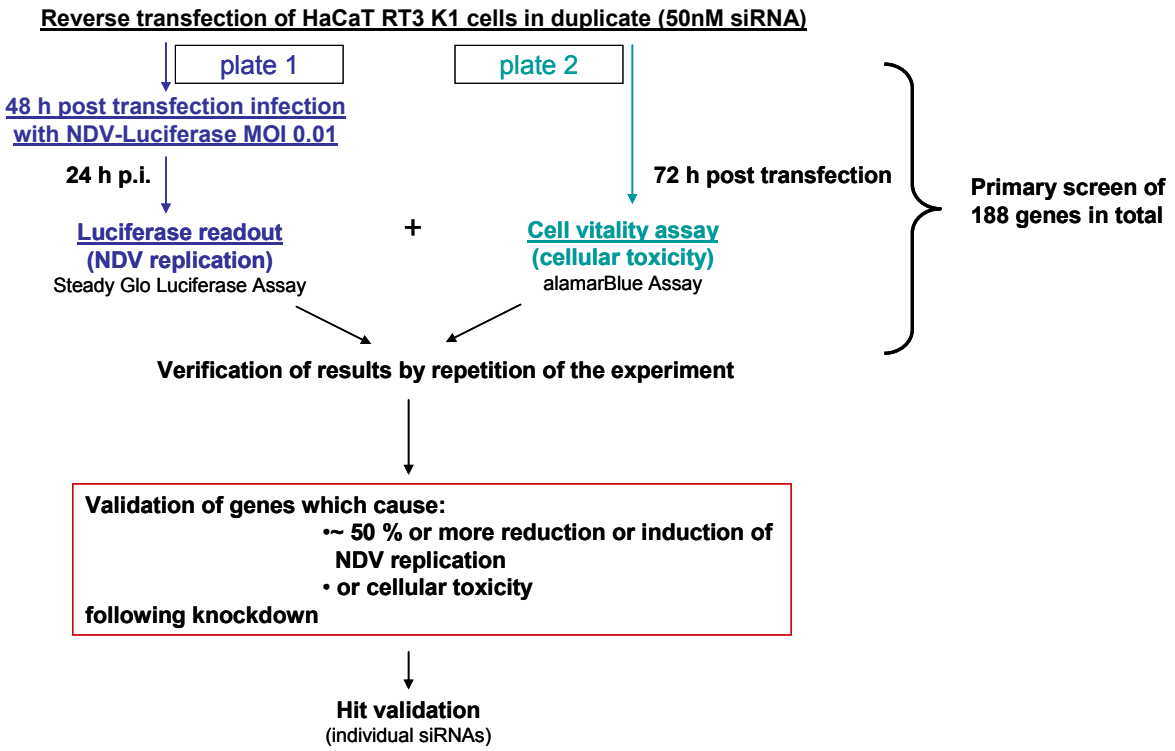

Figure 4-33: Scheme of the experimental procedure of the siRNA based functional screen

4.2.5 NDV-sensitizing and repressing candidates genes could be detected in the primary siRNA screen

Each library was screened twice and results averaged. The internal viral positive control indicated successful screening performances as the reduction of viral luciferase activity was reduced to at least 80 % compared to the RISC-free siRNA controls in each screen. All negative controls included did not severely differ in their luciferase signal intensities. The primary screen of the membrane trafficking and tyrosine kinase siRNA libraries for NDV-sensitizing genes resulted in the identification of gene-specific SMARTpool siRNAs which, when transfected, either did not cause changes in viral luciferase activities or enhancend or decreased it. Furthermore, almost no SMARTpool siRNA transfection resulted in cellular toxicity. However, due to the small number of repeats, there was no statistical analysis of the results possible. Therefore, NDV-sensitizing candidate genes were selected for a confirmatively secondary screen causing 50 % or more induction or reduction of viral replication. Cytotoxicity-inducing candidate genes were nominated when cell viability was reduced to more than 30 %. An overview about all screened genes in the primary screen is provided in the Appendix (Table 7-1 and Table 7-2). The screening of the membrane trafficking library resulted in the nomination of 15 candidate genes which, when down regulated, showed replication reducing properties and five candidate genes with replication

inducing features. There was one siRNA pool, which caused cytotoxicity in the tumorigenic RT3 K1 cells when transfected (Figure 4-34).

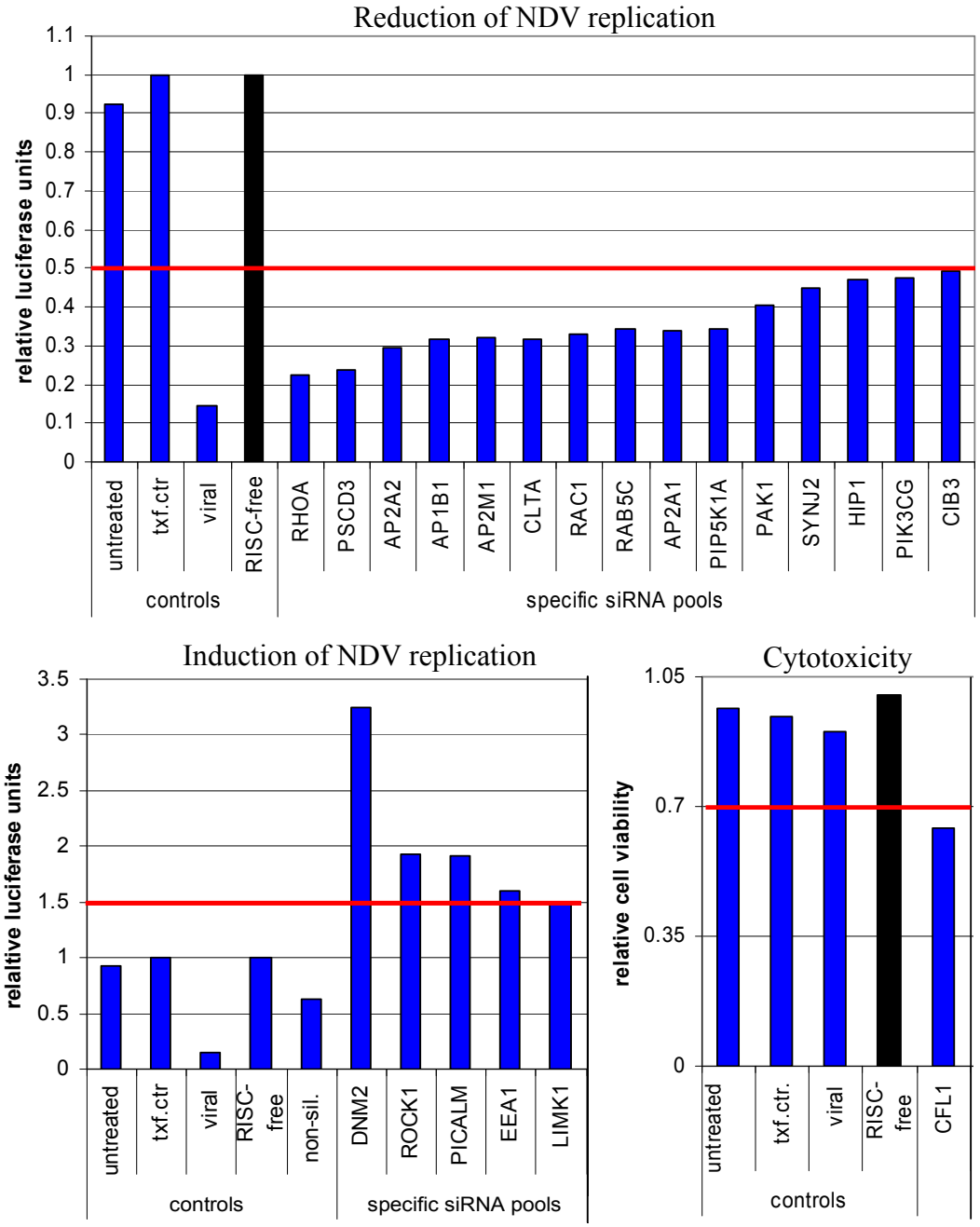

Figure 4-34: Membrane trafficking library hits which showed at least 50 % reduction or induction of NDV replication or cytotoxicity

RT3 K1 cells were reverse transfected with SMARTpool siRNA of the RTF membrane trafficking library. Untreated cells, a transfection reagent only control (txf.ctr.), a RISC-free siRNA (risc free) served as negative controls whereas a viral P+V pool was used as a positive control for reduction of viral replication. Fourty-eight hours post transfection cells were either infected with NDV-luciferase (MOI 0.01) or untreated for detection of cytotoxic effects. Twenty-four hour p.i. viral luciferase activitiy was measured and results are presented as relative viral luciferase activity normalized to the RISC-free siRNA control. Mock-infected plates were used for determination of cell viability following siRNA transfection using the alamarBlue assay. The RISC-free siRNA control was used for normalization. Results are presented as the mean of two experiments.

The screening of the tyrosine kinase library resulted in the nomination of seven candidate genes which, when down-regulated, showed replication reducing properties and six candidate genes with replication inducing features. There was one siRNA pool, which caused cytotoxicity when transfected (Figure 4-35).

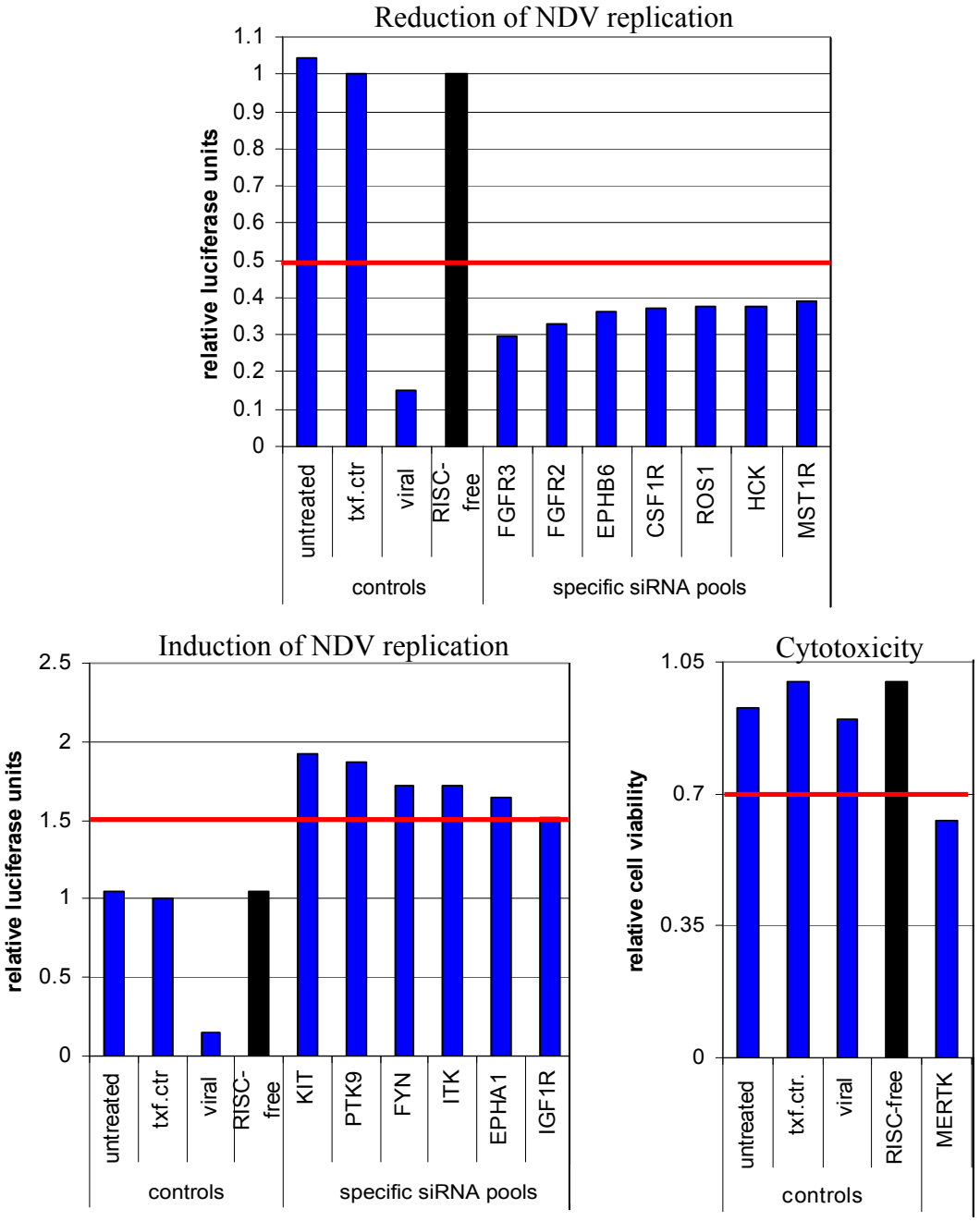

Figure 4-35: Tyrosine kinase library hits which showed at least 50 % reduction or induction of NDV replication or cytotoxicity

RT3 K1 cells were reverse transfected with SMARTpool siRNA of the RTF membrane trafficking library. Untreated cells, a transfection reagent only control (txf.ctr.), a risc-free siRNA (risc free) served as negative controls whereas a viral P+V pool was used as a positive control for reduction of viral replication. Fourty-eight hours post transfection cells were either infected with NDV-luciferase (MOI 0.01) or untreated for detection of cytotoxic effects. Twenty-four hour p.i. viral luciferase activitiy was measured and results are presented as relative viral luciferase activity normalized to the RISC-free siRNA control. Mock-infected plates were used for determination of cell viability following siRNA transfection using the alamarBlue assay. The RISC-free siRNA control was used for normalization. Results are presented as the mean of two experiments.

In summary, primary screening of both siRNA libraries led to the identification and nomination of candidate genes potentially inducing either repressing or increasing viral replication when knocked down in the tumorigenic RT3 K1 cells. Besides, two candidate genes were selected which potentially lead to cellular toxicity in tumor cells when inhibited.

4.2.6 Confirmation of NDV-sensitizing hits in the secondary siRNA screen

In order to validate the NDV-sensitizing features of the nominated candidate genes and the cytotoxity hits of the primary screen, a secondary siRNA screen was performed using four individual siRNAs per target gene separately.

The custom library containing 144 siRNAs (36 hits x four individual siRNAs) were delivered as lyophilisates in a masterplate. For the screening, individual siRNAs had to be transferred to the screening plates first. Besides, the screening procedure was identical to the primary screen. Untreated cells, transfection reagent only controls and a non-silencing siRNA #3 were used as negative controls. As an internal positive control, viral P+V siRNA #3 was utilized. High knockdown efficiencies of the internal positive controls indicated optimal screening performances. Candidate genes were considered as validated when 50 % or more reduction or induction of NDV replication compared to the non-silencing siRNA was caused. As a second condition, at least three out of four individual specific siRNAs per target gene had to show the same replication inducing or reducing phenotype (and no cytotoxicity). An overview about all screened genes in the secondary screen is provided in the Appendix Table 7-3.

Except for fibroblast growth factor receptor 3 (FGFR3), all secondary screen hits were components of the Membrane Trafficking library. In total, 12 candidate genes were nominated. Furthermore, only replication reducing candidate genes following siRNA knockdown could be validated (Figure 4-36).

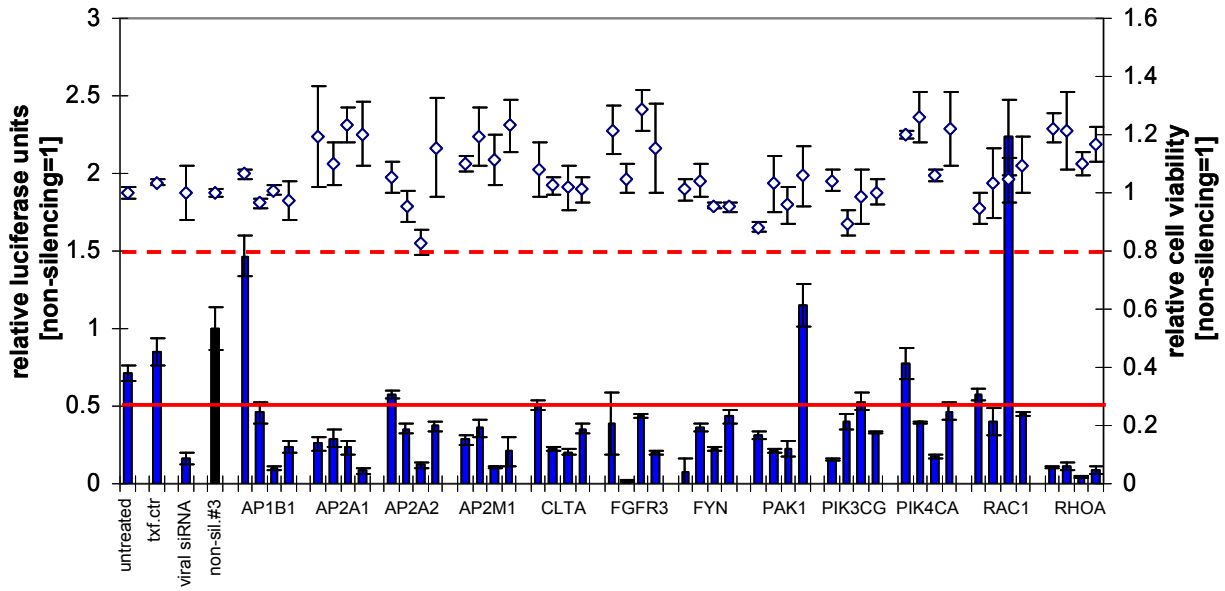

Figure 4-36: Nomination of 12 validated candidate genes inducing 50 % or more reduction of NDV replication in a secondary screen
RT3 K1 cells were reverse transfected with four individual specific siRNAs per candidate gene of the primary screen in sextuple. Untreated cells, a transfection reagent only control (txf.ctr.) and a non-silencing siRNA (non-sil. #3.) served as negative controls whereas a viral P+V #3 siRNA (viral siRNA) was used as a positive control for reduction of replication. Fourty-eight hours post transfection cells were infected with NDV-luciferase (MOI 0.01) or mock infected. Twenty-four hours p.i. viral luciferase activitiy was measured and results are presented as relative viral luciferase activity normalized to the non-silencing control siRNA. Cell vitality of transfected but mock-infected cells was measured using alamarBlue. Results are normalized to the non-silencing siRNA control. Error bars represent ±SD of triplicate values. (Red line= threshold relative luciferase activity, red dotted line= threshold relative cell vitality)

In summary, in the secondary confirmative siRNA screen, 12 NDV-sensitizing candidate genes were validated which led to a reduction of viral replication when knocked down.

4.2.7 Validation of siRNA-induced knockdowns for NDV-sensitizing genes involved in clathrin-mediated processes or actin cytoskeletal rearrangements

Subsequently, the NDV-sensitizing effects of the 12 nominated candidate genes had to be ascribed to specific siRNA-based knockdown effects. Therefore, the knockdown experiments in RT3 K1 cells using four individual siRNAs separately per candidate gene were repeated. The knockdown performance of each specific target siRNA was evaluated by Western Blot analysis. Protein expression and siRNA-related knockdowns were confirmed for six candidates which could be grouped concerning their main functions (Figure 4-37). The adaptor proteins AP2α (whereby knockdown validation was performed for AP2A1 representatively for all detected AP2 subunits in the screening), AP1B1 as well as clathrin light chain A (CLTA) are involved in clathrin-mediated processes such as endocytosis or protein-sorting. The Rho GTPases Ras-related C3 botulinum toxin substrate 1 (Rac1), Ras homolog gene familiy, member A (RhoA) and the Rac effector kinase p21 protein (cell

division cycle 42 (Cdc42)/Rac)-activated kinase 1 (Pak1) mediate actin reorganisations of the cytoskeleton (Table 4-2).

Although each of the four specific siRNAs targeting Rac1, Pak1 and AP1B1 caused target protein reduction, not all of them induced a decrease in NDV replication but an increase (see Figure 4-36). However, these contrary phenotypes could be due to unspecific off target effects and was only shown for one out of the four target specific siRNAs.

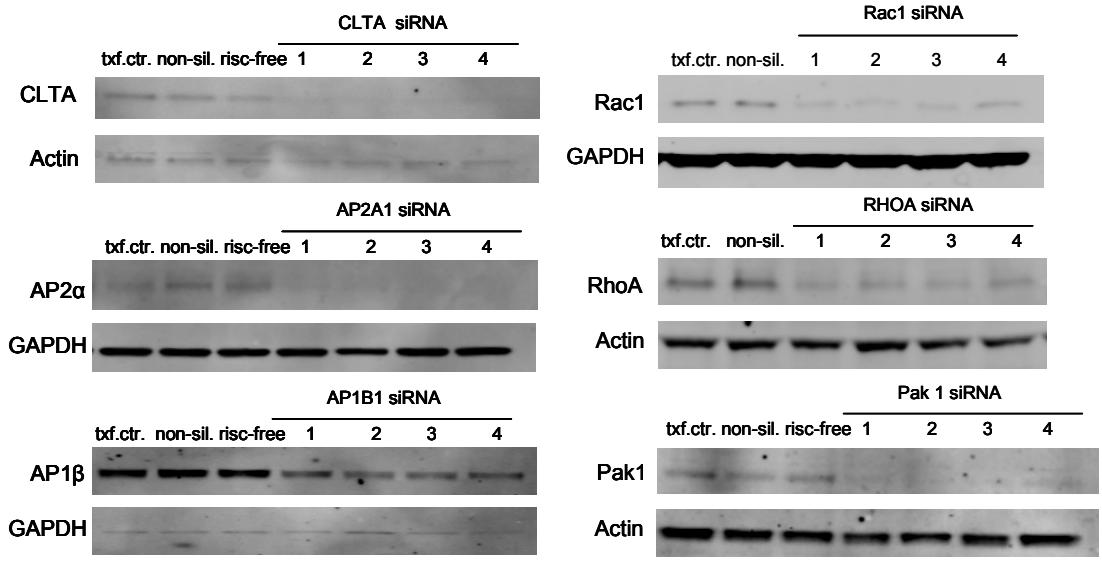

Figure 4-37: Validation of siRNA-mediated knockdowns of six candidate genes in RT3 K1 cells
RT3 K1 cells were reverse transfected with four individual specific siRNAs (siRNA 1-4) targeting AP1β (AP1B1), AP2α (AP2A1), Clathrin light chain A (CLTA), Rac1, RhoA and Pak1. A transfection reagent only control (txf.control), a non-silencing siRNA #3 (non-sil.) or a risc-free siRNA control (risc free) were used as negative controls. Fourty-eight hours post transfection, cells were harvested and lysed for protein extraction. Subsequently, SDS page of equal amounts of protein samples and Western Blot analysis was performed. SiRNA-mediated candidate protein knockdown was detected by specific primary antibodies. Actin or GAPDH expression served as endogenous controls.

Table 4-2: Knockdown validated candidate genes with NDV-sensitizing activity in RT3 K1 cells and their main, common functions

Gene symbol	Protein name and main function
	Clathrin-mediated processes
AP1B1	Clathrin-associated adaptor-related protein complex 1, beta 1 subunit (AP1); epithelium-specific; basolateral sorting adaptor; present in late-Golgi/trans-Golgi network and endosomes
AP2A1	Clathrin-associated adaptor-related protein complex 2, alpha 1 subunit (AP2) on endocytic vesicles; links receptors to clathrin
CLTA	Clathrin light chain A; major structural component of clathrin, involved in endocytosis, intracellular trafficking, protein-sorting
	Actin cytoskeleton reorganization
Rac1	Ras-related C3 botulinum toxin substrate 1; member of the RAS superfamily of Rho GTPases; regulates actin cytoskeletal reorganization (lamellipodia formation and membrane ruffles)
RhoA	Ras homolog gene family, member A; member of the RAS superfamily of Rho GTPases; mainly regulates reorganization of the actin cytoskeleton (stress fibre formation)
Pak1	p21 protein/Cdc42/Rac1 activated kinase 1; effector serine/threonine kinase of Rac1 and Cdc42; mediates actin cytoskeletal reorganization (lamellipodia and filopodia formation and membrane ruffles)

Candidate genes such as the protein tyrosine kinase FYN oncogene related to SRC, FGR, YES (Fyn) and the phosphatidylinositol 4-kinase, catalytic, alpha (PIK4CA) were not detectable on protein level. The candidate genes phosphoinositide-3-kinase, catalytic, gamma polypeptide (PIK3CG) and FGFR3 did not show siRNA-mediated knockdowns.

In the primary and secondary screen, viral luciferase transgene expression was used as a readout for NDV replication. However, the possibility could not be ruled out that the specific siRNAs of the candidate genes caused off-target effects which could have influenced viral luciferase transgene expression or activity. This could have led to false positive results. Therefore, individual siRNA based knockdowns for the previously validated candidate genes were repeated and EGFP expressing NDV was used instead. In Figure 4-38, results of the detection of viral EGFP expression by fluorescence microscopy 24 h p.i. (72 h post transfection) are depicted. For all candidate genes tested, an obvious decrease in viral EGFP expression by using three individual siRNAs per target gene compared to the non-silencing control was detectable. Results correlated with the luciferase based readout.

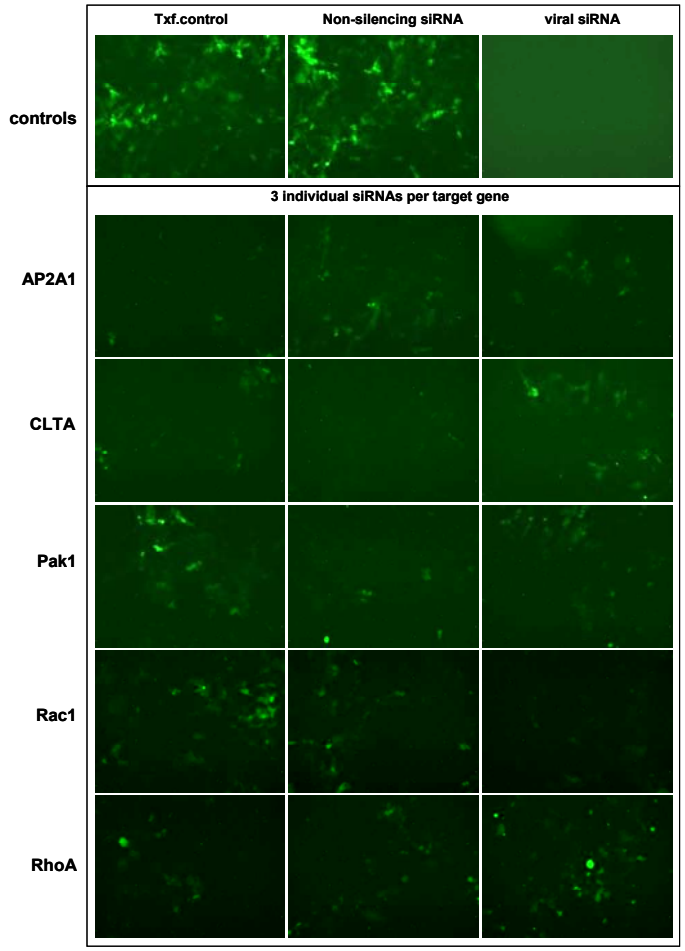

Figure 4-38: Representative fluorescence pictures showing viral replication reducing effects of secondary screen hits
RT3 K1 cells were reverse transfected with three individual specific siRNAs per candidate gene AP2A1, CLTA, PAK1, Rac1 and RhoA. A transfection reagent only control (txf.control) and a non-silencing siRNA served as negative controls whereas a viral P+V #3 siRNA (viral siRNA) was used as a positive control for reduction of viral replication. Fourty-eight hours post transfection cells were infected with NDV-EGFP (MOI 0.01). Twenty-four hours p.i. viral EGFP expression was monitored by fluorescence microscopy (scale bar= 100 µm).

In summary, out of 12 nominated candidate genes six were found to be expressed on protein level and were shown to be specifically knocked down via its corresponding siRNAs. In addition, the replication reducing effect following specific siRNA knockdowns measured by viral luciferase activity could be confirmed by detection of reduced viral EGFP expressions.

4.2.8 Detection of tumor cell-specific overexpressed NDV-sensitizing factors in the HaCaT-derived transformation model

Protein expressions of the NDV-sensitizing genes in RT3 K1 cells had been confirmed. In the following experiment it was analyzed whether these candidates were tumor cell-specifically overexpressed in RT3 cells as well as in the RT3 K1 cells compared to the non-tumorigenic HaCaT cells. Infection of the transfected cells started when cells were (nearly) confluent.

Consequently, protein lysates of confluent cells were tested by Western Blot analysis as the degree of confluency could influence protein expression levels in the cells. Comparision of candidate protein expressions revealed a clear tumor cell-specific overexpression of the adaptor protein AP2α and CLTA as well as Pak1 (overexpression indicated by a red font color of candidate names) (Figure 4-39).

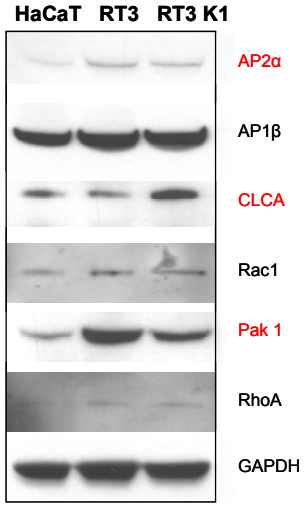

Figure 4-39: Tumor cell-specific overexpression of NDV-sensitizing candidate genes in the HaCaT-derived model for tumorigenic transformation
Confluent cells were harvested and lysed for protein extraction and equal amounts of protein samples were subjected to SDS page and subsequent Western Blot analysis of protein expression of secondary screen candidate genes AP2α, AP1β, CLTA, Rac1, Pak1 and RhoA in HaCaT, RT3 and RT3 K1 cells. GAPDH expression served as an endogenous control. Tumor specific overexpressions of candidates are indicated by the red font color of the candidate names.

In summary, three out of the six NDV-sensitizing candidate genes involved in clathrin-mediated processes or actin reorganization of the cytoskeleton revealed tumor cell-specific overexpression in the HaCaT derived transformation model.

4.2.9 Verification and functional analysis of the screening candidate Rac1

The Rho GTPase Rac1 was one of the validated siRNA screening candidates reducing NDV replication when knocked down. It is known for its virus-sensitizing activity for e.g. hepatitis B virus (HBV) [152], HSV-1 [153], HIV-1 [154] or Ebola virus [155]. Besides there is striking evidence that it is also involved in transformational processes induced by oncogenes including Ras or the Rac1-specific GEF TIAM1. TIAM1 has recently been shown to directly interact with oncogenic Ras [156-159]. A specific connection with the life cycle of naturally oncolytic viruses has not been shown. Hence, Rac1 was chosen for verification experiments and functional analysis with regard to its NDV-sensitizing activity and connection with tumorigenesis.

4.2.10 Observation of increased Rac1-induced lamellipodia formation in RT3 K1 cells compared to HaCaT cells

Although tumor cell-specific overexpression of Rac1 in RT3 K1 cells compared to HaCaT cells was not observed, Rac1 GTPase activitiy could be increased.

Rac1 is known to induce lamellipodia formation and membrane ruffling by promoting actin-branching in the leading edge of motile cells [160]. A hallmark of invasive and metastasizing tumor cells is increased membrane protrusion activity mediated by Rho GTPases, such as Rac1. Comparative immunofluorescence staining of filamentous polymers of actin (F-actin) in subconfluent HaCaT and RT3 K1 cells was performed to detect differences in actin cytoskeleton organisation which could hint to enhanced Rac1 activity in the tumorigenic HaCaT cells (Figure 4-40). In peripheral HaCaT cells, F-actin filaments were mainly bundled in parallel (examples indicated by white dotted arrows) and only few areas with actin-branching could be detected. In contrast, the peripheral tumorigenic RT3 K1 cells showed almost no parallel organisation of F-actin fibres but enhanced membrane protrusions (white arrows) which could hint to increased Rho GTPase activity.

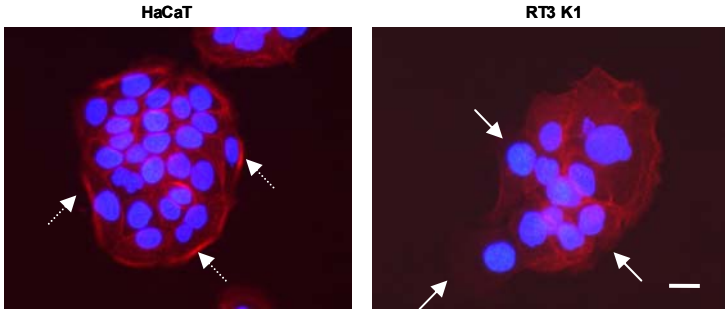

Figure 4-40: Representative fluorescence pictures showing differences in F-actin organisation in peripheral HaCaT and RT3 K1 cells
Subconfluent HaCaT and RT3 K1 cells grown on cover slides were fixed and immunofluorescently stained for F-actin using Phalloidin labelled with Alexa Fluor 488 (red staining). Cell nuclei were stained with Hoechst 33258 (blue staining). Fluorescence images were captured by fluorescence microscopy (scale bar= 20 µm).

4.2.11 The Rac1-GEF TIAM1 was overexpressed in HaCaT tumor cell lines

Enhanced lamellipodia formation in the Ras-transformed RT3 K1 cells hinted to deregulated Rac1 activity. To further prove this, tumor specific overexpression of the Rac1-GEF TIAM1 in the tumorigenic HaCaT cell lines was investigated as it could hint to increased Rac1 activation. Therefore, protein lysates of confluent HaCaT, II4, RT3 and RT3 K1 cells were tested by a comparative Western Blot analysis for TIAM1 protein expression (Figure 4-41). In the malignant cell lines II4 and RT3, TIAM1 expression was increased compared to the non-tumorigenic HaCaT cells. Furthermore, in RT3 K1 cells which were characterized by

enhanced tumor growth *in vivo* compared to the parental RT3 cells, TIAM1 expression was even stronger than in the II4 and RT3 cell lines. These results pointed to an activated TIAM1-mediated Rac1 pathway in tumorigenic, Ras-transformed HaCaT cells.

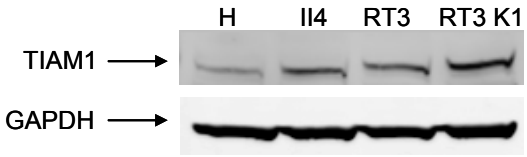

Figure 4-41: Tumor cell-specific overexpression of TIAM1 in the HaCaT-derived transformation model
HaCaT (H), II4, RT3 and RT3 K1 cells were harvested and lysed for protein extraction. Equal amounts of protein samples were subjected to SDS page and subsequent Western Blot analysis of TIAM1 expression using a TIAM1-specific polyclonal anti-rabbit antibody. GAPDH expression served as an endogenous control.

4.2.12 Expression of the dominant negative mutant Rac1T17N reduced viral replication and anchorage-independent growth

To independently confirm the siRNA-based NDV-sensitizing results for Rac1 as well as its impact on tumorigenesis of RT3 K1 cells a dominant negative (DN) mutant of Rac1 (Rac1T17N) was constructed [141]. Stable transfection of the mutant form into RT3 K1 cells resulted in a slight increase of *Rac1* mRNA expression as determined by Taqman realtime PCR (Figure 4-42 A). Despite the low expression level of the dominant negative mutant of Rac1 in the pool of transfected RT3 K1 cells, an infection experiment using NDV-luciferase was performed. Low expression of Rac1T17N could potentially be sufficient to induce a mutant-specific phenotype. In Figure 4-42 B it is shown, that NDV replication in RT3 K1 Rac1T17N cells was decreased by more than 20 % compared to the pool of RT3 K1 cells transfected with the vector control only. It was indicated by reduced viral luciferase expression.

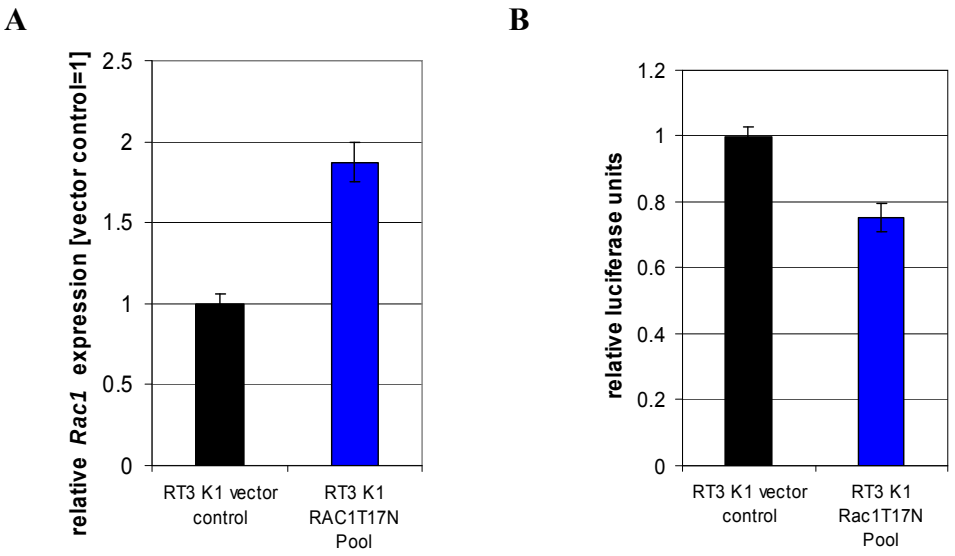

Figure 4-42: Stable Expression of Rac1T17N (DN) in RT3 K1 cells led to a significant reduction of viral replication
(A) RT3 K1 vector control cells and RT3 K1 Rac1T17N cells per 96-well were harvested for cDNA synthesis. Relative *Rac1* mRNA expression was determined by Taqman realtime PCR using the vector control for normalization. Error bars represent ±SD of triplicate values.
(B) RT3 K1 vector control cells and RT3 K1 Rac1T17N cells per 96-well were infected with NDV-luciferase (MOI 0.01). Twenty-four hours p.i. viral luciferase activitiy was measured and results are presented as relative viral luciferase activity normalized to the vector control. Error bars represent ±SD of sextuple values.

RT3 K1_Rac1T17N cells were then tested in a colony formation assay to assess the influence of Rac1 activity on the transformed phenotype of RT3 K1 cells (Figure 4-43). Four weeks after seeding of single cells, untreated RT3 K1 cells were characterized by enhanced colony growth. Nearly the same colony size could be detected in RT3 K1 cells stably transfected with an empty vector as a control. For RT3 K1 cells transfected with *Rac1T17N*, a severely reduced colony growth in soft agar was visible.

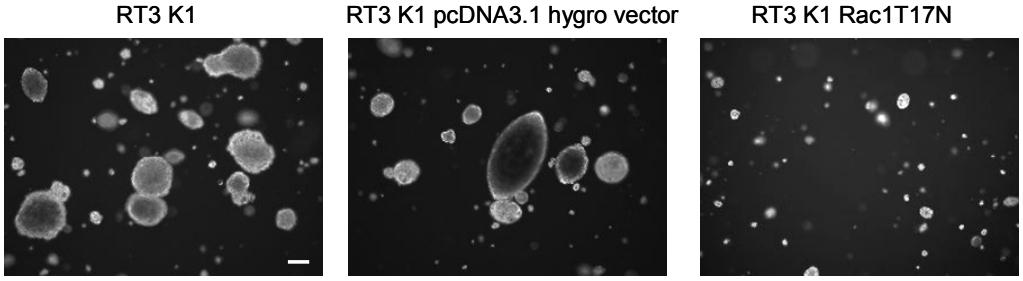

Figure 4-43: Inhibition of anchorage-independent growth in RT3 K1 cells expressing the dominant negative mutant of Rac1
Single RT3 K1, RT3 K1 vector control cells or RT3 K1_Rac1T17N_Pool cells were seeded in soft agar. Cells were incubated for 4 weeks before pictures of colony formation were taken using by inverse microscopy (scale bar= 500µm).

This showed that Rac1 activity is necessary for anchorage-independent growth in the tumorigenic Ras-transformed RT3 K1 cells.

4.2.13 Inhibition of Rac1 by a small molecule inhibitor decreased viral replication in a dose dependent manner

NDV-sensitizing effects of Rac1 were thus far shown via siRNA-based knockdown experiments and by dominant negative mutant experiments in RT3 K1 cells. As a third method, the Rac1-small molecule inhibitor NSC 23766 was tested. Tumorigenic RT3 K1 cells were pretreated with increasing concentrations of the Rac1 inhibitor (IC_{50} = 50 µM) for 1 h before NDV-luciferase infection at an MOI of 0.01 was performed (Figure 4-44). While cell viability of mock-infected cells but inhibitor-treated cells was not seriously affected, viral luciferase activity decreased with increasing Rac1 inhibitor concentrations at 24 h p.i.. At 100 µM viral replication was even lower than in the non-susceptible and non-tumorigenic HaCaT cells which were used as a negative control for NDV replication. Inhibition of Rac1 by a small molecule inhibitor could therefore confirm its NDV-sensitizing feature.

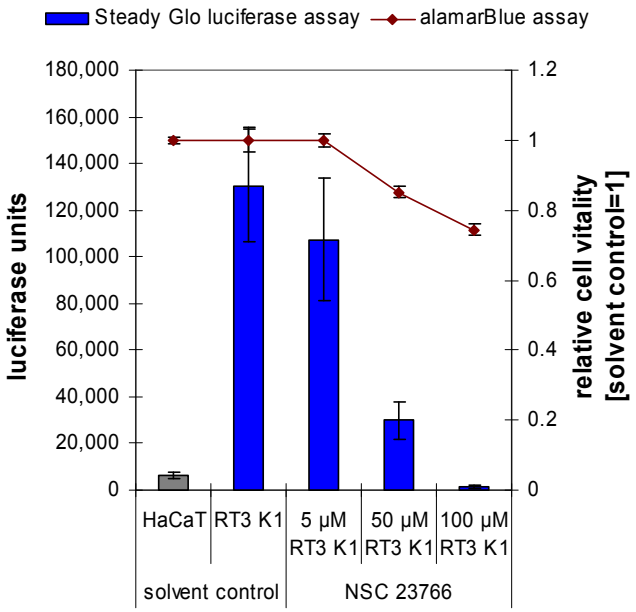

Figure 4-44: Dose-dependent decrease in viral luciferase activity in infected RT3 K1 cells treated with Rac1 small molecule inhibitor
RT3 K1 cells were pretreated with increasing NSC 23766 concentrations for 1 h. Subsequently, cells were infected with NDV-luciferase at an MOI of 0.01 in the presence of the inhibitor. HaCaT cells and RT3 K1 cells treated with solvent only were used as negative controls for inhibition of viral replication. Twenty-four hours p.i. viral luciferase activitiy was measured. Simultaneously, a duplicate plate with inhibitor treated but mock-infected cells was used for determination of cell viability using an alamarBlue assay. Cell vitalities were normalized to the solvent control. Error bars represent ±SD.

In summary, the NDV-sensitizing effect of Rac1 was shown by siRNA-mediated knockdown of Rac1 protein as well as by blockage of Rac1 activity.

4.2.14 Inhibition of PI3K led to a reduction of viral replication

Rac1 GTPase activity is regulated by a variety of factors which are regulated by major upstream components as well. As known from the literature, PI3K can activate Rac1 [161]. In order to determine whether PI3K-signaling is involved in mediating NDV susceptibility in RT3 K1 cells, a PI3K small molecule inhibitor experiment was performed. RT3 K1 cells were pretreated with increasing concentrations of the PI3K inhibitor LY 294002 (IC_{50} = 50 µM) for 1 h before cells were infected with NDV-luciferase in the presence of the PI3K inhibitor. As shown in Figure 4-45, viral replication decreased 24 h p.i. in a dose dependent manner in RT3 K1 cells compared to the solvent control while cells stayed vital. Treatment of cells with 10 µM PI3K inhibitor led to a reduction of viral luciferase activity comparable the level in non-susceptible HaCaT cells which were used as a negative control for viral replication.

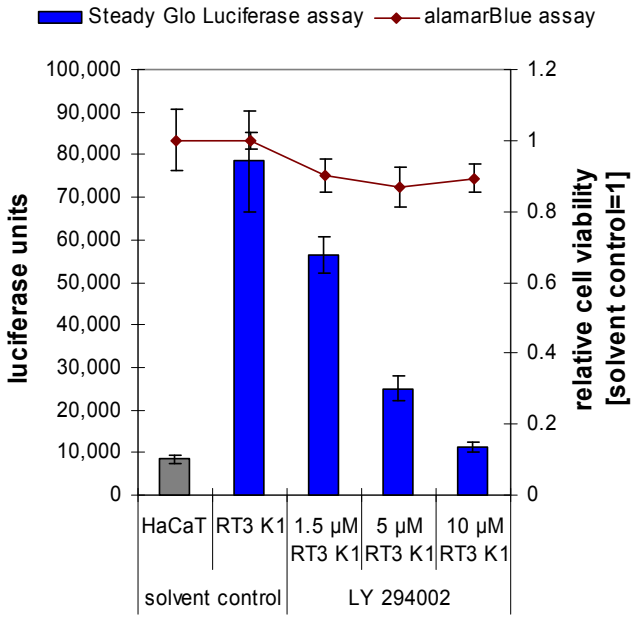

Figure 4-45: Decreasing viral luciferase activity in infected RT3 K1 cells in the presence of increasing PI3K small molecule inhibitor concentrations
RT3 K1 cells were pretreated with increasing LY294002 concentrations for 1 h. Subsequently, cells were infected with NDV-luciferase at an MOI of 0.01 in the presence of the inhibitor. HaCaT cells and RT3 K1 cells treated with solvent only were used as negative controls. Twenty-four hour p.i. viral luciferase activitiy was measured. In parallel, a duplicate plate with inhibitor treated cells but mock-infected cells was used for determination of cell viability using an alamarBlue assay. Cell vitalities were normalized to the solvent control. Error bars represent ±SD of sextuple values.

This result indicated that PI3K signaling influenced NDV susceptibility in the tumorigenic RT3 K1 cells.

4.2.15 Rac1 inhibition negatively influenced early stages of the viral life cycle

In order to detect the NDV-sensitizing function of Rac1 with respect to the NDV life cycle, an experiment was performed to evaluate the Rac1 function during early stages of the viral life cycle.

Subconfluent RT3 K1 cells were pretreated with 50 µM NSC 23766, a dose which induced a severe decrease in viral luciferase activity but no cytotoxicity in the previous inhibitor study experiment. Subsequently, cells were infected with NDV in presence of the Rac1 inhibitor. Untreated but infected cells served as a control. Three hours p.i. cells were fixed and immunofluorescently stained for F-actin in order to detect any inhibitor mediated changes in the actin cytoskeleton and for NDV proteins to determine NDV uptake into the cells (Figure 4-46).

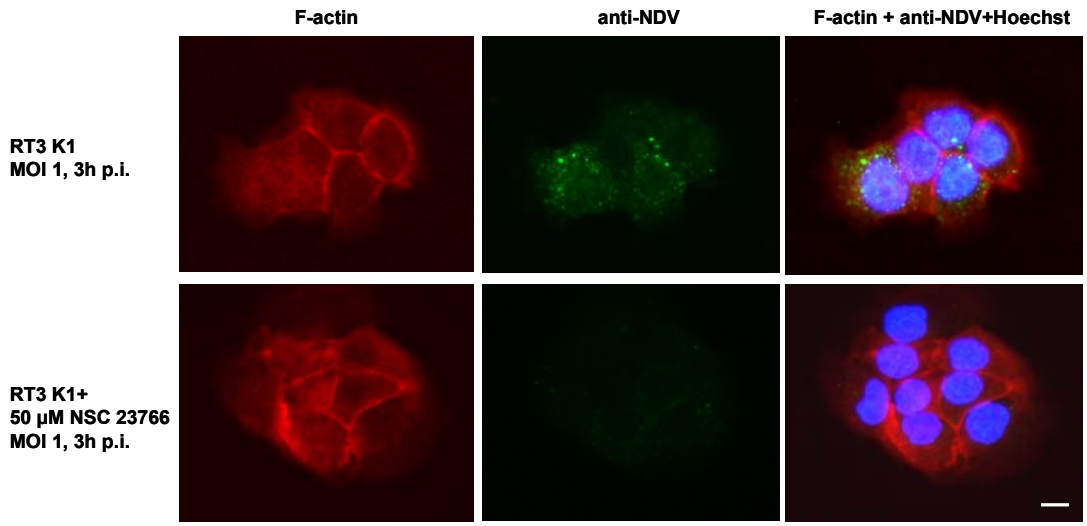

Figure 4-46: Representative fluorescence pictures showing no NDV-specific proteins in RT3 K1 cells treated with the Rac1 inhibitor
Cells grown on cover slides were preteated with 50 µM NSC 23766 for 1 h. Subsequently, cells were infected with NDV at an MOI of 1 in the presence of inhibitor. Solvent only-treated but infected RT3 K1 cells served as a control for virus uptake. 3 h p.i. cells were fixed and immunofluorescently stained for F-actin using Phalloidin labelled with Alexa Fluor 488 (red staining). NDV proteins were detected by using a rabbit polyclonal NDV antiserum and anti-rabbit Cy-2 as a secondary antibody (green staining). Cell nuclei were stained with Hoechst 33258 (blue staining). Fluoresence images were captured by fluorescence microscopy (scale bar= 10µm).

In the control cells, 3 h p.i. NDV proteins were detected which was indicated by a strong dotted green staining within the cells. In contrast, cells treated with the Rac1 inhibitor did not show any NDV-specific staining. This indicated that Rac1 could be involved in virus internalization processes. However, at this magnification there were no obvious inhibitor mediated changes in the actin cytoskeleton visible.

4.2.16 Overexpression of Rac1 in HaCaT cells increased viral replication

As Rac1 inhibition in RT3 K1 cells was shown to decrease NDV replication the question arose whether overexpression of *Rac1*wt alone, in contrast to oncogenic *Ras,* could have an influence on NDV susceptibility in non-NDV-susceptible HaCaT cells. Hence, HaCaT cells were stably transfected with *Rac1*wt or an empty vector as a control. Overexpression was confirmed by Taqman realtime PCR. The pool of *Rac1* transfected HaCaT cells showed only a slight overexpression of Rac1 compared to the vector control (Figure 4-47 A). However, when a pool of HaCaT Rac1wt cells were infected with NDV-luciferase, viral luciferase activity was three times as high as in infected HaCaT vector control cells and constituted an intermediate phenotype compared to the viral replication in RT3 K1 cells (Figure 4-47 B).

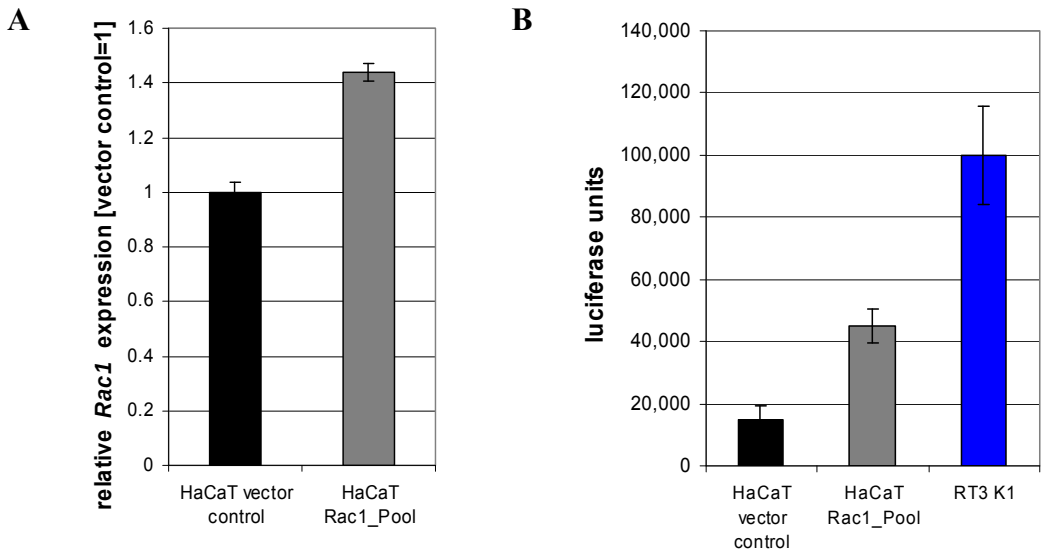

Figure 4-47: Increase in viral replication following *Rac1wt* overexpression in HaCaT cells
(A) HaCaT empty vector control cells and HaCaT Rac1wt cells were harvested for cDNA synthesis. Relative *Rac1* mRNA expression was determined by Taqman realtime PCR using the vector control for normalization. Error bars represent ±SD of triplicate values.
(B) HaCaT vector control cells and HaCaT Rac1wt cells were infected with NDV-luciferase (MOI 0.01). Twenty-four hours p.i. viral luciferase activitiy was measured and results are presented as relative viral luciferase activity normalized to the vector control. Error bars represent ±SD of sextuple values.

Results could be confirmed by repetition of the infection experiment using NDV-EGFP for detection of viral replication. Infection of a pool of HaCaT Rac1wt cells resulted in an increase in EGFP expressing cells compared to the vector control cells but the number of EGFP expressing cells was not as high as in RT3 K1 cells (Figure 4-48).

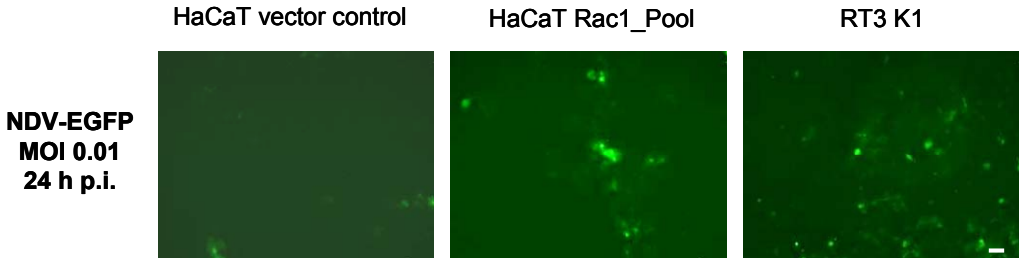

Figure 4-48: Representative fluorescence pictures showing a partial increase in viral EGFP expression in *Rac1*wt transfected HaCaT cells compared to vector control cells
HaCaT vector control cells, HaCaT Rac1wt_Pool cells and RT3 K1 cells were infected with NDV-EGFP (MOI 0.01). HaCaT vector control cells served as a negative control and highly susceptible RT3 K1 cells as a positive control for viral replication. Twenty-four hours p.i. fluorescence microscopy was performed for detection of viral EGFP expression (scale bar=100µm).

Overexpression of Rac1 was not very strong (as shown in Figure 4-47 A). The positive effect of Rac1 on NDV replication may therefore have been underestimated. In order to directly correlate the increase in viral replication in HaCaT cells with Rac1wt overexpression a co-localization experiment was performed. The pool of HaCaT Rac1wt cells and HaCaT vector control cells were infected with NDV and fixed at 24 h after infection. Cells were immunofluorescently stained for Rac1 overexpression and NDV proteins (Figure 4-49). HaCaT vector control cells did not show any Rac1-specific overexpression or areas of increased NDV protein detection. Instead, the pool of HaCaT Rac1wt cells showed cells with increased Rac1 expression (red staining). In these cells, elevated NDV replication (green staining) could be observed indicated by a strong orange overlay when both fluorescence channels were combined.

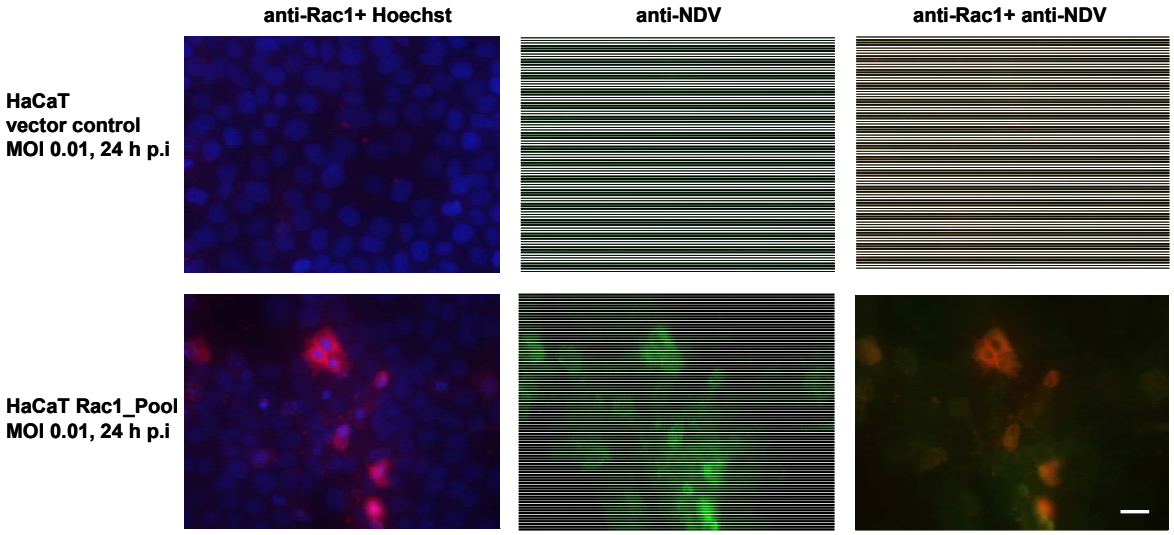

Figure 4-49: Representative fluorescence pictures showing co-localization of Rac1wt overexpression and increased NDV replication in HaCaT cells
HaCaT vector control cells and HaCaT Rac1wt (pool) cells were infected with NDV (MOI 0.01). Twenty-four hours p.i. cells were fixed with and immunofluorescently stained for Rac1 expression using a Rac1-specific mouse monoclonal antibody and anti-mouse Cy-3 (red staining) and a rabbit polyclonal anti-NDV sera and anti-rabbit Cy-2 (green staining) for detection of NDV proteins. Cell nuclei were stained with Hoechst 33258 (blue staining). Fluorescence pictures were captured by fluorescence microcopy (scale bar= 50 µm).

In summary, HaCaT cells were rendered NDV susceptible by overexpression of Rac1wt.

4.2.17 Validation of the NDV-sensitizing feature of Rac1 in highly NDV susceptible HCT 116 and MDA-MB-231 cells

In order to exclude that the NDV-sensitizing effect of Rac1 were restricted to the HaCaT derived cell line model, highly NDV-susceptible MDA-MB-231 cells (human breast adenocarcinoma cell line) and HCT 116 cells (human colon carcinoma cell line) were used in Rac1 inhibitor and infection studies. In both cell lines Rac1 inhibition decreased viral luciferase activity in a dose dependent manner as detected at 24 h p.i. with a low MOI of NDV (Figure 4-50). In MDA-MB-231 cells, 50 µM of NSC 23766 led to strong decrease in viral replication while no serious effect on cell viability was detectable. A severe decrease in viral luciferase activity but no serious loss of cell viability could be shown for HCT 116 cells when treated with 100 µM of NSC 23766.

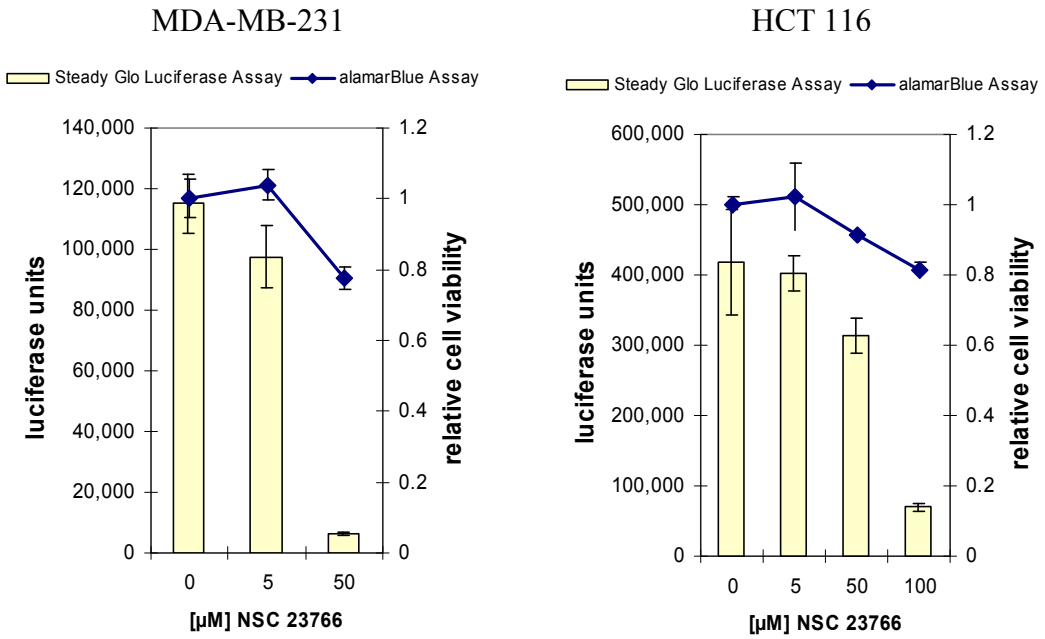

Figure 4-50: Decrease in viral luciferase activity in infected MDA-MB-231 and HCT 116 cells in the presence of increasing Rac1 small molecule inhibitor concentrations
MDA-MB-231 or HCT 116 cells were pretreated with increasing NSC 23766 concentrations for 1 h. Subsequently, cells were infected with NDV-luciferase at an MOI of 0.01 in the presence of the inhibitor. Twenty-four hours p.i. viral luciferase activitiy was measured. In parallel, cells were treated with increasing inhibitor concentrations for 25 h. Cell viability was then measured by alamarBlue assay and normalized to the solvent control. Error bars represent ±SD of sextuple values.

The NDV-sensitizing feature of Rac1 in HCT 116 cells was confirmed by siRNA knockdown experiments and subsequent infection with NDV-luciferase. Cells were transfected with four individual Rac1-specific siRNAs. Knockdown efficacy on protein level was confirmed by Western Blot analysis at 48 h post transfection. The Rac1 specific siRNAs 1, 2 and 3 showed a strong Rac1 knockdown compared to the transfection and non-silencing controls. Rac1 expression in cells treated with siRNA 4 was decreased but not as reduced as with siRNAs 1-3 (Figure 4-51).

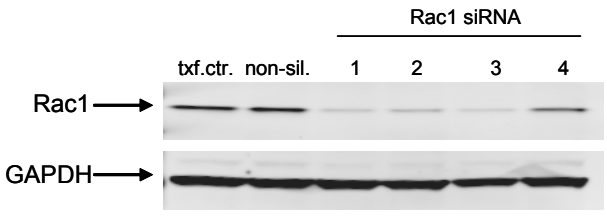

Figure 4-51: SiRNA-mediated knockdown of Rac1 in HCT 116 cells
HCT 116 cells were reverse transfected using four individual Rac1-specific siRNAs (siRNA 1-4). A non-silencing siRNA pool (non-sil.) as well as a transfection reagent only control (txf.control.) were used as negative controls. Fourty-eight hours post transfection, cells were harvested and lysed for protein extraction. Subsequently, SDS page of the equal amounts of protein samples and Western Blot analysis was performed. SiRNA-mediated Rac1 knockdown was detected by using a Rac1-specific monoclonal anti-mouse antibody. GAPDH expression served as an endogenous control.

Following siRNA-mediated Rac1 knockdown, cells were infected with NDV-luciferase and viral luciferase activity was measured 24 h p.i. (Figure 4-52). In parallel, cell vitality of cells following siRNA-mediated Rac1 knockdown was measured in order to exclude cytotoxic effects. Cells treated with the Rac1 siRNA 1, 2 or 3 showed reduction in viral luciferase activity between 40 % and 90 % compared to the non-silencing control. The weak Rac1 protein knockdown obtained by siRNA 4 correlated with a slight reduction of viral luciferase activity of 20 %. As the viral positive control dramatically decreased the viral luciferase signal, the assay performance was optimal and cytotoxic effects which could have influenced viral luciferase activity could be excluded.

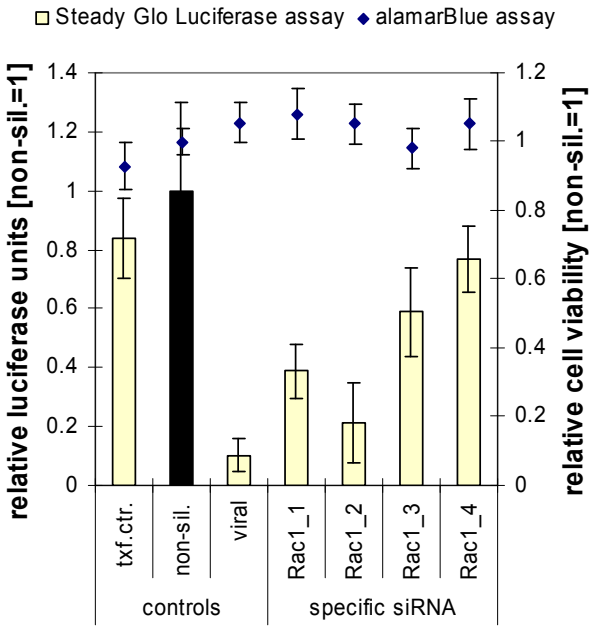

Figure 4-52: Reduction of viral luciferase activity following siRNA-mediated Rac1 knockdown in HCT 116 cells and infection
HCT 116 cells were reverse transfected using four individual Rac1-specific siRNAs (siRNA 1-4). A non-silencing siRNA pool (non-sil.) as well as a transfection reagent only control (txf.ctr.) were used as negative controls. Viral P+V siRNA served as a positive control. Fourty-eight hours post transfection, cells were infected with NDV-luciferase at an MOI of 0.01 and 24 h p.i. viral luciferase activitiy was measured. Results are presented as relative viral luciferase activity normalized to the non-silencing siRNA control. In parallel, cells were siRNA transfected and 72 h post transfection a cell viability assay was performed an alamarBlue assay. Results were normalized to the non-silencing control. Error bars represent ±SD of sextuple values.

In summary, the Rac1-mediated NDV-sensitizing effect shown for the HaCaT derived cell line model was verified for the NDV susceptible cell lines MDA-MB-231 and HCT 116 as well.

5 DISCUSSION

5.1 Tumor cell-specific replication of NDV

NDV features a preference for replicating in a variety of tumor cells but not in normal cells [55]. In contrast to many other genetically modified oncolytic viruses, the tumor selectivity of NDV is inherent which makes it an attractive candidate for virotherapy [104, 105, 162].

In this study, its specific oncolytic property was demonstrated by performing a mixed cell culture experiment. Tumorigenic HT-29 cells were efficiently lysed by oncolytic NDV as a consequence of uninhibited replication. In contrast, almost all non-tumorigenic HaCaT cells stayed viable as they counteracted viral replication. So far, tumor selective replication of NDV has been shown to correlate with defects in IFN type I-mediated antiviral activity in tumorigenic cells [90, 92]. However, oncolytic NDV replication is generally poorly understood and still needs to be analyzed in more detail to improve anti-tumor efficacy.

In order to systematically investigate tumor-specific NDV-sensitizing factors, it was necessary to identify a pair of genetically closely related cell lines comprising a non-tumorigenic, non-NDV-susceptible cell line and a tumorigenic, NDV susceptible cell line. This cell line model for oncolysis then allows the detection, verification and analysis of tumor cell-specific cellular factors supporting oncolytic virus replication. Eventually, it could lay the basis for the discovery of novel drug candidates for anti-tumor therapy as well as biomarkers for efficient NDV-replication.

Such a cellular system was provided by the well characterized multistep skin carcinogenesis HaCaT model developed by Boukamp and colleagues [118, 120, 121].

5.2 The HaCaT-derived model for skin carcinogenesis as a model for NDV-mediated oncolysis

From this HaCaT-derived cell transformation model, the immortal but non-tumorigenic parental HaCaT cell line, which had already been described to be resistant to oncolytic NDV-replication [140], as well as the H-RasV12 transformed malignant subclonal cell line II4 and the highly malignant RT3 cell line [118, 121] were utilized. Infection of these three cell lines demonstrated that although II4 and RT3 cells were proven to be tumorigenic by forming malignant subcutaneous tumors in nude mice [120, 121], they were not simultaneously highly permissive for NDV replication. This results indicated that there must exist specific deregulated cellular factors which render tumor cells susceptible to NDV.

In contrast to II4 cells, the highly malignant RT3 cell line showed at least transient NDV susceptibility. Subcloning of RT3 cells led to the isolation of a clone (K1) which was characterized by an increased malignant phenotype in terms of anchorage-independent growth in soft agar. Although *in vitro* proliferation was not increased, tumor growth *in vivo* was significantly elevated compared to RT3 cells which hints to improved adaptation to the *in vivo* growth environment.

H-Ras protein expression levels did not differ in RT3 K1 cells compared to parental RT3 cells and could therefore not account for the enhanced malignant phenotype. This result indicated that there had to be additional deregulated pathways leading to the increased malignancy of RT3 K1 cells. Previous attempts (in 2001) by Mueller and colleagues [121] to gain such subclonal cells were unsuccessful. *In vitro* subcloning of benign or malignant Ras-transfomed HaCaT cell lines did not reveal clones with malignant or increased malignant phenotypes, respectively [121]. However, these cell lines were originally isolated following one round of *in vivo* passaging. In this study, the highly malignant RT3 cells, which were a result of three rounds of *in vivo* passaging, were used for the subcloning experiments. Due to the repeated selective pressure and cultivation *in vivo,* the likelyhood to gain cells with enhanced malignant phenotypes increased. The subclonal cell line RT3 K1 could thus have featured genetic alterations that caused not only increased malignancy but also elevated NDV susceptibility. Enhanced NDV susceptibility of RT3 K1 cells compared to the parental RT3 cell line and HaCaT cells was demonstrated by different approaches. RT3 K1 cells showed elevated viral transgene expressions and increased oncolysis. Furthermore, NDV replication in this cell line was characterized by enhanced production and release of infectious progeny virus compared to RT3 and HaCaT cells. Viral protein production following NDV infection demonstrated, that a general lack of cell binding, entry of the virus and viral protein synthesis could be ruled out as a reason for the non-susceptibility of HaCaT cells. However, levels of viral protein expression and release of infectious viruses was decreased in HaCaT cells compared to RT3 and RT3 K1 cells. It indicated that there must exist deregulated tumor cell-specific cellular factors or pathways that do not counteract but support the NDV life cycle.

Consequently, these utilized epithelial cell lines of the HaCaT-derived model for tumorigenic transformation constituted an ideal cellular model to investigate the tumor cell-specific NDV replication systematically and in more detail. As 85 % of all cancers are cancers of epithelial cells (http://www.cancerhelp.org.uk/help/default.asp?page=98#epith), such a unique epithelial cell line model for oncolysis, established and validated in this study, could be a valid tool to discover novel drug candidates or tumor biomarkers for NDV replication.

5.3 Tumorigenic HaCaT cells show no eIF-2Bε-mediateted deregulated translational control but defects in the IFN-mediated antiviral response

There are several mechanisms proposed which potentially mediate oncolytic virus susceptibility. For example, in a diverse range of oncolytic VSV-susceptible rodent and human tumor cells, increased expression levels of eIF-2Bε were demonstrated [97]. Overexpression of this subunit of eIF-2B was supposed to mediate a partial overcome of translational blockade induced by eIF-2α phosphorylation following VSV infection [97]. In the Ras-transformed HaCaT cell lines with varying degree of NDV susceptibility, no differences in eIF-2Bε expression levels were detected (see Figure 4-11). Hence, translational deregulation induced by increased expression of eIF-2Bε could be ruled out as a reason for increased NDV susceptibility in RT3 K1 cells.

Furthermore, tumorigenic cells are often characterized by mutations of gene products in the IFN-signaling pathway e.g. deletions of the IFN type I genes or STAT1 or 2 deficiency [144, 163]. These IFN-non-responsive cancer cells may have acquired a growth and survival advantage over their normal counterparts which simultaneously renders them susceptible to oncolytic virus replication [89]. Severe defects in the IFN-signaling pathway, as a reason for enhanced NDV susceptibility of RT3 K1 cells, could not be confirmed in this study. Instead, secretion of biological active IFN type I was even elevated in both tumorigenic RT3 and RT3 K1 cells compared to HaCaT cells following infection with NDV. Furthermore, RT3 K1 cells could be protected from NDV-mediated oncolysis when pre-stimulated with IFN type I. It indicated, that there was no general insensitivity to IFN-mediated antiviral response in these cells. These observations could be confirmed by the finding that STAT1 and 2 were still constitutively expressed in all three cell lines. However, when cells were infected with NDV, activation of both transcription factors STAT1 and 2 by phosphorylation was found to be retarded in RT3 and RT3 K1 cells compared to HaCaT cells (see Figure 4-13). Delayed and decreased STAT1 and 2 activation could be a result of reduced levels of the IFNAR on the cell surface of these cancer cells [164]. Another cause for this lower STAT activation might be the impaired activation or activity of the JAK1 and/ or TYK2 kinases which normally provide IFN-mediated signal transduction via STAT phosphorylation. In normal cells, induction of the IFN pathway leads to an increase of STAT protein expression due to a positive feedback loop mechanism. In contrast to HaCaT and RT3 cells, inductions of STAT1 and 2 protein expression following infection of RT3 K1 cells was found to be absent (see Figure 4-13). The absence of induction together with the retarded phosphorylation of STAT1

and 2 could hint to a reduced persistence of an antiviral state in RT3 K1 cells and might explain the increased production of viral proteins and progeny virus in this cell line. The loss of STAT protein inductions might be explained by negative regulation caused by oncogenic H-Ras activity in these cells similar to what was shown for activated K-Ras transformed human colon cancer cell lines [165].

A consequence of defects in the JAK/STAT-signaling cascade should be a reduced induction kinetic and expression level of IFN-stimulated antiviral genes such as MxA, OAS1, PKR or IFITM1. In the investigated cell lines, all four antiviral genes were found to be expressed. The basal expression level of constitutively expressed PKR and OAS1 were not tumor cell-specifically reduced in RT3 and RT3 K1 cells compared to HaCaT cells. Thus, it could be shown in this study that generally reduced basal levels of antiviral genes are not determinant for enhanced NDV susceptibility in the tumorigenic HaCaT cells. Furthermore, NDV infection resulted in an indisputable induction of the antiviral genes PKR, OAS1 and MxA not only in HaCaT cells but also in RT3 and RT3 K1 cells. Nevertheless, MxA protein expression was clearly delayed and decreased in RT3 compared to HaCaT cells. In addition, IFITM1 expression was severely impaired both on RNA level and on protein level in RT3 cells (see Figure 4-17). This phenomenon was even more obvious in the highly NDV-susceptible RT3 K1 cells. The observed differences in the induction and expression levels of antiviral factors might be the leading cause for NDV-replication in the tumorigenic HaCaT cells and could explain the increased NDV susceptibility of RT3 K1 cells compared to the parental RT3 cell line. However, in contrast to VSV-replication which was shown to be directly or indirectly inhibited by MxA or IFITM1 antiviral activities [166, 167], IFN-inducible antiviral proteins that function specifically against NDV replication had not been demonstrated so far. Up to now, defects in antiviral gene induction were only demonstrated to correlate with NDV susceptibility of tumor cells [91, 92]. Therefore, the ISG IFITM1, which was shown to be most severely inhibited in the highly NDV-susceptible RT3 K1 cells, was chosen to be further investigated with respect to its NDV-directed antiviral function. Following siRNA-mediated knockdown in non-susceptible HaCaT cells, no elevated NDV replication could be detected. This result led to the conclusion, that the antiviral activity of IFIMT1 against NDV was not critical for the HaCaT derived model for oncolysis. In the future it has to be clarified if MxA and/ or OAS1 activity directly interfere with NDV-replication Furthermore, it would be of interest, whether the observed strongly reduced protein induction level of MxA directly cause NDV susceptibility in the tumorigenic HaCaT cells.

Oncolytic reovirus replication had been demonstrated to be connected with an activated Ras-pathway [93]. It is currently predicted that multiple Ras-signaling pathways cooperate in viral oncolysis by augmenting different reovirus replication steps [95]. However, in a mouse embryonic fibroblast cell line NIH-3T3, Ras transformation was shown to mediate PKR inhibition. As a consequence, translational blockage following reovirus infection was prevented and viral protein synthesis could proceed [93]. Despite Rastransformation of RT3 and RT3 K1 cells, these cells still exhibited PKR phosporylation and no delay in PKR activation following NDV infection compared to HaCaT cells (see Figure 4-16). Therefore, unlike reovirus replication in these rodent cells, tumor cell-specific NDV replication in human HaCaT-derived tumor cell lines must be caused by different mechanisms than Ras-mediated inhibition of PKR activation.

In summary it was found in this study, that the NDV-susceptible cell lines RT3 and RT3 K1 did not show a complete shut down of IFN-signaling as described for other tumor cells. However, the observed delayed induction of the JAK/STAT-signaling cascade as well as impaired MxA and IFITM1 protein inductions and expressions, especially in the highly NDV-susceptible cell line RT3 K1, might hint to a reduced or weakened antiviral activity in this cell line. Nevertheless, it remains to be determined whether the reduced and delayed induction levels of the antiviral effector MxA, unlike IFITM1, mediate NDV susceptibility and could account for increased virus production in RT3 K1 cells.

5.4 Ras is necessary but not sufficient to render non-susceptible HaCaT cells NDV-susceptible

A severe disruption of the IFN-signaling pathway as a leading cause for NDV susceptibility of Ras-transformed HaCaT cells could not be demonstrated. Subsequently, it was investigated whether NDV susceptibility of RT3 K1 cells was generally mediated by oncogenic Ras. In fact, in 1994, Lorence and colleagues [98] reported that human fibroblasts were rendered 1000 times more NDV-susceptible after transformation with activated N-Ras. In the present study, siRNA-mediated H-Ras depletion indeed rendered RT3 K1 cells non-susceptible to NDV. This demonstrated that H-Ras activity was necessary for efficient NDV replication in this tumor cell line. However, in the reverse experiment, overexpression of oncogenic H-Ras in HaCaT cells alone (HaCaT-Ras subclone H6, see Figure 4-24) as well as H-Ras transformation with subsequent *in vivo* tumor growth (II4 cells, see Figure 4-2) was not generally sufficient to induce NDV susceptibility. Severely differing expression levels of H-Ras protein could not be the reason for the inconsistent phenotypes with respect to NDV

permissiveness of these oncogenic Ras-transformed or tranfected cell lines as shown in Figure 4-22. Furthermore, oncogenic Ras activity of any of these cell lines was indirectly proven by anchorage-independent growth in soft agar (see Figure 4-23). However, the highly NDV-susceptible RT3 K1 cells excelled in increased colony sizes which could hint to an elevated Ras activity. An *in vitro* assay for quantification of Ras activity might clarify, if varying degrees of Ras activity in these cells are responsible for different NDV-susceptibilities. Beside the isolation of a non-susceptible HaCaT-Ras subclone (H6), a NDV-susceptible HaCaT-Ras subclone (H5) was also isolated. The susceptible Ras-clone neither showed obvious differences in Ras protein expression nor increased colony formation in soft agar compared to the non-susceptible Ras-clone (see Figure 4-22 and Figure 4-23). This contradictory result could indicate, that the individual genetic background of the recipient cell, e.g. pre-existing deregulated factors or pathways, might be determinant for Ras-mediated susceptibility. Another explanation might be the specific integration site of the lentiviral transduced Ras oncogene in the genome of this recipient cell. Integration of the transgene might have interrupted a gene whose gene product normally provides viral resistance.
This led to the conclusion that there must be deregulated factors or pathways in addition to Ras that support NDV susceptibility. An siRNA-based screening was utilized to reveal such NDV-sensitizing factors.

5.5 An siRNA-based screen identifies several oncolytic NDV-sensitizing candidate genes in tumorigenic RT3 K1 cells

The siRNA-based screening approach was established and performed to identify NDV-sensitizing factors in the Ras-transformed NDV-susceptible RT3 K1 cell line. Two focussed siRNA libraries targeting tyrosine kinases and membrane trafficking/ remodeling factors were chosen to be applied in the non-automated screen. Tyrosine kinases are important signal transducers of a variety of cellular signaling pathways and are frequently found to be deregulated or aberrantly expressed in human malignancies [150]. Besides, candidate genes involved in membrane trafficking/remodeling could potentially play an important role in the life cycle of NDV in terms of internalization, intracellular trafficking or release. As the NDV viral life cycle is not completely understood any of these chosen siRNA library candidate genes could potentially support or inhibit viral replication.
In order to evaluate and compare the performances of the siRNA screenings, three siRNA-based positive controls for inhibition of viral replication were designed. Simultaneous targeting of viral P- and V-mRNA, by utilizing any of the three designed siRNAs, resulted in

a strong reduction of viral replication. It was demonstrated by reduced viral luciferase activity following infection and inhibition of oncolysis of NDV-infected RT3 K1 cells. Furthermore, results were confirmed by decreased levels of released progeny virus in supernatants of infected RT3 K1 cells. Deprivation of P-protein severely impairs RNA synthesis as it is an essential component of the RNA-dependent RNA transcriptase activity complex. The influence of siRNA-mediated V-protein withdrawal on viral replication in human tumor cells is currently unknown. However, it was demonstrated to target avian STAT1 for protein degradation [43]. It is therefore a major virulence factor in poultry leading to inhibition of IFN-mediated antiviral defense. These results illustrated that targeted knockdown of these specific viral mRNAs is sufficient to efficiently block viral replication. SiRNAs targeting viral P- and V-RNA could therefore successfully be applied as positive controls for reduction of viral replication and to confirm the comparable performances of the siRNA screenings.

The established siRNA screening approach, based on oncolytic NDV replication in tumor cells, resulted in the identification of six NDV-sensitizing genes out of 188 candidate genes (see Table 4-2). NDV-sensitizing effects were detected by altered viral luciferase activity and additionally by modified expression of the viral transgene EGFP. Expressions of these proteins and their specific siRNA-mediated knockdown were confirmed independently.

All of these identified genes had never been connected with oncolytic NDV replication before.

Interestingly, only the membrane trafficking library revealed new candidate genes whilst no tyrosine kinases were among the validated NDV-sensitizing genes. Furthermore, only genes leading to a reduction of viral replication after knock down were identified. No genes that induce NDV replication or cytotoxicity when knocked down were found. It was likely that based on the stringent selection procedure of NDV-sensitizing genes as well as the chosen screening conditions the identification of NDV replication-reducing genes was more favorable. Additionally, by utilizing the already highly NDV-susceptible RT3 K1 cells in the screen it could be possible, that there was no dramatic increase of viral replication feasible due to limitations of exploited cellular processes. However, in the secondary siRNA screen, one out of four individual siRNAs per target gene (AP1B1, Pak1 or Rac1) induced a strong increase in viral luciferase activity following transfection. It could be due to individual off-target effects directly influencing viral luciferase activity.

The screening revealed a number of genes reducing viral replication to at least 50 % compared to the control. This finding illustrates that the replication cycle of NDV strongly depends on the cellular machinery. Due to the fact that the knockdown of single genes already

resulted in a dramatic reduction of viral replication, it can be concluded that NDV-reproduction is highly dependent on the function and activity of single cellular factors.

In this screen the confirmed NDV-sensitizing genes could either be grouped to or associated with clathrin-mediated endocytosis or protein-sorting (CLTA, AP2A1 and AP1B1) or actin cytoskeletal reorganization processes (Rac1, RhoA and Pak1). Clathrin, which is composed of three heavy chains and three light chains, acts as an multifunctional protein and mediates not only endocytosis and intracellular trafficking on the trans-Golgi network (TGN) but also participates in sorting of basolateral proteins at the TGN of polarized epithelial cells [168]. Adaptor-protein complexes such as AP2 and AP1, which comprise of different subunits, mediate the sorting of membrane proteins in the endocytic and secretory pathways and are involved in the formation of clathrin-coated vesicles by recruiting clathrin [169]. The cellular factors CLTA (a light chain of clathrin), AP2A1 (subunit of the AP2 complex) and AP1B1 (subunit of the AP1 complex), that were confirmed in the siRNA screen to support NDV susceptibility, could potentially participate in viral internalization processes or protein trafficking e.g. of the glycoproteins HN and F to the plasma membrane.

Rac1 and RhoA are prototypic members of the Rho-family of small GTPases and the serine/ threonine kinase Pak1 is known to be a Rac1 effector. The best characterized function of these proteins is their role as regulators of the actin cytoskeleton [170]. The actin cytoskeleton mediates a variety of essential biological functions in all eukaryotic cells. It provides a structural framework for defining cell shape and polarity. Furthermore, its dynamic properties provide the driving force for cells to move and to divide [170]. Rho GTPase-controlled cytoskeletal rearrangements promote, for example, cell shape and motility as well as cell-cell and cell-matrix contacts [171]. Viruses are known to exploit the cellular actin cytoskeleton to facilitate different steps of their viral life cycles e.g. entry, intracellular trafficking or release [172]. The siRNA confirmed cellular factors Rac1, RhoA and Pak1, which were shown to promote NDV susceptibility in this study, could potentially support any of the actin-dependent processes during the viral life cycle.

None of the above described NDV-sensitizing factors have been connected with the viral life cycle of NDV before. Therefore, this novel siRNA-based cellular screening approach proved to be a valid tool to further elucidate cellular factors essential for oncolytic NDV replication.

Interestingly, when comparing protein expression levels of all siRNA-confirmed hits in non-tumorigenic HaCaT cells and tumorigenic RT3 and RT3 K1 cells, three (AP2, CLTA and Pak1) out of the six identified genes showed tumor cell-specific overexpression (see Figure 4-39). This indicated that the screening approach could potentially be utilized to identify

biomarkers for efficient NDV replication (virotherapy) as well as novel tumor biomarkers or targets for anti-cancer therapy. Indeed, these assumptions could be supported by the following publications about clathrin and Pak1:

Clathrin heavy chain (CHC) was recently found to be tumor-specifically overexpressed, when a comprehensive proteome analysis of hepatocellular carcinomas (HCC) and adjacent non-tumor tissues was performed. These results could be confirmed by immunohistochemical analysis. Detection of CHC was suggested to be used as a biomarker which could substantially contribute to early diagnosis of HCC [173]. In the present study, CLTA was found to be overexpressed in RT3 K1 cells but not in HaCaT or RT3 cells. Because RT3 K1 cells were characterized by increased malignancy *in vivo* compared to the parental RT3 cells, it might be a marker of tumorigenic progression in this HaCaT-derived squamous cell carcinoma cell line model.

In addition, Pak1 upregulation or hyperactivation could not only be detected in this present study but has also been detected in a variety of other human tumors e.g. cancer of the breast, liver, kidney, colon and ovarian (reviewed in [174]). Pak1 functions in a variety of cellular processes e.g. cell motility, mitosis and survival [175, 176] and its activation can occur via multiple GTPase-dependent (e.g. via Ras and/ or Rac1) or GTPase-independent mechanism (e.g. via PI3K) [177]. However, its signaling is thought to act as a convergence point in transformation processes induced by various oncogenes e.g. Ras or Rac1. Upregulation of Pak1 expression has been shown to correlate with breast cancer invasiveness as well as tumor cell-specifically increased cyclin D1 expression (reviewed in [177]). Pak1 is therefore considered as a potential therapeutic target for interrupting cancer progression. However, no highly selective inhibitors have been identified, yet (reviewed in [178]).

The identification of three tumor cell-specifically overexpressed cellular factors out of 188 candidate genes indicate, that it could be worth to further extend the screening approach in the future. A genome-wide screening could potentially reveal a variety of biomarkers or targets for anti-cancer therapy.

5.6 The screening candidate Rac1 is essential for NDV susceptibility in tumorigenic RT3 K1 cells as well as in other tumor cells

The siRNA-confirmed NDV-sensitizing Rac1 was chosen to be further validated and analyzed. It was reported to be involved in virus sensitizing activities as well as connected with transformational processes in cells. Up to now, there had been no hints for its involvement in oncolytic virus replication.

The Rho GTPase Rac1 is ubiquitously expressed and like all GTPases, it can exist in two conformational states, an inactive GDP-bound form and an active GTP-bound form. In response to extracellular stimuli (such as receptor kinases, G-protein-coupled receptors or integrins), the interconversion of these states occurs. GEFs thereby convert Rac1 to its active form and GAPs inactivate Rac1 [179]. Rac1 interacts with specific effectors through domains that coordinate activation of a variety of signaling cascades and therefore influences diverse physiological outcomes. One of the first described Rac1 effector proteins was the family of p21 activating kinases (Pak). However, some of the Rac1-mediated functions are cell type-specific and new roles are still emerging. In particular, keratinocytes are known to rely on Rac1 signaling to establish and maintain E-cadherin-mediated cell–cell adhesion [180]. It was demonstrated that Rac1 regulates adherens junctions through endocytosis of E-cadherin in an actin-dependent manner. E-cadherin was found to be recycled. This mechanism is therefore supposed to play a role in tissue remodeling events, such as a wound healing, where dynamic regulation of E-cadherin by Rac1 would allow the continual disruption and reformation of cell–cell contacts [181].

5.6.1 Rac1 influences the life cycle of oncolytic NDV

In this study, a previously unknown pivotal role for Rac1 in the life cycle of oncolytic NDV could be demonstrated. The NDV-sensitizing activity of Rac1 in RT3 K1 cells was confirmed by three independent experimental procedures using (I) Rac1-specific siRNAs, (II) a Rac1 small molecule inhibitor and (III) expression of a dominant negative mutant Rac1T17N. This clearly demonstrated that Rac1 is an essential NDV-sensitizing cellular factor in RT3 K1 cells. In addition, the Rac1 effector kinase Pak1 was also among the validated screening candidates which reduced viral replication when knocked down.

Rac1 seems to be primarily located at the plasma membrane [182]. It is best-known for its pivotal role in the reorganization of the actin cytoskeleton. Studies predominantly performed in fibroblasts revealed, that it participates in the regulation of cell shape and motility by

promoting lamellipodia formation (sheet-like plasma membrane protrusions formed by F-actin polymerisation) and membrane ruffling (motile wave like cell-surface structures) [141]. As actin cytoskeletal dynamics are closely linked to endocytosis and vesicular trafficking, Rac1 has also been implicated in these processes (reviewed in [183]).

It is known that viruses can make use or manipulate the cytoskeletal network of actin filaments during their life cycles. Virus-induced Rac1 activity has been linked to infection or trafficking processes as well as release of several viruses causing severe human diseases, such as HIV [154], Ebola [155], HSV-1 [153] and HBV [152]. For paramyxoviruses of different genera, Simian virus 5 and Hendra virus, increased F-protein-induced cell-cell fusions have been observed in cells transfected with activated Rac1. It remained to be determined whether it could play a role for viral entry or syncytia formation [184]. However, NDV replication in RT3 K1 cells was not accompanied by syncytia formation which excluded a role for Rac1 in that process in this cell line. However, an immunofluoresence experiment hinted to a role for Rac1 in early steps in the viral life cycle. In this experiment RT3 K1 cells were pretreated with the NSC 23766 inhibitor demonstrated to selectively inhibit Rac1 activation but not Cdc42 or RhoA activation [138]. Subsequent to inhibitor treatment, cells were infected with NDV. When these permeabilized cells were immunofluorescently stained for NDV-specific proteins, a dramatically decreased level of viral proteins was detected compared to the solvent control. As cells were fixed at an early time point after infection, this result could hint to a role for Rac1 in viral internalization processes. For NDV it was recently shown that it may enter cells not only via membrane fusion but also by caveolae-dependent endocytosis as an alternative route [46]. It has also been demonstrated for other virus e.g. HIV [185] or Vaccinia virus [186] that they can enter cells through direct fusion at the plasma membrane or through diverse endocytotic processes. In most cases the mode of internalization was shown to be cell-type-specific. For example, single-particle tracking of influenza virus in cultured simian kidney epithelial cells showed, that although 60 % of the viral particles entered cells via clathrin-coated pits, 40 % used a clathrin-independent pathway [187].

5.6.2 NDV-sensitizing feature of Rac1 is potentially mediated by its involvement in virus internalization processes

In human keratinocytes, Rac1 has been reported to regulate adherens junctions through endocytosis of E-cadherin [181]. In fact, one of the first described functions of Rac1 was the stimulation of macropinocytosis [141]. Interestingly, one of the most important effector kinases which is needed during all stages of macropinocytosis is Pak1 (reviewed in [188]).

Furthermore, it is known that macropinocytosis is also highly dependent on PI3K activity. PI3K inhibitors, such as LY294002, have been shown to block macropinocytosis in cells [189, 190]. One has to bear in mind that kinase inhibitors are often characterized by non-specific side effects. However, NDV replication clearly decreased in RT3 K1 cells pretreated with LY294002 in a dose-dependent manner. Macropinocytosis is a clathrin-independent but actin-dependent endocytotic process characterized by large, heterogenous vesicular structures (macropinosomes) caused by the closure of lamellipodia at sides of membrane ruffling [191]. It is considered as a non-specific mechanism for internalization of fluids and membrane, activated in response to cell stimulation. However, a variety of viruses can directly or indirectly induce this typical membrane ruffling behavior e.g. Vaccinia virus, HIV and HSV-1 (reviewed in [188]). As a result, they can be internalized together with fluid in macropinosomes. With respect to HSV infection, which can occur by utilizing endocytic or non-endocytic (membrane fusion) mechanisms, infection of HaCaT cells was proposed to depend on macropinocytosis [192]. As epithelial cells, such as keratinocytes, are characterized by a dense layer of cortical actin underneath the plasma membrane, HSV might exploit this distinct entry mechanism in order to bypass this barrier [192]. This implicated that viral entry via macropinocytosis is generally feasible in HaCaT-derived cell lines. With respect to the NDV-susceptible RT3 K1 cells, Pak1 overexpression could hint to increased macropinocytotic activity in this tumorigenic cell line. It could therefore be possible that enhanced macropinocytosis could promote a passive mechanism of viral entry in RT3 K1 cells.

Overexpression of constitutively activated H-Ras has been demonstrated to stimulate Rac1 activation, leading to plasma membrane ruffling and macropinocytosis in fibroblasts [141, 193, 194]. However, neither expression of oncogenic H-Ras (HaCaT-Ras subclones) nor H-Ras transformation with subsequent *in vivo* tumor growth (II4 cells) was shown to render HaCaT cells generally susceptible to NDV in this study. In 1990, Boukamp and colleagues [120] reported, that no obvious change in cell morphology was observed when HaCaT cells were overexpressed with activated H-Ras. The different effects of oncogenic H-Ras and Rac1wt transfection on NDV susceptibility of HaCaT cells could be explained by Ras-isoform-specific, cell type or cell line specific differences in cell signaling. For example, H-Ras was shown to be a more potent activator of PI3K than K-Ras [195]. In contrast, Walsh and colleagues [10] demonstrated, that Rac1-mediated membrane ruffling and macropinocytosis was more efficiently induced following microinjection of activated K-Ras than H-Ras in rat embryonic fibroblasts. This phenomenon was explained by distinct

membrane domain localizations of the Ras isoforms. Different localizations could influence the efficiency of activating the Rac1 pathway [10].

Rac1 and PI3K were also described to affect other endocytic pathways e.g. clathrin-mediated endocytosis [196, 197]. This endocytotic pathway is the major transport pathway from the plasma membrane to early endosomes. It comprises plasma membrane invagination into clathrin-coated pits whereby adaptor protein complexes, e.g. AP2, bridge the interaction of clathrin with cargo [198]. So far, Rho GTPases, such as Rac1, were not supposed to have obligate functions in this specific endocytotic process but seem to regulate the efficiency of internalization [196]. Up to now, there were no hints for a clathrin-mediated endocytotic pathway for NDV internalization. By considering the fact that genes involved in clathrin-mediated endocytosis like CLTA and AP2A1 (a subunit of AP2) were among the validated NDV-sensitizing genes, this alternative mode of cell entry seemed conceivable, too. In this study, not only Pak1 but also CLTA and AP2A1 were shown to be tumor cell-specifically overexpressed in RT3 K1 cells. It could hint to enhanced or deregulated endocytotic processes in this malignant cell line. This phenomenon is currently also discussed as being a common feature of tumor cells [199]. However, there are no data supporting Rac1-dependent clathrin-mediated endocytosis of NDV so far. By performing immunofluorescence co-localization studies of Rac1 and clathrin early after NDV infection, the importance of these factors during NDV internalization in RT3 K1 cells could be revealed.

In general, the increase of viral replication could be caused by an elevated uptake rate of viral particles via endocytotic processes or increased membrane fusion triggered by Rac1. Clathrin-mediated endocytosis or macropinocytosis could constitute alternative routes of NDV internalization. In this study, entry of NDV into non-susceptible HaCaT cells was indirectly demonstrated by Western blot analysis of viral protein production following infection. However, this experiment did not allow a quantitative evaluation of virus entry and could therefore not be used to prove the hypothesis. In order to compare the efficiency of viral entry in HaCaT and RT3 K1 cells, quantitative internalization experiments are necessary. For example, internalized viruses could be measured by using radioactive-labeled NDV or counted by electron microscopy shortly after infection of these cells.

The hypothetic role for Rac1 in virus internalization processes is based on an initial immunofluorescence experiment in this study. It can not be ruled out that NDV also exploits other Rac1-mediated actin-dependent processes during its reproduction in the cell. Giuffre and colleagues demonstrated in 1982 [200], that the viral M-protein of NDV interacts with cellular actin. The M-protein is essential for viral assembly at the plasma membrane before

budding can take place. Beside regulation of actin dynamics, Rac1 is also a regulator of several other, partially cell type dependent, cellular processes, for example, proliferation, gene transcription and microtubule stabilization [183]. Further experiments are necessary to elucidate the exact NDV-sensitizing mechanism of Rac1. Nevertheless, Rac1 likewise influenced the NDV susceptibility of other epithelial tumor cell lines with activated K-Ras mutations in this study MDA-MB-231 [201, 202] and HCT 116 [202, 203].
In summary, the data might indicate a general NDV-sensitizing effect of Rac1 that is not only restricted to the HaCaT cell line model.

5.6.3 Rac1 potentially influences tumorigenesis in the HaCaT-derived, Ras-transformed tumor cell line model

There is striking evidence that Rac1 is also involved in cell transformation processes (reviewed in [183]). *In vitro* and *in vivo* studies using tumor-derived cell lines, primary tumors and mouse-models clearly show, that deregulated signaling of small Rho GTPases, such as Rac1, play important roles in the initiation as well as the progression of cancer. For example, in 2001, Coniglio and colleagues [204] observed that activated Rac1 can suppress apoptosis in epithelial cells cultured in anchorage-independent conditions. Besides, in 2005, Chan and colleagues [205] described a role of Rac1 in human breast and glioma tumor cell invasion. So far, there have been no mutations in Rac1 proteins detected. It strongly suggests that its aberrant signaling in cancer is caused by alterations at the level of Rac1 regulators rather than by mutations at the level of this small Rho GTPase [206]. In addition to aberrant Rac1 activation, overexpression of Rac1 has been found in many tumor types including cancers of the breast, lung and colon (reviewed in [183]). Specific mechanism by which Rac1 influences transformation and tumor progression are still subject of investigations. However, it is proposed that deregulated Rac1-signaling promotes tumorigenesis by modulating the activities of several transcription factors e.g. nuclear factor-kappaB (NF-κB), activator protein-1 (AP-1) and STAT3. These transcription factors regulate the expression of genes involved in tumorigenic events like cell proliferation, tumor angiogenesis and cell survival [207]. There exists evidence that deregulated Rac1 can lead to a loss of adhesion to the extracellular matrix (ECM) and increased invasiveness. These features are not only caused by modulation of the actin cytoskeleton but also by increasing transcriptions of metalloproteinases (enzymes which are capable of degrading ECM) or by regulating levels of their antagonists (reviewed in [208] and [183]).

Interestingly, Rac1 activity has been shown to be required for Ras transformation [156, 157] Rac1-promoted malignant phenotypes of skin keratinocytes was demonstrated in a H-Ras transformed mouse squamous cell carcinoma cell line. By expression of the dominant negative mutant Rac1T17N, markers of malignancy decreased including colony formation in soft agar and *in vivo* tumor growth [209]. In human Ras-transformed RT3 K1 cells, Rac1 was not found to be overexpressed and the activity of Rac1 in this cell line was unknown (see Figure 4-39). Nevertheless, just as in the experiment performed in malignant mouse skin keratinocytes by Kwei and colleagues [209], the expression of the dominant negative mutant Rac1T17N in RT3 K1 cells led to a loss of colony formation in soft agar. This effect indicated that Rac1 was involved in the maintainance of anchorage-independent growth in this human Ras-transformed tumor cell line. Currently, anchorage-independence is best understood in terms of constitutive oncogene-generated signals, which are thought to replace the normal integrin-dependent signaling required for anchorage-dependent cell growth and survival. Indeed, Rac1 is an effector of normal integrin signaling cascades, and its activated counterpart is known to be a potent driver of anchorage-independent growth [204]. *In vivo* tumor growth experiments will have to clarify if the loss of anchorage-independent growth in RT3 K1_Rac1T17N cells also correlates with decreased tumorigenic growth, reduced tumor vascularization and/or metastasation.

Activation of Rac1 by (oncogenic) Ras has been shown to either occur via PI3K [16] or by the Rac1-specific GEF TIAM1 [210], which was recently identified to be a relevant effector of Ras. It is proposed that TIAM1 is a critical downstream mediator of Ras-induced oncogenesis by sustained activation of the Rac1-signaling pathway [159]. Overexpression of TIAM1 has been reported in highly invasive breast tumors and colon carcinomas. Its aberrant expression in these cancers is also proposed to contribute to elevated Rac1 signaling [207].

In fact, in Ras-transformed HaCaT tumor cell lines, TIAM1 expression was found to be increased compared to the parental HaCaT cells (see Figure 4-41). Interestingly, the degree of TIAM1 overexpression correlated with the stage of malignancy in RT3 and RT3 K1 cells. Further investigations would be necessary to analyze, if TIAM1 can function as a prognostic marker for cancer progression in this squamous cell carcinoma cell line model. So far, a correlation was demonstrated, for example, for prostate [211] and breast tumors [212].

RT3 K1 cells showed signs of increased lamellipodia formation compared to HaCaT cells. Furthermore, a Rac1-dependent ability of anchorage-independent growth was demonstrated as well as enhanced expression of the Rac1-GEF TIAM1. These observations could hint to elevated Rac1 activity in RT3 K1 cells. This assumption might be proven by analysing and

comparing the Rac1 activity in the HaCaT-derived cell line model by utilizing an *in vitro* Rac1 activity assay.

Altogether, unlike Ras, Rac1 was shown to be sufficient to induce viral susceptibility in HaCaT cells and to be essential for viral replication in RT3 K1 cells. In addition to that, malignant Ras-transformed RT3 K1 cells were demonstrated to depend on Rac1 activity with respect to anchorage-independent growth, and increased expression of the Rac1-GEF TIAM1 correlated with enhanced malignancy. Rac1 could therefore establish a missing link between tumorigenesis and oncolytic virus replication in the HaCaT-derived multistage model for skin carcinogenesis. As a next step, NDV-susceptible tumor cell lines could be analyzed with respect to Rac1 overexpression or increased Rac1 activity. In case of correlations between NDV susceptibility and aberrant Rac1-signaling, this cellular factor could be used as a biomarker for efficient replication of oncolytic NDV.

5.7 Conclusions

The developed siRNA-based screening approach, which utilizes oncolytic NDV replication in the NDV-susceptible HaCaT-derived tumor cell line RT3 K1, has proven to be a valid tool to detect novel tumor cell-specific NDV-sensitizing genes. This screening approach therefore provides a basis for the identification of novel tumor-associated drug targets as well as biomarkers for therapeutic oncolytic virus replication.

In this study it was demonstrated, that NDV susceptibility of the Ras-transformed RT3 K1 cells is not only determined by defects in the antiviral IFN-signaling pathway and oncogenic Ras but also by a variety of additional cellular factors, such as AP1B1, AP2A1, CLTA, Pak1, Rac1 and RhoA.

A subsequent comparison of protein expression levels of these genes in the HaCaT-derived model for oncolysis allowed for the detection of tumor cell-specifically overexpressed NDV-sensitizing genes (AP2A1, CLTA, Pak1). In addition, it enabled to evaluate the potential of such genes to directly mediate NDV-susceptiblity and tumorigenic transformation of cells (demonstrated for Rac1). The screening approach and its final outcome is depicted in Figure 5-1.

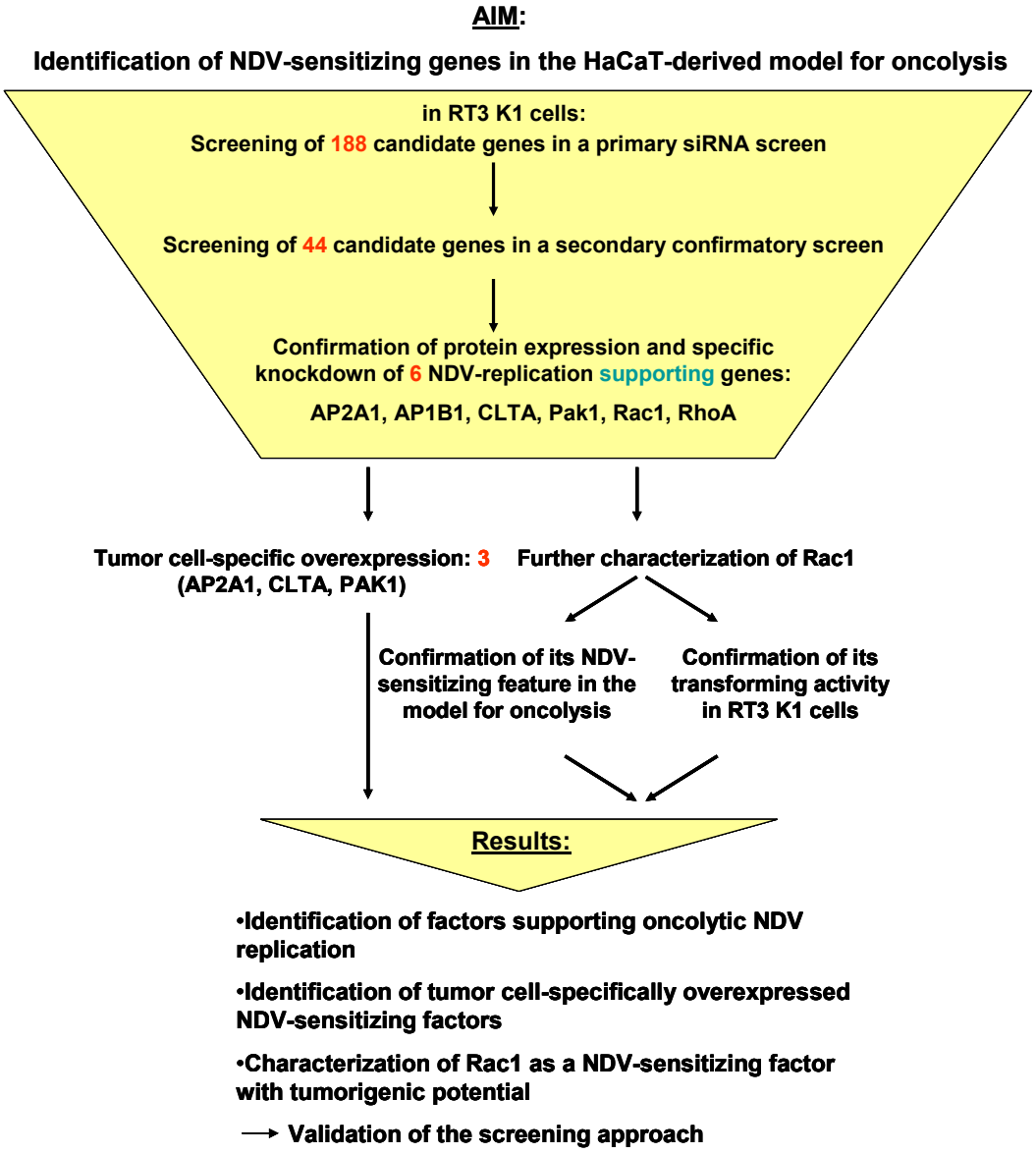

Figure 5-1: Flowchart of the siRNA-based screening approach and its outcome
The HaCaT-derived model for oncolysis was used to identify novel NDV-sensitizing genes in human tumor cells.

The siRNA screening candidate Rac1 was illustrated to be essential for NDV replication in the HaCaT-derived model for oncolysis as well as in other NDV-susceptible tumor cell lines with activated Ras. In Figure 5-2, one possible link between Ras-induced tumorigenesis and sensitivity to oncolytic NDV is depicted. Deregulated Rac1 possibly leads to an increased endocytotic activity in Ras-transformed tumor cells. This aberrant condition could promote enhanced viral uptake in RT3 K1 cells compared to non-tumorigenic HaCaT cells (Figure 5-2, part 1). In addition to that, decreased antiviral activity in RT3 K1 cells could then provide a basis for efficient viral replication and further spread (Figure 5-2, part 2+3).

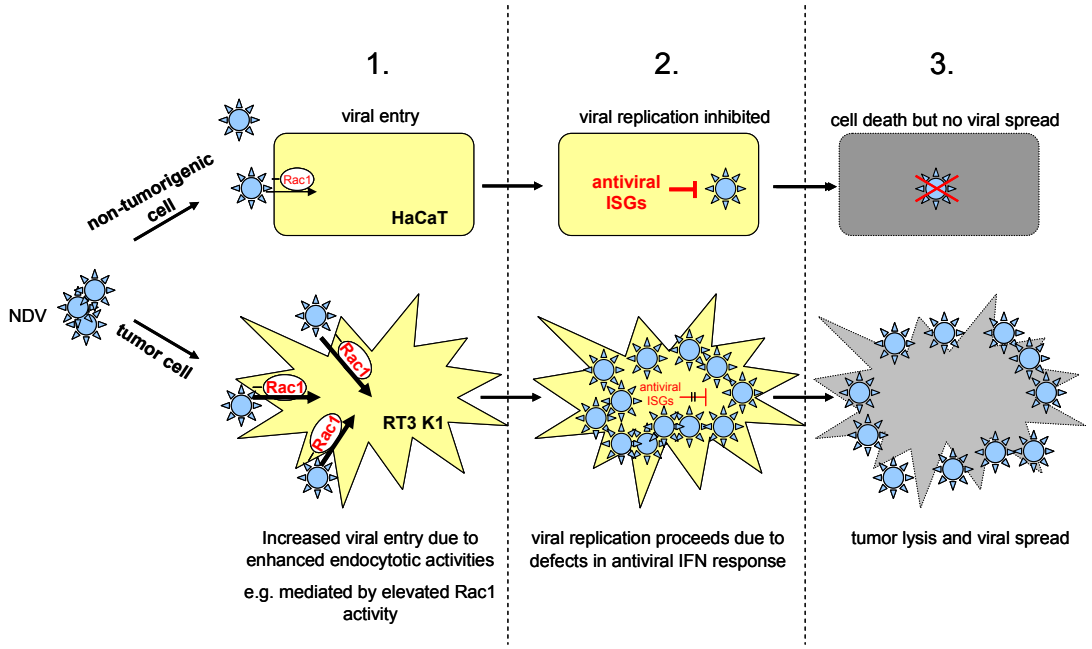

Figure 5-2: Hypothesized model for tumor cell-specific replication of NDV
NDV susceptibility of Ras-transformed tumor cells e.g. RT3 K1 cells is determined by enhanced Rac1-mediated endocytotic activities leading to increased viral uptake compared to non-tumorigenic cells e.g. HaCaT cells (part 1). Following infection, viral replication, cell killing and viral spread are not inhibited in tumor cells due to defects in antiviral defence (part 2+3). In contrast, antiviral ISGs defend viral invaders in non-tumorigenic cells leading to a block of viral replication and spread.

Until now, only limited information was available regarding the link between tumorigenesis and susceptibility to oncolytic viruses, such as NDV. With the help of this study, clathrin-mediated and actin cytoskeleton reorganization processes were identified as additional NDV-sensitizing pathways (besides IFN) in Ras-transformed tumor cells. These findings provide a valid basis to further elucidate the tumor-selective replication of such viruses and could help to improve the efficacy of anti-cancer therapy.

6 REFERENCES

1. Hanahan D, Weinberg RA: **The hallmarks of cancer.** *Cell* 2000, **100:**57-70.
2. Luo J, Solimini NL, Elledge SJ: **Principles of cancer therapy: oncogene and non-oncogene addiction.** *Cell* 2009, **136:**823-837.
3. Kroemer G, Pouyssegur J: **Tumor cell metabolism: cancer's Achilles' heel.** *Cancer Cell* 2008, **13:**472-482.
4. Cherfils J, Chardin P: **GEFs: structural basis for their activation of small GTP-binding proteins.** *Trends Biochem Sci* 1999, **24:**306-311.
5. Donovan S, Shannon KM, Bollag G: **GTPase activating proteins: critical regulators of intracellular signaling.** *Biochim Biophys Acta* 2002, **1602:**23-45.
6. Herrmann C: **Ras-effector interactions: after one decade.** *Curr Opin Struct Biol* 2003, **13:**122-129.
7. Dhillon AS, Meikle S, Yazici Z, Eulitz M, Kolch W: **Regulation of Raf-1 activation and signalling by dephosphorylation.** *Embo J* 2002, **21:**64-71.
8. Wymann MP, Zvelebil M, Laffargue M: **Phosphoinositide 3-kinase signalling--which way to target?** *Trends Pharmacol Sci* 2003, **24:**366-376.
9. Ehrhardt A, Ehrhardt GR, Guo X, Schrader JW: **Ras and relatives--job sharing and networking keep an old family together.** *Exp Hematol* 2002, **30:**1089-1106.
10. Walsh AB, Bar-Sagi D: **Differential activation of the Rac pathway by Ha-Ras and K-Ras.** *J Biol Chem* 2001, **276:**15609-15615.
11. Campbell PM, Der CJ: **Oncogenic Ras and its role in tumor cell invasion and metastasis.** *Semin Cancer Biol* 2004, **14:**105-114.
12. Barbacid M: **ras genes.** *Annu Rev Biochem* 1987, **56:**779-827.
13. Bos JL: **ras oncogenes in human cancer: a review.** *Cancer Res* 1989, **49:**4682-4689.
14. Scheffzek K, Ahmadian MR, Kabsch W, Wiesmuller L, Lautwein A, Schmitz F, Wittinghofer A: **The Ras-RasGAP complex: structural basis for GTPase activation and its loss in oncogenic Ras mutants.** *Science* 1997, **277:**333-338.
15. Khosravi-Far R, Campbell S, Rossman KL, Der CJ: **Increasing complexity of Ras signal transduction: involvement of Rho family proteins.** *Adv Cancer Res* 1998, **72:**57-107.
16. Rodriguez-Viciana P, Warne PH, Khwaja A, Marte BM, Pappin D, Das P, Waterfield MD, Ridley A, Downward J: **Role of phosphoinositide 3-OH kinase in cell transformation and control of the actin cytoskeleton by Ras.** *Cell* 1997, **89:**457-467.
17. Montagut C, Settleman J: **Targeting the RAF-MEK-ERK pathway in cancer therapy.** *Cancer Lett* 2009, **283:**125-134.
18. Franke TF, Hornik CP, Segev L, Shostak GA, Sugimoto C: **PI3K/Akt and apoptosis: size matters.** *Oncogene* 2003, **22:**8983-8998.
19. Nimnual AS, Yatsula BA, Bar-Sagi D: **Coupling of Ras and Rac guanosine triphosphatases through the Ras exchanger Sos.** *Science* 1998, **279:**560-563.
20. Han J, Luby-Phelps K, Das B, Shu X, Xia Y, Mosteller RD, Krishna UM, Falck JR, White MA, Broek D: **Role of substrates and products of PI 3-kinase in regulating activation of Rac-related guanosine triphosphatases by Vav.** *Science* 1998, **279:**558-560.
21. Etienne-Manneville S, Hall A: **Rho GTPases in cell biology.** *Nature* 2002, **420:**629-635.
22. Liu TC, Galanis E, Kirn D: **Clinical trial results with oncolytic virotherapy: a century of promise, a decade of progress.** *Nat Clin Pract Oncol* 2007, **4:**101-117.

23. Huebner RJ, Rowe WP, Schatten WE, Smith RR, Thomas LB: **Studies on the use of viruses in the treatment of carcinoma of the cervix.** *Cancer* 1956, **9:**1211-1218.
24. Southam CM: **Present status of oncolytic virus studies.** *Trans N Y Acad Sci* 1960, **22:**657-673.
25. Everts B, van der Poel HG: **Replication-selective oncolytic viruses in the treatment of cancer.** *Cancer Gene Ther* 2005, **12:**141-161.
26. Garber K: **China approves world's first oncolytic virus therapy for cancer treatment.** *J Natl Cancer Inst* 2006, **98:**298-300.
27. Doyle TM: **A hitherto unrecorded disease of fowls due to a filter-passing virus.** *Journal of Comparative Pathology and Therapeutics* 1927, **40:**144-169.
28. Alexander DJ: *Newcastle disease.* Norwell, Massachusetts: Kluwer Academic Publishers; 1988.
29. Hanson RP: **The reemergence of Newcastle disease.** *Adv Vet Sci Comp Med* 1974, **18:**213-229.
30. Alexander DJ, Allan W.H.: **Newcastle disease virus pathotypes.** *Avian Pathology* 1974, **3:**269-278.
31. Alexander DJ: **Newcastle disease and other Paramyxoviridae infections.** *Desease of Poultry* 1997**:**541-569.
32. Lorence R.M. RMS, Groene W.S., Rabin H.: **Replication-competent, oncolytic Newcastle disease virus for cancer therapy.** *Replication-Competent Viruses for Cancer Therapy* 2003**:**160-182.
33. Alexander DJ: **Newcastle disease and other avian paramyxoviruses.** *Rev Sci Tech* 2000, **19:**443-462.
34. de Leeuw O, Peeters B: **Complete nucleotide sequence of Newcastle disease virus: evidence for the existence of a new genus within the subfamily Paramyxovirinae.** *J Gen Virol* 1999, **80 (Pt 1):**131-136.
35. Fields: *Virology.* 5 edn: Lippincott, Williams & Wilkins, Wolters Kluwer Health; 2007.
36. Schirrmacher V FP: **Newcastle disease virus: a promising vector for viral therapy, immune therapy, and gene therapy of cancer.** *Methods Mol Biol* 2009, **542:**565-605.
37. Garten W, Berk W, Nagai Y, Rott R, Klenk HD: **Mutational changes of the protease susceptibility of glycoprotein F of Newcastle disease virus: effects on pathogenicity.** *J Gen Virol* 1980, **50:**135-147.
38. Nagai Y, Klenk HD, Rott R: **Proteolytic cleavage of the viral glycoproteins and its significance for the virulence of Newcastle disease virus.** *Virology* 1976, **72:**494-508.
39. Nagai Y, Klenk HD: **Activation of precursors to both glycoporteins of Newcastle disease virus by proteolytic cleavage.** *Virology* 1977, **77:**125-134.
40. Iorio RM, Glickman RL, Sheehan JP: **Inhibition of fusion by neutralizing monoclonal antibodies to the haemagglutinin-neuraminidase glycoprotein of Newcastle disease virus.** *J Gen Virol* 1992, **73 (Pt 5):**1167-1176.
41. Takimoto T, Taylor GL, Connaris HC, Crennell SJ, Portner A: **Role of the hemagglutinin-neuraminidase protein in the mechanism of paramyxovirus-cell membrane fusion.** *J Virol* 2002, **76:**13028-13033.
42. Pantua HD, McGinnes LW, Peeples ME, Morrison TG: **Requirements for the assembly and release of Newcastle disease virus-like particles.** *J Virol* 2006, **80:**11062-11073.
43. Huang Z, Krishnamurthy S, Panda A, Samal SK: **Newcastle disease virus V protein is associated with viral pathogenesis and functions as an alpha interferon antagonist.** *J Virol* 2003, **77:**8676-8685.

44. Modrow S. FD, Truyen: **Molecular Virology.** *Spektrum Akademischer Verlag Heidelberg* 2002**:**265-300.
45. Lamb RA, Paterson RG, Jardetzky TS: **Paramyxovirus membrane fusion: Lessons from the F and HN atomic structures.** *Virology* 2006, **344:**30-37.
46. Cantin C, Holguera J, Ferreira L, Villar E, Munoz-Barroso I: **Newcastle disease virus may enter cells by caveolae-mediated endocytosis.** *J Gen Virol* 2007, **88:**559-569.
47. Calain P, Roux L: **The rule of six, a basic feature for efficient replication of Sendai virus defective interfering RNA.** *J Virol* 1993, **67:**4822-4830.
48. Nagai Y, Hamaguchi M, Toyoda T: **Molecular biology of Newcastle disease virus.** *Prog Vet Microbiol Immunol* 1989, **5:**16-64.
49. Yusoff K, Tan WS: **Newcastle disease virus: macromolecules and opportunities.** *Avian Pathol* 2001, **30:**439-455.
50. Laliberte JP, McGinnes LW, Peeples ME, Morrison TG: **Integrity of membrane lipid rafts is necessary for the ordered assembly and release of infectious Newcastle disease virus particles.** *J Virol* 2006, **80:**10652-10662.
51. Alexander DJ: **Newcastle disease, A laboratory manual for the isolation and identification of avian pathogens.** *American Association of Avian Pathologists, In H G Purchase, L H Arp, C H Domermuth, and J E Pearson* 1989.
52. Glickman RL, Syddall RJ, Iorio RM, Sheehan JP, Bratt MA: **Quantitative basic residue requirements in the cleavage-activation site of the fusion glycoprotein as a determinant of virulence for Newcastle disease virus.** *J Virol* 1988, **62:**354-356.
53. Hodder AN, Selleck PW, White JR, Gorman JJ: **Analysis of pathotype-specific structural features and cleavage activation of Newcastle disease virus membrane glycoproteins using antipeptide antibodies.** *J Gen Virol* 1993, **74 (Pt 6):**1081-1091.
54. de Leeuw OS, Koch G, Hartog L, Ravenshorst N, Peeters BP: **Virulence of Newcastle disease virus is determined by the cleavage site of the fusion protein and by both the stem region and globular head of the haemagglutinin-neuraminidase protein.** *J Gen Virol* 2005, **86:**1759-1769.
55. Reichard KW, Lorence RM, Cascino CJ, Peeples ME, Walter RJ, Fernando MB, Reyes HM, Greager JA: **Newcastle disease virus selectively kills human tumor cells.** *J Surg Res* 1992, **52:**448-453.
56. Bar-Eli N, Giloh H, Schlesinger M, Zakay-Rones Z: **Preferential cytotoxic effect of Newcastle disease virus on lymphoma cells.** *J Cancer Res Clin Oncol* 1996, **122:**409-415.
57. Schirrmacher V, Haas C, Bonifer R, Ahlert T, Gerhards R, Ertel C: **Human tumor cell modification by virus infection: an efficient and safe way to produce cancer vaccine with pleiotropic immune stimulatory properties when using Newcastle disease virus.** *Gene Ther* 1999, **6:**63-73.
58. Fabian Z, Csatary CM, Szeberenyi J, Csatary LK: **p53-independent endoplasmic reticulum stress-mediated cytotoxicity of a Newcastle disease virus strain in tumor cell lines.** *J Virol* 2007, **81:**2817-2830.
59. Elankumaran S, Rockemann D, Samal SK: **Newcastle Disease Virus Exerts Oncolysis by both Intrinsic and Extrinsic Caspase-Dependent Pathways of Cell Death.** *J Virol* 2006, **80:**7522-7534.
60. Schirrmacher V, Jurianz K, Roth C, Griesbach A, Bonifer R, Zawatzky R: **Tumor stimulator cell modification by infection with Newcastle Disease Virus: analysis of effects and mechanism in MLTC-CML cultures.** *Int J Oncol* 1999, **14:**205-215.
61. Csatary LK, Bakacs T: **Use of Newcastle disease virus vaccine (MTH-68/H) in a patient with high-grade glioblastoma.** *Jama* 1999, **281:**1588-1589.
62. Csatary LK: **Viruses in the treatment of cancer.** *Lancet* 1971, **2:**825.

63. Isaacs L: **Virus interference. 1. The interferon. .** *Proc R Soc Lond B Biol Sci* 1957, **147:**258-267.
64. Pestka S, Krause CD, Walter MR: **Interferons, interferon-like cytokines, and their receptors.** *Immunol Rev* 2004, **202:**8-32.
65. Guha-Thakurta N, Majde JA: **Early induction of proinflammatory cytokine and type I interferon mRNAs following Newcastle disease virus, poly [rI:rC], or low-dose LPS challenge of the mouse.** *J Interferon Cytokine Res* 1997, **17:**197-204.
66. Washburn B, Schirrmacher V: **Human tumor cell infection by Newcastle Disease Virus leads to upregulation of HLA and cell adhesion molecules and to induction of interferons, chemokines and finally apoptosis.** *Int J Oncol* 2002, **21:**85-93.
67. Weissmann C, Weber H: **The interferon genes.** *Prog Nucleic Acid Res Mol Biol* 1986, **33:**251-300.
68. Barchet W, Cella M, Colonna M: **Plasmacytoid dendritic cells--virus experts of innate immunity.** *Semin Immunol* 2005, **17:**253-261.
69. Kato H, Sato S, Yoneyama M, Yamamoto M, Uematsu S, Matsui K, Tsujimura T, Takeda K, Fujita T, Takeuchi O, Akira S: **Cell type-specific involvement of RIG-I in antiviral response.** *Immunity* 2005, **23:**19-28.
70. Kumagai Y, Kumar H, Koyama S, Kawai T, Takeuchi O, Akira S: **Cutting Edge: TLR-Dependent viral recognition along with type I IFN positive feedback signaling masks the requirement of viral replication for IFN-alpha production in plasmacytoid dendritic cells.** *J Immunol* 2009, **182:**3960-3964.
71. Fournier S: **Newcastle disease virus: a promising vector for viral therapy, immune therapy, and gene therapy of cancer.** *Methods in molecular biology* 2009, **542:**565-605.
72. Yoneyama M, Kikuchi M, Natsukawa T, Shinobu N, Imaizumi T, Miyagishi M, Taira K, Akira S, Fujita T: **The RNA helicase RIG-I has an essential function in double-stranded RNA-induced innate antiviral responses.** *Nat Immunol* 2004, **5:**730-737.
73. Kato H, Takeuchi O, Sato S, Yoneyama M, Yamamoto M, Matsui K, Uematsu S, Jung A, Kawai T, Ishii KJ, et al: **Differential roles of MDA5 and RIG-I helicases in the recognition of RNA viruses.** *Nature* 2006, **441:**101-105.
74. Hornung V, Ellegast J, Kim S, Brzozka K, Jung A, Kato H, Poeck H, Akira S, Conzelmann KK, Schlee M, et al: **5'-Triphosphate RNA is the ligand for RIG-I.** *Science* 2006, **314:**994-997.
75. Kawai T, Takahashi K, Sato S, Coban C, Kumar H, Kato H, Ishii KJ, Takeuchi O, Akira S: **IPS-1, an adaptor triggering RIG-I- and Mda5-mediated type I interferon induction.** *Nat Immunol* 2005, **6:**981-988.
76. Kawai T, Akira S: **[Role of IPS-1 in type I IFN induction].** *Nippon Rinsho* 2006, **64:**1231-1235.
77. Kumar H, Kawai T, Kato H, Sato S, Takahashi K, Coban C, Yamamoto M, Uematsu S, Ishii KJ, Takeuchi O, Akira S: **Essential role of IPS-1 in innate immune responses against RNA viruses.** *J Exp Med* 2006, **203:**1795-1803.
78. Prakash A, Smith E, Lee CK, Levy DE: **Tissue-specific positive feedback requirements for production of type I interferon following virus infection.** *J Biol Chem* 2005, **280:**18651-18657.
79. Marie I, Durbin JE, Levy DE: **Differential viral induction of distinct interferon-alpha genes by positive feedback through interferon regulatory factor-7.** *Embo J* 1998, **17:**6660-6669.
80. Haller O, Staeheli P, Kochs G: **Interferon-induced Mx proteins in antiviral host defense.** *Biochimie* 2007, **89:**812-818.

81. Rebouillat D, Hovanessian AG: **The human 2',5'-oligoadenylate synthetase family: interferon-induced proteins with unique enzymatic properties.** *J Interferon Cytokine Res* 1999, **19:**295-308.
82. Stark GR, Kerr IM, Williams BR, Silverman RH, Schreiber RD: **How cells respond to interferons.** *Annu Rev Biochem* 1998, **67:**227-264.
83. Williams BR: **PKR; a sentinel kinase for cellular stress.** *Oncogene* 1999, **18:**6112-6120.
84. Chen YX, Welte K, Gebhard DH, Evans RL: **Induction of T cell aggregation by antibody to a 16kd human leukocyte surface antigen.** *J Immunol* 1984, **133:**2496-2501.
85. Yang G, Xu Y, Chen X, Hu G: **IFITM1 plays an essential role in the antiproliferative action of interferon-gamma.** *Oncogene* 2007, **26:**594-603.
86. Staeheli Aa: **Partial Inhibition of Vesicular Stomatitis Virus by the Interferon-Induced Human 9-27 Protein.** *Journal of Interferon and Cytokine Research* 1996, **16:**375-380.
87. Garcia MA, Meurs EF, Esteban M: **The dsRNA protein kinase PKR: virus and cell control.** *Biochimie* 2007, **89:**799-811.
88. Castelli J, Wood KA, Youle RJ: **The 2-5A system in viral infection and apoptosis.** *Biomed Pharmacother* 1998, **52:**386-390.
89. Stojdl DF, Lichty B, Knowles S, Marius R, Atkins H, Sonenberg N, Bell JC: **Exploiting tumor-specific defects in the interferon pathway with a previously unknown oncolytic virus.** *Nat Med* 2000, **6:**821-825.
90. Krishnamurthy S, Takimoto T, Scroggs RA, Portner A: **Differentially regulated interferon response determines the outcome of Newcastle disease virus infection in normal and tumor cell lines.** *J Virol* 2006, **80:**5145-5155.
91. Fiola C, Peeters B, Fournier P, Arnold A, Bucur M, Schirrmacher V: **Tumor selective replication of Newcastle disease virus: association with defects of tumor cells in antiviral defence.** *Int J Cancer* 2006, **119:**328-338.
92. Wilden H, Fournier P, Zawatzky R, Schirrmacher V: **Expression of RIG-I, IRF3, IFN-beta and IRF7 determines resistance or susceptibility of cells to infection by Newcastle Disease Virus.** *Int J Oncol* 2009, **34:**971-982.
93. Strong JE, Coffey MC, Tang D, Sabinin P, Lee PW: **The molecular basis of viral oncolysis: usurpation of the Ras signaling pathway by reovirus.** *Embo J* 1998, **17:**3351-3362.
94. Shmulevitz M, Marcato P, Lee PW: **Unshackling the links between reovirus oncolysis, Ras signaling, translational control and cancer.** *Oncogene* 2005, **24:**7720-7728.
95. Marcato P, Shmulevitz M, Pan D, Stoltz D, Lee PW: **Ras transformation mediates reovirus oncolysis by enhancing virus uncoating, particle infectivity, and apoptosis-dependent release.** *Mol Ther* 2007, **15:**1522-1530.
96. Noser JA, Mael AA, Sakuma R, Ohmine S, Marcato P, Wk Lee P, Ikeda Y: **The RAS/Raf1/MEK/ERK Signaling Pathway Facilitates VSV-mediated Oncolysis: Implication for the Defective Interferon Response in Cancer Cells.** *Mol Ther* 2007, **15:**1531-1536.
97. Balachandran S, Barber GN: **Defective translational control facilitates vesicular stomatitis virus oncolysis.** *Cancer Cell* 2004, **5:**51-65.
98. Lorence RM, Katubig BB, Reichard KW, Reyes HM, Phuangsab A, Sassetti MD, Walter RJ, Peeples ME: **Complete regression of human fibrosarcoma xenografts after local Newcastle disease virus therapy.** *Cancer Res* 1994, **54:**6017-6021.

99. Wheelock EF, Dingle JH: **Observations on the Repeated Administration of Viruses to a Patient with Acute Leukemia. a Preliminary Report.** *N Engl J Med* 1964, **271:**645-651.
100. Sinkovics JG, Horvath JC: **Newcastle disease virus (NDV): brief history of its oncolytic strains.** *J Clin Virol* 2000, **16:**1-15.
101. Hotte SJ, Lorence RM, Hirte HW, Polawski SR, Bamat MK, O'Neil JD, Roberts MS, Groene WS, Major PP: **An optimized clinical regimen for the oncolytic virus PV701.** *Clin Cancer Res* 2007, **13:**977-985.
102. Laurie SA, Bell JC, Atkins HL, Roach J, Bamat MK, O'Neil JD, Roberts MS, Groene WS, Lorence RM: **A phase 1 clinical study of intravenous administration of PV701, an oncolytic virus, using two-step desensitization.** *Clin Cancer Res* 2006, **12:**2555-2562.
103. Pecora AL, Rizvi N, Cohen GI, Meropol NJ, Sterman D, Marshall JL, Goldberg S, Gross P, O'Neil JD, Groene WS, et al: **Phase I trial of intravenous administration of PV701, an oncolytic virus, in patients with advanced solid cancers.** *J Clin Oncol* 2002, **20:**2251-2266.
104. Freeman AI, Zakay-Rones Z, Gomori JM, Linetsky E, Rasooly L, Greenbaum E, Rozenman-Yair S, Panet A, Libson E, Irving CS, et al: **Phase I/II trial of intravenous NDV-HUJ oncolytic virus in recurrent glioblastoma multiforme.** *Mol Ther* 2006, **13:**221-228.
105. Csatary LK, Gosztonyi G, Szeberenyi J, Fabian Z, Liszka V, Bodey B, Csatary CM: **MTH-68/H oncolytic viral treatment in human high-grade gliomas.** *J Neurooncol* 2004, **67:**83-93.
106. Csatary LK, Eckhardt S, Bukosza I, Czegledi F, Fenyvesi C, Gergely P, Bodey B, Csatary CM: **Attenuated veterinary virus vaccine for the treatment of cancer.** *Cancer Detect Prev* 1993, **17:**619-627.
107. Batliwalla FM, Bateman BA, Serrano D, Murray D, Macphail S, Maino VC, Ansel JC, Gregersen PK, Armstrong CA: **A 15-year follow-up of AJCC stage III malignant melanoma patients treated postsurgically with Newcastle disease virus (NDV) oncolysate and determination of alterations in the CD8 T cell repertoire.** *Mol Med* 1998, **4:**783-794.
108. Schirrmacher V: **Clinical trials of antitumor vaccination with an autologous tumor cell vaccine modified by virus infection: improvement of patient survival based on improved antitumor immune memory.** *Cancer Immunol Immunother* 2005, **54:**587-598.
109. Stewart SA, Weinberg RA: **Telomeres: cancer to human aging.** *Annu Rev Cell Dev Biol* 2006, **22:**531-557.
110. Shay JW, Pereira-Smith OM, Wright WE: **A role for both RB and p53 in the regulation of human cellular senescence.** *Exp Cell Res* 1991, **196:**33-39.
111. Shay JW, Wright WE: **Senescence and immortalization: role of telomeres and telomerase.** *Carcinogenesis* 2005, **26:**867-874.
112. de Lange T, Jacks T: **For better or worse? Telomerase inhibition and cancer.** *Cell* 1999, **98:**273-275.
113. Campisi J: **Cellular senescence as a tumor-suppressor mechanism.** *Trends Cell Biol* 2001, **11:**S27-31.
114. de Lange T: **Protection of mammalian telomeres.** *Oncogene* 2002, **21:**532-540.
115. Verdun RE, Karlseder J: **Replication and protection of telomeres.** *Nature* 2007, **447:**924-931.
116. Hahn WC, Counter CM, Lundberg AS, Beijersbergen RL, Brooks MW, Weinberg RA: **Creation of human tumour cells with defined genetic elements.** *Nature* 1999, **400:**464-468.

117. Hahn WC, Weinberg RA: **Modelling the molecular circuitry of cancer.** *Nat Rev Cancer* 2002, **2:**331-341.
118. Boukamp P, Petrussevska RT, Breitkreutz D, Hornung J, Markham A, Fusenig NE: **Normal keratinization in a spontaneously immortalized aneuploid human keratinocyte cell line.** *J Cell Biol* 1988, **106:**761-771.
119. Fusenig NE, Boukamp P: **Multiple stages and genetic alterations in immortalization, malignant transformation, and tumor progression of human skin keratinocytes.** *Mol Carcinog* 1998, **23:**144-158.
120. Boukamp P, Stanbridge EJ, Foo DY, Cerutti PA, Fusenig NE: **c-Ha-ras oncogene expression in immortalized human keratinocytes (HaCaT) alters growth potential in vivo but lacks correlation with malignancy.** *Cancer Res* 1990, **50:**2840-2847.
121. Mueller MM, Peter W, Mappes M, Huelsen A, Steinbauer H, Boukamp P, Vaccariello M, Garlick J, Fusenig NE: **Tumor progression of skin carcinoma cells in vivo promoted by clonal selection, mutagenesis, and autocrine growth regulation by granulocyte colony-stimulating factor and granulocyte-macrophage colony-stimulating factor.** *Am J Pathol* 2001, **159:**1567-1579.
122. Cerutti H, Casas-Mollano JA: **On the origin and functions of RNA-mediated silencing: from protists to man.** *Curr Genet* 2006, **50:**81-99.
123. Shrey K, Suchit A, Nishant M, Vibha R: **RNA interference: emerging diagnostics and therapeutics tool.** *Biochem Biophys Res Commun* 2009, **386:**273-277.
124. Fire A, Xu S, Montgomery MK, Kostas SA, Driver SE, Mello CC: **Potent and specific genetic interference by double-stranded RNA in Caenorhabditis elegans.** *Nature* 1998, **391:**806-811.
125. Grimm D: **Small silencing RNAs: state-of-the-art.** *Adv Drug Deliv Rev* 2009, **61:**672-703.
126. Tuschl T: **RNA interference and small interfering RNAs.** *Chembiochem* 2001, **2:**239-245.
127. Elbashir SM, Lendeckel W, Tuschl T: **RNA interference is mediated by 21- and 22-nucleotide RNAs.** *Genes Dev* 2001, **15:**188-200.
128. Pei Y, Tuschl T: **On the art of identifying effective and specific siRNAs.** *Nat Methods* 2006, **3:**670-676.
129. Fedorov Y, Anderson EM, Birmingham A, Reynolds A, Karpilow J, Robinson K, Leake D, Marshall WS, Khvorova A: **Off-target effects by siRNA can induce toxic phenotype.** *Rna* 2006, **12:**1188-1196.
130. Quon K, Kassner PD: **RNA interference screening for the discovery of oncology targets.** *Expert Opin Ther Targets* 2009, **13:**1027-1035.
131. Nguyen DG, Wolff KC, Yin H, Caldwell JS, Kuhen KL: **"UnPAKing" human immunodeficiency virus (HIV) replication: using small interfering RNA screening to identify novel cofactors and elucidate the role of group I PAKs in HIV infection.** *J Virol* 2006, **80:**130-137.
132. Zhou H, Xu M, Huang Q, Gates AT, Zhang XD, Castle JC, Stec E, Ferrer M, Strulovici B, Hazuda DJ, Espeseth AS: **Genome-scale RNAi screen for host factors required for HIV replication.** *Cell Host Microbe* 2008, **4:**495-504.
133. Brass AL, Dykxhoorn DM, Benita Y, Yan N, Engelman A, Xavier RJ, Lieberman J, Elledge SJ: **Identification of host proteins required for HIV infection through a functional genomic screen.** *Science* 2008, **319:**921-926.
134. Ng TI, Mo H, Pilot-Matias T, He Y, Koev G, Krishnan P, Mondal R, Pithawalla R, He W, Dekhtyar T, et al: **Identification of host genes involved in hepatitis C virus replication by small interfering RNA technology.** *Hepatology* 2007, **45:**1413-1421.

135. Kolokoltsov AA, Deniger D, Fleming EH, Roberts NJ, Jr., Karpilow JM, Davey RA: **Small interfering RNA profiling reveals key role of clathrin-mediated endocytosis and early endosome formation for infection by respiratory syncytial virus.** *J Virol* 2007, **81:**7786-7800.
136. Krishnan MN, Ng A, Sukumaran B, Gilfoy FD, Uchil PD, Sultana H, Brass AL, Adametz R, Tsui M, Qian F, et al: **RNA interference screen for human genes associated with West Nile virus infection.** *Nature* 2008, **455:**242-245.
137. Pelkmans L, Fava E, Grabner H, Hannus M, Habermann B, Krausz E, Zerial M: **Genome-wide analysis of human kinases in clathrin- and caveolae/raft-mediated endocytosis.** *Nature* 2005, **436:**78-86.
138. Gao Y, Dickerson JB, Guo F, Zheng J, Zheng Y: **Rational design and characterization of a Rac GTPase-specific small molecule inhibitor.** *Proc Natl Acad Sci U S A* 2004, **101:**7618-7623.
139. Vlahos CJ, Matter WF, Hui KY, Brown RF: **A specific inhibitor of phosphatidylinositol 3-kinase, 2-(4-morpholinyl)-8-phenyl-4H-1-benzopyran-4-one (LY294002).** *J Biol Chem* 1994, **269:**5241-5248.
140. Puhler F, Willuda J, Puhlmann J, Mumberg D, Romer-Oberdorfer A, Beier R: **Generation of a recombinant oncolytic Newcastle disease virus and expression of a full IgG antibody from two transgenes.** *Gene Ther* 2008.
141. Ridley AJ, Paterson HF, Johnston CL, Diekmann D, Hall A: **The small GTP-binding protein rac regulates growth factor-induced membrane ruffling.** *Cell* 1992, **70:**401-410.
142. Kang JS, Krauss RS: **Ras induces anchorage-independent growth by subverting multiple adhesion-regulated cell cycle events.** *Mol Cell Biol* 1996, **16:**3370-3380.
143. Schwartz MA: **Integrins, oncogenes, and anchorage independence.** *J Cell Biol* 1997, **139:**575-578.
144. Wong LH, Krauer KG, Hatzinisiriou I, Estcourt MJ, Hersey P, Tam ND, Edmondson S, Devenish RJ, Ralph SJ: **Interferon-resistant human melanoma cells are deficient in ISGF3 components, STAT1, STAT2, and p48-ISGF3gamma.** *J Biol Chem* 1997, **272:**28779-28785.
145. Xi S, Dyer KF, Kimak M, Zhang Q, Gooding WE, Chaillet JR, Chai RL, Ferrell RE, Zamboni B, Hunt J, Grandis JR: **Decreased STAT1 expression by promoter methylation in squamous cell carcinogenesis.** *J Natl Cancer Inst* 2006, **98:**181-189.
146. Kim DJ, Chan KS, Sano S, Digiovanni J: **Signal transducer and activator of transcription 3 (Stat3) in epithelial carcinogenesis.** *Mol Carcinog* 2007, **46:**725-731.
147. Mundschau LJ, Faller DV: **Oncogenic ras induces an inhibitor of double-stranded RNA-dependent eukaryotic initiation factor 2 alpha-kinase activation.** *J Biol Chem* 1992, **267:**23092-23098.
148. Norman KL, Hirasawa K, Yang AD, Shields MA, Lee PW: **Reovirus oncolysis: the Ras/RalGEF/p38 pathway dictates host cell permissiveness to reovirus infection.** *Proc Natl Acad Sci U S A* 2004, **101:**11099-11104.
149. Schlessinger J: **Cell signaling by receptor tyrosine kinases.** *Cell* 2000, **103:**211-225.
150. Blume-Jensen P, Hunter T: **Oncogenic kinase signalling.** *Nature* 2001, **411:**355-365.
151. Barik S: **Control of nonsegmented negative-strand RNA virus replication by siRNA.** *Virus Res* 2004, **102:**27-35.
152. Tan TL, Fang N, Neo TL, Singh P, Zhang J, Zhou R, Koh CG, Chan V, Lim SG, Chen WN: **Rac1 GTPase is activated by hepatitis B virus replication--involvement of HBX.** *Biochim Biophys Acta* 2008, **1783:**360-374.

153. Hoppe S, Schelhaas M, Jaeger V, Liebig T, Petermann P, Knebel-Morsdorf D: **Early herpes simplex virus type 1 infection is dependent on regulated Rac1/Cdc42 signalling in epithelial MDCKII cells.** *J Gen Virol* 2006, **87:**3483-3494.
154. Lu X, Wu X, Plemenitas A, Yu H, Sawai ET, Abo A, Peterlin BM: **CDC42 and Rac1 are implicated in the activation of the Nef-associated kinase and replication of HIV-1.** *Curr Biol* 1996, **6:**1677-1684.
155. Saeed MF, Kolokoltsov AA, Freiberg AN, Holbrook MR, Davey RA: **Phosphoinositide-3 kinase-Akt pathway controls cellular entry of Ebola virus.** *PLoS Pathog* 2008, **4:**e1000141.
156. Qiu RG, Chen J, Kirn D, McCormick F, Symons M: **An essential role for Rac in Ras transformation.** *Nature* 1995, **374:**457-459.
157. Khosravi-Far R, Solski PA, Clark GJ, Kinch MS, Der CJ: **Activation of Rac1, RhoA, and mitogen-activated protein kinases is required for Ras transformation.** *Mol Cell Biol* 1995, **15:**6443-6453.
158. Malliri A, van der Kammen RA, Clark K, van der Valk M, Michiels F, Collard JG: **Mice deficient in the Rac activator Tiam1 are resistant to Ras-induced skin tumours.** *Nature* 2002, **417:**867-871.
159. Lambert JM, Lambert QT, Reuther GW, Malliri A, Siderovski DP, Sondek J, Collard JG, Der CJ: **Tiam1 mediates Ras activation of Rac by a PI(3)K-independent mechanism.** *Nat Cell Biol* 2002, **4:**621-625.
160. Small JV, Stradal T, Vignal E, Rottner K: **The lamellipodium: where motility begins.** *Trends Cell Biol* 2002, **12:**112-120.
161. Scita G, Tenca P, Frittoli E, Tocchetti A, Innocenti M, Giardina G, Di Fiore PP: **Signaling from Ras to Rac and beyond: not just a matter of GEFs.** *Embo J* 2000, **19:**2393-2398.
162. Lorence RM, Roberts MS, O'Neil JD, Groene WS, Miller JA, Mueller SN, Bamat MK: **Phase 1 clinical experience using intravenous administration of PV701, an oncolytic Newcastle disease virus.** *Curr Cancer Drug Targets* 2007, **7:**157-167.
163. Colamonici OR, Domanski P, Platanias LC, Diaz MO: **Correlation between interferon (IFN) alpha resistance and deletion of the IFN alpha/beta genes in acute leukemia cell lines suggests selection against the IFN system.** *Blood* 1992, **80:**744-749.
164. Wagner TC, Velichko S, Chesney SK, Biroc S, Harde D, Vogel D, Croze E: **Interferon receptor expression regulates the antiproliferative effects of interferons on cancer cells and solid tumors.** *Int J Cancer* 2004, **111:**32-42.
165. Klampfer L, Huang J, Corner G, Mariadason J, Arango D, Sasazuki T, Shirasawa S, Augenlicht L: **Oncogenic Ki-ras inhibits the expression of interferon-responsive genes through inhibition of STAT1 and STAT2 expression.** *J Biol Chem* 2003, **278:**46278-46287.
166. Staeheli P, Pavlovic J: **Inhibition of vesicular stomatitis virus mRNA synthesis by human MxA protein.** *J Virol* 1991, **65:**4498-4501.
167. Alber D, Staeheli P: **Partial inhibition of vesicular stomatitis virus by the interferon-induced human 9-27 protein.** *J Interferon Cytokine Res* 1996, **16:**375-380.
168. Roth MG: **Cell biology: porter and sorter.** *Nature* 2008, **452:**706-707.
169. Nakatsu F, Ohno H: **Adaptor protein complexes as the key regulators of protein sorting in the post-Golgi network.** *Cell Struct Funct* 2003, **28:**419-429.
170. Hall A: **Rho GTPases and the actin cytoskeleton.** *Science* 1998, **279:**509-514.
171. Ridley AJ: **Rho GTPases and actin dynamics in membrane protrusions and vesicle trafficking.** *Trends Cell Biol* 2006, **16:**522-529.

172. Cudmore S, Reckmann I, Way M: **Viral manipulations of the actin cytoskeleton.** *Trends Microbiol* 1997, **5:**142-148.
173. Seimiya M, Tomonaga T, Matsushita K, Sunaga M, Oh-Ishi M, Kodera Y, Maeda T, Takano S, Togawa A, Yoshitomi H, et al: **Identification of novel immunohistochemical tumor markers for primary hepatocellular carcinoma; clathrin heavy chain and formiminotransferase cyclodeaminase.** *Hepatology* 2008, **48:**519-530.
174. Dummler B, Ohshiro K, Kumar R, Field J: **Pak protein kinases and their role in cancer.** *Cancer Metastasis Rev* 2009, **28:**51-63.
175. Bokoch GM: **Biology of the p21-activated kinases.** *Annu Rev Biochem* 2003, **72:**743-781.
176. Vadlamudi RK, Kumar R: **P21-activated kinases in human cancer.** *Cancer Metastasis Rev* 2003, **22:**385-393.
177. Kumar R, Gururaj AE, Barnes CJ: **p21-activated kinases in cancer.** *Nat Rev Cancer* 2006, **6:**459-471.
178. Deacon SW, Beeser A, Fukui JA, Rennefahrt UE, Myers C, Chernoff J, Peterson JR: **An isoform-selective, small-molecule inhibitor targets the autoregulatory mechanism of p21-activated kinase.** *Chem Biol* 2008, **15:**322-331.
179. Boguski MS, McCormick F: **Proteins regulating Ras and its relatives.** *Nature* 1993, **366:**643-654.
180. Takaishi K, Sasaki T, Kotani H, Nishioka H, Takai Y: **Regulation of cell-cell adhesion by rac and rho small G proteins in MDCK cells.** *J Cell Biol* 1997, **139:**1047-1059.
181. Akhtar N, Hotchin NA: **RAC1 regulates adherens junctions through endocytosis of E-cadherin.** *Mol Biol Cell* 2001, **12:**847-862.
182. Michaelson D, Silletti J, Murphy G, D'Eustachio P, Rush M, Philips MR: **Differential localization of Rho GTPases in live cells: regulation by hypervariable regions and RhoGDI binding.** *J Cell Biol* 2001, **152:**111-126.
183. Bosco EE, Mulloy JC, Zheng Y: **Rac1 GTPase: a "Rac" of all trades.** *Cell Mol Life Sci* 2009, **66:**370-374.
184. Schowalter RM, Wurth MA, Aguilar HC, Lee B, Moncman CL, McCann RO, Dutch RE: **Rho GTPase activity modulates paramyxovirus fusion protein-mediated cell-cell fusion.** *Virology* 2006, **350:**323-334.
185. Daecke J, Fackler OT, Dittmar MT, Krausslich HG: **Involvement of clathrin-mediated endocytosis in human immunodeficiency virus type 1 entry.** *J Virol* 2005, **79:**1581-1594.
186. Townsley AC, Weisberg AS, Wagenaar TR, Moss B: **Vaccinia virus entry into cells via a low-pH-dependent endosomal pathway.** *J Virol* 2006, **80:**8899-8908.
187. Rust MJ, Lakadamyali M, Zhang F, Zhuang X: **Assembly of endocytic machinery around individual influenza viruses during viral entry.** *Nat Struct Mol Biol* 2004, **11:**567-573.
188. Mercer J, Helenius A: **Virus entry by macropinocytosis.** *Nat Cell Biol* 2009, **11:**510-520.
189. Araki N, Johnson MT, Swanson JA: **A role for phosphoinositide 3-kinase in the completion of macropinocytosis and phagocytosis by macrophages.** *J Cell Biol* 1996, **135:**1249-1260.
190. Sieczkarski SB, Whittaker GR: **Dissecting virus entry via endocytosis.** *J Gen Virol* 2002, **83:**1535-1545.
191. Amyere M, Mettlen M, Van Der Smissen P, Platek A, Payrastre B, Veithen A, Courtoy PJ: **Origin, originality, functions, subversions and molecular signalling of macropinocytosis.** *Int J Med Microbiol* 2002, **291:**487-494.

192. Nicola AV, Hou J, Major EO, Straus SE: **Herpes simplex virus type 1 enters human epidermal keratinocytes, but not neurons, via a pH-dependent endocytic pathway.** *J Virol* 2005, **79:**7609-7616.
193. Bar-Sagi D, Feramisco JR: **Induction of membrane ruffling and fluid-phase pinocytosis in quiescent fibroblasts by ras proteins.** *Science* 1986, **233:**1061-1068.
194. Li G, D'Souza-Schorey C, Barbieri MA, Cooper JA, Stahl PD: **Uncoupling of membrane ruffling and pinocytosis during Ras signal transduction.** *J Biol Chem* 1997, **272:**10337-10340.
195. Yan J, Roy S, Apolloni A, Lane A, Hancock JF: **Ras isoforms vary in their ability to activate Raf-1 and phosphoinositide 3-kinase.** *J Biol Chem* 1998, **273:**24052-24056.
196. Qualmann B, Mellor H: **Regulation of endocytic traffic by Rho GTPases.** *Biochem J* 2003, **371:**233-241.
197. Corvera S: **Phosphatidylinositol 3-kinase and the control of endosome dynamics: new players defined by structural motifs.** *Traffic* 2001, **2:**859-866.
198. Kaksonen M, Toret CP, Drubin DG: **Harnessing actin dynamics for clathrin-mediated endocytosis.** *Nat Rev Mol Cell Biol* 2006, **7:**404-414.
199. Mosesson Y, Mills GB, Yarden Y: **Derailed endocytosis: an emerging feature of cancer.** *Nat Rev Cancer* 2008, **8:**835-850.
200. Giuffre RM, Tovell DR, Kay CM, Tyrrell DL: **Evidence for an interaction between the membrane protein of a paramyxovirus and actin.** *J Virol* 1982, **42:**963-968.
201. Kozma SC, Bogaard ME, Buser K, Saurer SM, Bos JL, Groner B, Hynes NE: **The human c-Kirsten ras gene is activated by a novel mutation in codon 13 in the breast carcinoma cell line MDA-MB231.** *Nucleic Acids Res* 1987, **15:**5963-5971.
202. Ikediobi ON, Davies H, Bignell G, Edkins S, Stevens C, O'Meara S, Santarius T, Avis T, Barthorpe S, Brackenbury L, et al: **Mutation analysis of 24 known cancer genes in the NCI-60 cell line set.** *Mol Cancer Ther* 2006, **5:**2606-2612.
203. Bjorheim J, Minarik M, Gaudernack G, Ekstrom PO: **Mutation detection in KRAS Exon 1 by constant denaturant capillary electrophoresis in 96 parallel capillaries.** *Anal Biochem* 2002, **304:**200-205.
204. Coniglio SJ, Jou TS, Symons M: **Rac1 protects epithelial cells against anoikis.** *J Biol Chem* 2001, **276:**28113-28120.
205. Chan AY, Coniglio SJ, Chuang YY, Michaelson D, Knaus UG, Philips MR, Symons M: **Roles of the Rac1 and Rac3 GTPases in human tumor cell invasion.** *Oncogene* 2005, **24:**7821-7829.
206. Ellenbroek SI, Collard JG: **Rho GTPases: functions and association with cancer.** *Clin Exp Metastasis* 2007, **24:**657-672.
207. Buongiorno P, Pethe VV, Charames GS, Esufali S, Bapat B: **Rac1 GTPase and the Rac1 exchange factor Tiam1 associate with Wnt-responsive promoters to enhance beta-catenin/TCF-dependent transcription in colorectal cancer cells.** *Mol Cancer* 2008, **7:**73.
208. Sahai E, Marshall CJ: **RHO-GTPases and cancer.** *Nat Rev Cancer* 2002, **2:**133-142.
209. Kwei KA, Finch JS, Ranger-Moore J, Bowden GT: **The role of Rac1 in maintaining malignant phenotype of mouse skin tumor cells.** *Cancer Lett* 2006, **231:**326-338.
210. Michiels F, Habets GG, Stam JC, van der Kammen RA, Collard JG: **A role for Rac in Tiam1-induced membrane ruffling and invasion.** *Nature* 1995, **375:**338-340.
211. Engers R, Mueller M, Walter A, Collard JG, Willers R, Gabbert HE: **Prognostic relevance of Tiam1 protein expression in prostate carcinomas.** *Br J Cancer* 2006, **95:**1081-1086.
212. Adam L, Vadlamudi RK, McCrea P, Kumar R: **Tiam1 overexpression potentiates heregulin-induced lymphoid enhancer factor-1/beta -catenin nuclear signaling in**

breast cancer cells by modulating the intercellular stability. *J Biol Chem* 2001, **276:**28443-28450.

7 APPENDIX

7.1 Plasmid cards

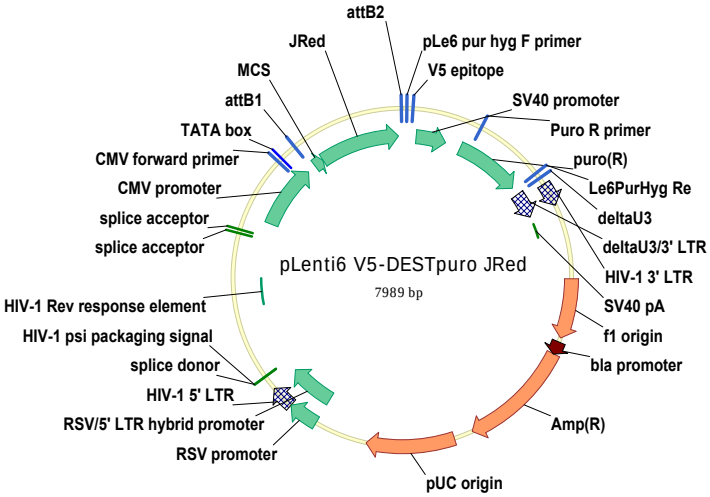

Figure 7-1: Lentiviral destination vector for *JRED* transduction control

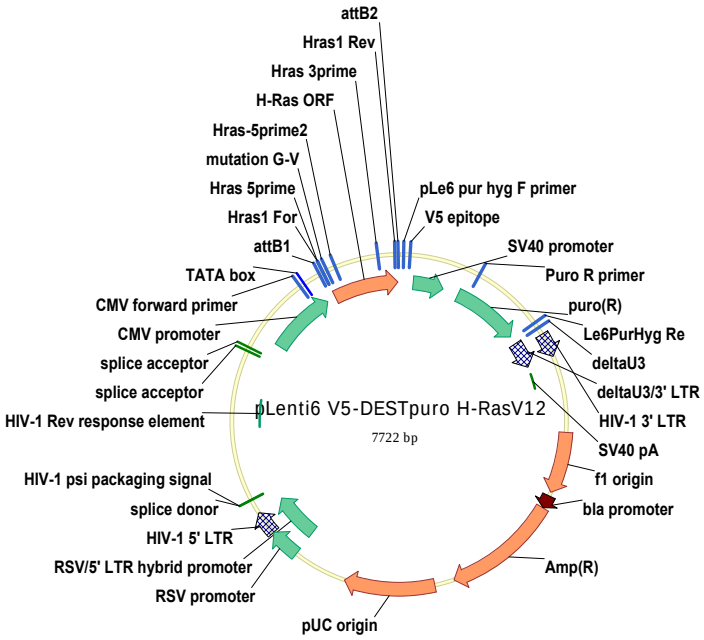

Figure 7-2: Lentiviral destination vector for *H-RasV12*

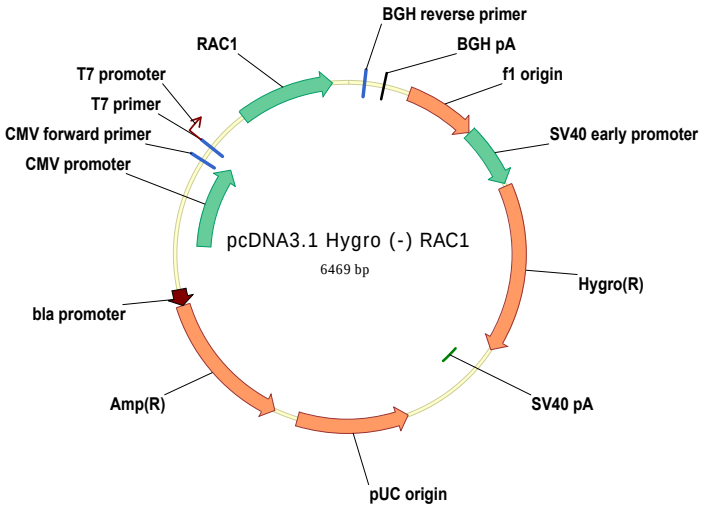

Figure 7-3: Expression vector for *Rac1wt*

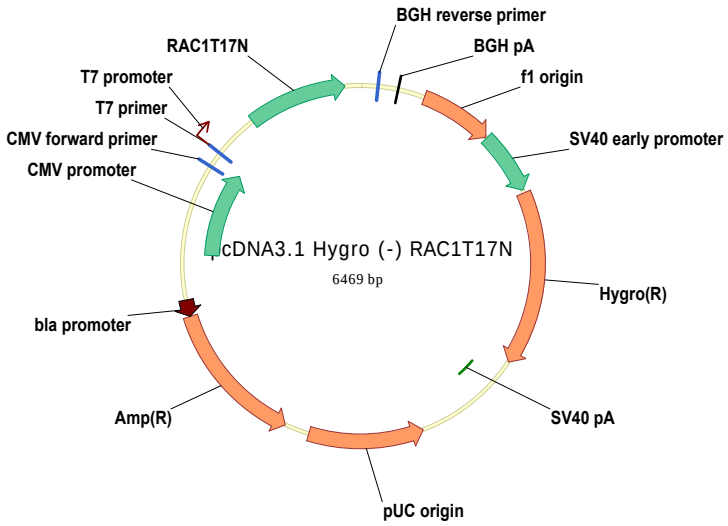

Figure 7-4: Expression vector for the dominant negative mutant *Rac1T17N*

7.2 List of screening candidates and screening results

Table 7-1: List of membrane trafficking library candidate genes and the screening outcome relative to the RISC-free siRNA control

Gene symbol	Accession number	RLU	relative cell viability
ACTR2	NM_005722	0,60	1,07
ACTR3	NM_005721	0,95	1,00
ADAM10	NM_001110	0,68	1,04
AMPH	NM_139316	0,86	1,06
AP1B1	NM_145730	0,32	1,06
AP1M1	NM_032493	1,37	1,05
AP1M2	NM_005498	0,90	1,01
AP2A1	NM_130787	0,34	0,93
AP2A2	NM_012305	0,30	0,92
AP2B1	NM_001282	0,74	1,07
AP2M1	NM_004068	0,32	0,99
ARF1	NM_001658	0,76	0,97
ARF6	NM_001663	0,70	0,93
ARFIP2	NM_012402	0,70	0,99
ARPC1B	NM_005720	1,12	0,92
ARPC2	NM_152862	0,59	0,98
ARPC3	NM_005719	0,92	0,98
ARPC4	NM_005718	0,87	0,94
ARPC5	NM_005717	0,73	1,01
ARRB1	NM_020251	1,11	1,03
ARRB2	NM_199004	0,75	0,98
ATM	NM_138293	1,49	0,98
ATP6V0A1	NM_005177	0,86	0,99
BIN1	NM_139351	1,30	0,88
CAMK1	NM_003656	1,39	1,00
CAV1	NM_001753	1,09	1,02
CAV2	NM_198212	0,63	0,96
CBLB	NM_170662	1,32	1,03
CBLC	NM_012116	0,76	0,91
CDC42	NM_044472	0,85	0,98
CFL1	NM_005507	0,99	0,67
CIB2	NM_006383	1,03	0,93
CIB3	NM_054113	0,49	0,92
CLTA	NM_007096	0,32	0,91
CLTB	NM_007097	0,90	0,85
CLTC	NM_004859	0,87	1,03
CLTCL1	NM_007098	1,06	1,05
DAB2	NM_001343	0,63	0,87
DDEF2	NM_003887	0,85	1,00
DIAPH1	NM_005219	0,81	0,96
DNM2	NM_004945	3,25	1,03
DNM3	NM_015569	0,96	0,95
EEA1	NM_003566	1,61	0,94
EFS	NM_032459	0,68	0,89
ELKS	NM_178040	0,63	0,97
ENTH	NM_014666	0,80	0,90
EPN1	NM_013333	0,82	0,89
EPN2	NM_148921	0,62	0,98
EPN3	NM_017957	0,58	0,94
EPS15	NM_001981	1,42	1,02
EPS15L1	NM_021235	0,69	0,79
FYN	NM_153048	1,33	1,01
GAF1	NM_015470	0,78	0,90
GIT1	NM_014030	1,40	0,90
GORASP1	NM_031899	0,66	0,84
HIP1	NM_005338	0,47	0,85
HIP1R	XM_290592	0,60	0,97
IHPK3	NM_054111	1,25	0,97
ITSN1	NM_003024	0,76	0,91
LIMK1	NM_016735	1,49	0,96
MAPK8IP1	NM_005456	0,66	0,98
MAPK8IP2	NM_139124	1,03	0,81
MAPK8IP3	NM_033392	0,60	0,96
NEDD4	NM_198400	1,39	1,00
NEDD4L	NM_015277	0,74	0,98
NSF	NM_006178	0,77	1,00
PACSIN1	NM_020804	0,59	0,88
PACSIN3	NM_016223	0,55	0,93
PAK1	NM_002576	0,40	0,96
PICALM	NM_007166	1,92	1,00
PIK3CG	NM_002649	0,48	0,97
PIK4CA	NM_058004	1,65	0,99
PIP5K1A	NM_003557	0,35	1,06
PSCD3	NM_004227	0,24	1,06
RAB11A	NM_004663	0,75	1,10
RAB11B	NM_004218	0,67	1,05
RAB3A	NM_002866	0,77	1,03
RAB3B	NM_002867	0,95	1,01
RAB3C	NM_138453	1,09	1,06
RAB3D	NM_004283	1,16	1,02
RAB4A	NM_004578	0,65	1,04
RAB4B	NM_016154	0,95	1,06
RAB5A	NM_004162	0,52	1,16
RAB5B	NM_002868	1,31	1,04
RAB5C	NM_201434	0,34	0,99
RAB6A	NM_198896	1,39	1,01
RAB6B	NM_016577	1,30	0,97
RAB7B	NM_177403	0,63	0,92
RAB7L1	NM_003929	1,31	0,88
RAB8A	NM_005370	0,80	0,94
RAB8B	NM_016530	1,13	1,01
RAC1	NM_198829	0,33	0,89
RHOA	NM_001664	0,23	0,97
ROCK1	NM_005406	1,93	1,01
ROCK2	NM_004850	1,24	1,08
SH3GLB1	NM_016009	0,69	0,96
STAU	NM_017454	1,15	0,92
SYNJ1	NM_203446	1,02	0,94
SYNJ2	NM_003898	0,45	0,92
SYT1	NM_005639	1,00	0,90
SYT2	NM_177402	0,67	0,89
TNIK	XM_039796	0,95	1,06
VAMP1	NM_199245	1,29	0,93
VAMP2	NM_014232	0,89	1,00
VAPA	NM_194434	0,68	0,92
VAPB	NM_004738	0,67	0,89
VAV2	NM_003371	1,20	1,02
VIL2	NM_003379	0,64	0,93
WAS	NM_000377	0,53	0,95
WASF1	NM_003931	1,23	0,93
WASF2	NM_006990	1,03	0,91
WASF3	NM_006646	1,06	1,01

Table 7-2:List of tyrosine kinase library candidate genes and the screening outcome relative to the RISC-free siRNA control

Gene symbol	Accession number	RLU	relative cell viability
ABL2	NM_007314	0,79	1,14
ALK	NM_004304	0,69	1,04
AXL	NM_021913	0,78	0,99
BLK	NM_001715	1,23	1,07
BMX	NM_001721	1,31	1,11
BTK	NM_000061	1,12	1,03
CSF1R	NM_005211	0,37	0,88
CSK	NM_004383	0,84	1,05
DDR1	NM_013994	0,61	0,97
DDR2	NM_006182	0,94	1,01
STYK1	NM_018423	0,57	0,93
EGFR	NM_005228	0,64	0,95
EPHA1	NM_005232	1,64	0,89
EPHA2	NM_004431	1,01	0,97
EPHA3	NM_005233	1,01	0,93
EPHA4	NM_004438	0,56	0,92
EPHA7	NM_004440	0,72	0,87
EPHA8	NM_020526	0,96	1,05
EPHB1	NM_004441	0,60	0,97
EPHB2	NM_017449	0,68	0,92
EPHB3	NM_004443	1,46	0,97
EPHB4	NM_004444	0,54	0,90
EPHB6	NM_004445	0,36	0,83
ERBB2	NM_004448	0,65	0,92
ERBB4	NM_005235	0,68	0,87
FER	NM_005246	0,44	0,96
FES	NM_002005	0,83	0,89
FGFR1	NM_000604	0,76	0,96
FGFR2	NM_000141	0,33	0,78
FGFR3	NM_000142	0,30	0,87
FGFR4	NM_002011	1,09	0,84
FGR	NM_005248	1,14	0,89
FLT1	NM_002019	0,54	0,79
FLT3	NM_004119	0,82	0,81
FLT4	NM_002020	0,96	0,89
FRK	NM_002031	1,06	0,96
FYN	NM_002037	1,72	0,97
HCK	NM_002110	0,38	0,93
IGF1R	NM_000875	1,51	1,04
ITK	NM_005546	1,72	0,93
JAK1	NM_002227	1,22	0,83
JAK2	NM_004972	1,27	0,77
KDR	NM_002253	0,66	0,81
KIT	NM_000222	1,92	0,86
LCK	NM_005356	0,58	0,91
LTK	NM_002344	1,05	0,91
MERTK	NM_006343	0,57	0,65
MET	NM_000245	1,26	0,83
MST1R	NM_002447	0,39	0,78
MUSK	NM_005592	0,75	0,79
NTRK1	NM_002529	1,01	0,88
NTRK2	NM_006180	1,43	0,85
NTRK3	NM_002530	0,84	0,86
PDGFRA	NM_006206	1,39	0,88
PTK2	NM_005607	0,75	0,78
PTK2B	NM_004103	0,60	0,84
PTK6	NM_005975	0,61	0,80
PTK7	NM_002821	0,85	0,78
PTK9	NM_002822	1,87	0,88
PTK9L	NM_007284	0,96	0,88
RET	NM_000323	0,68	0,90
ROR1	NM_005012	1,39	0,91
ROR2	NM_004560	1,37	0,95
ROS1	NM_002944	0,37	0,84
RYK	NM_002958	1,03	0,96
SRC	NM_005417	0,51	0,92
SYK	NM_003177	0,42	0,91
TEC	NM_003215	1,30	0,99
TEK	NM_000459	0,73	0,89
TIE	NM_005424	0,81	0,97
TNK1	NM_003985	0,66	1,04
TNK2	NM_005781	0,67	1,06
TP53RK	NM_033550	1,43	1,05
TYK2	NM_003331	0,77	0,99
TYRO3	NM_006293	1,11	1,06
YES1	NM_005433	0,83	1,04

Table 7-3: List of secondary screening candidate genes and the screening outcome relative to the non-silencing siRNA control

gene symbol	RLU	STABW	relative cell viability	STABW
AP1B1	1,463935306	0,131003369	1,064013502	0,017770832
AP1B1	0,461019704	0,069917477	0,964297235	0,018605376
AP1B1	0,102087311	0,013870268	1,009292567	0,017429734
AP1B1	0,234843608	0,034560058	0,973767897	0,06744452
AP2A1	0,260543687	0,044037233	1,194160257	0,174620127
AP2A1	0,293178088	0,05852946	1,101542076	0,073867286
AP2A1	0,231611964	0,047219156	1,234953055	0,058499623
AP2A1	0,085243748	0,016624847	1,201311376	0,109158075
AP2A2	0,57482678	0,020149403	1,053142941	0,050328068
AP2A2	0,355057811	0,028003079	0,953719445	0,053239565
AP2A2	0,121197408	0,015605631	0,829429932	0,045046412
AP2A2	0,371384747	0,032238282	1,15547511	0,171842417
AP2M1	0,2822678	0,026973875	1,098712864	0,028355231
AP2M1	0,357892751	0,054363627	1,193569359	0,102095004
AP2M1	0,107134353	0,010123502	1,114187469	0,088010346
AP2M1	0,210496004	0,093377418	1,231552305	0,089661634
CFL1	0,495084538	0,054596462	0,686148501	0,069611174
CFL1	0,825163158	0,087299616	0,878142206	0,099202805
CFL1	1,031440677	0,024606148	0,84026409	0,056592765
CFL1	0,389110472	0,014482176	0,744984752	0,033164964
CIB3	0,820505275	0,061798742	0,993213563	0,040172512
CIB3	0,678074904	0,050023341	1,029152307	0,002075066
CIB3	0,434860425	0,082058607	0,958921859	0,039648394
CIB3	1,027490384	0,080760377	0,959982033	0,086023575
CLTA	0,506367341	0,035658385	1,07759782	0,093939904
CLTA	0,225685495	0,008594336	1,025439289	0,030446936
CLTA	0,203390754	0,017455658	1,017027271	0,078751896
CLTA	0,354152538	0,027769458	1,011756865	0,042486723
CSF1R	0,115233038	0,016097759	0,99685315	0,069067247
CSF1R	0,612124549	0,022096667	0,985375614	0,014918525
CSF1R	1,249075193	0,028628906	1,195434938	0,130043592
CSF1R	0,425108371	0,014854721	1,230945785	0,139696806
DNM2	0,614827828	0,032659073	1,127310287	0,117056904
DNM2	1,060845112	0,014930359	0,952653611	0,020445027
DNM2	0,986585332	0,112525416	1,115315836	0,13023091
DNM2	0,308831687	0,042075121	1,031168349	0,009865029
EEA1	0,871166675	0,056656793	0,795064517	0,039334732
EEA1	0,909661006	0,085058916	1,002935889	0,072195312
EEA1	0,50342534	0,089887614	0,955794525	0,00582378
EEA1	0,51131907	0,016687429	1,02573043	0,070405591
EPHA1	0,762594839	0,12981261	0,8133839	0,053969405
EPHA1	0,963972135	0,059330104	0,90298773	0,052092074
EPHA1	0,893105771	0,021586343	0,810160316	0,027305178
EPHA1	0,728556789	0,081389552	0,918687847	0,01135546
EPHB6	0,503450719	0,024165401	0,85690049	0,058458511
EPHB6	0,06511516	0,005078525	0,935131741	0,042694178
EPHB6	0,80076999	0,029052826	0,902180932	0,04990351
EPHB6	0,56591892	0,024536056	0,939730788	0,04179296
FGFR2	0,19588189	0,004714588	1,025042986	0,034247792
FGFR2	0,150639876	0,009807501	0,960233439	0,029810821
FGFR2	0,717696418	0,130520196	1,162380422	0,098028689
FGFR2	0,507787592	0,024415979	1,025969515	0,076269305
FGFR3	0,389364518	0,199726171	1,213924838	0,083328265
FGFR3	0,017914581	0,006156027	1,049545863	0,047530092
FGFR3	0,434606869	0,010242263	1,283686198	0,070813611
FGFR3	0,198889585	0,016165412	1,154368	0,151702188
FYN	0,075212073	0,090086461	1,01032405	0,035744551
FYN	0,364641048	0,024346215	1,043130852	0,0585305
FYN	0,225579934	0,011967106	0,956494205	0,007552422
FYN	0,432680123	0,042332494	0,950996018	0,014999869
HCK	1,495321878	0,184008486	1,114243779	0,075431132
HCK	0,590746565	0,117929839	1,042809296	0,04571196
HCK	0,053542586	0,012771252	1,01826857	0,060545408
HCK	0,745015209	0,044530093	0,957032652	0,019678963
HIP1	2,195598022	0,044127464	0,971174001	0,070807022
HIP1	0,192566118	0,017657986	0,973202376	0,063392838
HIP1	1,182300203	0,072406166	0,914205212	0,09709877
HIP1	0,131627935	0,006586933	0,913013278	0,078425138
IGF1R	1,041331053	0,055005259	0,860977856	0,026339745
IGF1R	0,102410077	0,010345159	0,926603	0,028989965
IGF1R	1,402604431	0,052848028	0,935477721	0,020875086
IGF1R	0,638833228	0,014734518	0,927467768	0,016783787

gene symbol	RLU	STABW	relative cell viability	STABW
ITK	0,592708504	0,026780982	0,970353909	0,060043299
ITK	0,824238664	0,126194864	0,915177883	0,040711454
ITK	1,456975556	0,190073973	0,950511343	0,060290643
ITK	0,762140231	0,017405428	0,929860738	0,055240412
KIT	0,231222832	0,015071823	0,985026564	0,053427413
KIT	1,260331068	0,056151753	0,86455243	0,025469281
KIT	1,36511648	0,066742411	0,96032251	0,074318526
KIT	0,438645274	0,059108708	0,881248388	0,055148375
MERTK	0,182343459	0,074360514	0,838020095	0,036922326
MERTK	0,451146742	0,004342088	0,819531616	0,024623214
MERTK	0,419401073	0,015583767	0,896484026	0,081207112
MERTK	0,542454671	0,014810498	1,045580807	0,138125681
MST1R	0,791206588	0,147439761	1,016695074	0,03471698
MST1R	1,212182974	0,175936205	0,896118089	0,036452385
MST1R	0,425876057	0,029080032	0,827567058	0,098940254
MST1R	0,653173095	0,039966347	0,853368197	0,067446586
PAK1	0,312467734	0,026197142	0,882129654	0,015618252
PAK1	0,213278944	0,009473852	1,032052321	0,096363394
PAK1	0,228854669	0,051531191	0,957276012	0,06266775
PAK1	1,148153709	0,134933759	1,058478953	0,102668004
PICALM	1,101566242	0,203120147	0,960429274	0,110743485
PICALM	1,375606174	0,175990495	1,001708788	0,048595228
PICALM	1,418558399	0,057211491	1,030129123	0,070171558
PICALM	1,127151411	0,051282768	1,021103582	0,049413
PIK3CG	0,154592659	0,005671147	1,0425784	0,034114752
PIK3CG	0,401155481	0,050122132	0,895706028	0,041800015
PIK3CG	0,529746077	0,060411992	0,984553007	0,093203327
PIK3CG	0,330435551	0,004513833	1,001977861	0,044603716
PIK4CA	0,774857265	0,099769876	1,19962139	0,010630142
PIK4CA	0,394288527	0,00184369	1,259874631	0,084403006
PIK4CA	0,176917052	0,013396023	1,06088408	0,021426182
PIK4CA	0,465602554	0,056960809	1,222371205	0,127444274
PIP5K1A	0,419193164	0,050649197	0,959939442	0,062779017
PIP5K1A	0,694510363	0,0783556	0,962045953	0,10287139
PIP5K1A	1,0044915	0,128393797	1,041221343	0,026335425
PIP5K1A	0,210904353	0,042144476	1,077575466	0,112736852
PSCD3	1,024452573	0,185551619	0,982416872	0,052981955
PSCD3	0,054100283	0,008344817	0,942007586	0,064276882
PSCD3	0,479220313	0,005913742	1,051632463	0,014806384
PSCD3	0,914548905	0,209946761	1,010029827	0,130811045
PTK9	0,594766898	0,058356964	0,996538302	0,014194302
PTK9	0,716217343	0,028822802	0,975497515	0,053154807
PTK9	0,719498683	0,189047032	0,989615012	0,050777466
PTK9	1,585718102	0,019063971	0,997626574	0,062181512
RAB5C	0,698920808	0,043453236	0,997468907	0,031102588
RAB5C	0,158876218	0,041716244	0,967171752	0,024219044
RAB5C	0,719581149	0,044280859	0,9802886	0,003275071
RAB5C	0,401280994	0,022352894	1,000482064	0,034600214
RAC1	0,573065875	0,036858524	0,948098889	0,053436466
RAC1	0,395154037	0,088087241	1,03293833	0,122129722
RAC1	2,232721487	0,239189605	1,043452797	0,07839917
RAC1	0,446234008	0,014240952	1,095313493	0,096364046
RHOA	0,104384888	0,007861502	1,22324437	0,04978591
RHOA	0,117937055	0,025225533	1,21364214	0,133254782
RHOA	0,040940369	0,004131704	1,098608138	0,041848332
RHOA	0,08925145	0,022508484	1,167970367	0,060801242
ROCK1	1,206742707	0,248050249	0,925676516	0,00469467
ROCK1	0,439793425	0,078517789	0,923008848	0,053648745
ROCK1	1,248722126	0,135153295	1,004285782	0,063991617
ROCK1	0,873524092	0,081411487	0,988809631	0,121074082
ROR1	0,872178715	0,023533179	0,872073138	0,024860021
ROR1	1,016660407	0,074641948	0,920701868	0,048437842
ROR1	0,493132674	0,02063549	0,855354977	0,012986215
ROR1	1,141644653	0,026263533	0,905629198	0,00663874
ROS1	0,389166547	0,028089464	0,892824477	0,043723273
ROS1	0,606124737	0,016610346	0,940899835	0,082677724
ROS1	0,114336625	0,005470229	0,708757237	0,017802266
ROS1	0,472998883	0,018146381	0,932725146	0,019214058
SYNJ2	0,722773781	0,108752961	1,009196085	0,131091569
SYNJ2	0,595600802	0,039118374	1,025259966	0,046198742
SYNJ2	0,830578202	0,144650366	1,036794794	0,131370482
SYNJ2	0,16559434	0,022437539	0,973541178	0,054897001

7.3 List of single siRNAs

Table 7-4: Assignment of duplex numbers of specific single siRNAs and non-silencing siRNAs

Target mRNA	Specific siRNA #	Dharmacon Duplex number
AP1B1	1	D-011200-01
	2	D-011200-02
	3	D-011200-03
	4	D-011200-04
AP2A1	1	D-012492-01
	2	D-012492-02
	3	D-012492-03
	4	D-012492-04
AP2A2	1	D-012812-01
	2	D-012812-02
	3	D-012812-03
	4	D-012812-04
AP2M1	1	D-008170-01
	2	D-008170-02
	3	D-008170-03
	4	D-008170-04
CLTA	1	D-004002-01
	2	D-004002-02
	3	D-004002-03
	4	D-004002-04
FGFR3	1	D-003133-05
	2	D-003133-06
	3	D-003133-07
	4	D-003133-08
FYN	1	D-003140-09
	2	D-003140-10
	3	D-003140-23
	4	D-003140-24
H-Ras	1	J-004142-07
	2	J-004142-08
	3	J-004142-09
	4	J-004142-10
IFITM1	1	J-019543-05
	2	J-019543-06
	3	J-019543-07
	4	J-019543-08
PAK1	1	D-003521-03
	2	D-003521-05
	3	D-003521-07
	4	D-003521-21
PIK3CG	1	D-005274-03
	2	D-005274-04
	3	D-005274-05
	4	D-005274-06
PIK4CA	1	D-006776-02
	2	D-006776-03
	3	D-006776-09
	4	D-006776-25
RAC1	1	D-003560-07
	2	D-003560-08
	3	D-003560-09
	4	D-003560-30
RHOA	1	D-003860-01
	2	D-003860-02
	3	D-003860-03
	4	D-003860-04
	Non-silencing siRNA #	
	3	D-001210-03
	Pool	D-001810-10

8 ACKNOWLEDGEMENTS

An dieser Stelle möchte ich mich bei allen Freunden und Kollegen bedanken, die mich bei der Erstellung dieser Arbeit unterstützt haben.

Ein ganz besonderes Dankeschön geht an meine beiden Betreuer Rudolf Beier und Florian Pühler, die mir immer mit Rat und Tat zur Seite standen, viele praktische Tipps für mich hatten (nicht nur von wissenschaftlicher Natur ;-)) und mich mit Ideen und wertvollen Verbesserungsvorschlägen nur so überhäuft haben. Eine bessere Betreuung hätte ich mir nicht vorstellen können!!!!

Ein großes Dankeschön möchte ich auch an Herrn Mumberg richten, der sich immer, wenn es seine Zeit zuließ, mit regem Interesse am Fortschreiten meiner Arbeit beteiligt hat. Darüberhinaus war er auch immer bereit, während Dienstreisen im Ausland oder im Urlaub, dringende Fragen und Anliegen meinerseits geduldig zu beantwortet und zu klären.

I am really grateful to my reviewer Sanna-Maria Käkönen for not only carefully reading my dissertation but also my paper. Many thanks for the valuable comments on both! Furthermore, I would like to thank you for the cordial and motivating talks.

Professor Mutzel Danke ich für die Übernahme der Gutachtertätigkeit.

Weiterhin möchte ich mich bei meinen beiden Laborkollegen Katja Köckritz und Steve Baethge bedanken, die mich geduldig beim Erlernen von virologischen Methoden unterstützt haben und auch sehr gute Diskussionspartner bei der Planung von Versuchen waren! Vielen Dank auch dafür, dass Ihr es mehr als 3 Jahre lang mit mir auf engsten Schreibraum ausgehalten habt. Ich werde mich auch mit Freude an die persönlichen und vor allem auch lustigen Gespräche erinnern sowie an die tollen Bastelnachmittage mit Katja, die mir so manch kurzfristige Rennerei vor dem Weihnachtsabend erspart haben!

Ein großes Dankeschön geht auch an meine Doktoranden- und Postdoktoraden-Gemeinschaft (nicht nur, aber vor allem aus der TRG Oncology!), die mir mit wertvollen technischen Tipps und Tricks sowie Gerätschaften und Labormaterialien auch in letzter Sekunde ausgeholfen

haben. Nicht zu vergessen sind natürlich auch die Lady Lunches und netten Abende und Ausflüge zusammen!

Außerdem möchte ich mich beim ehemaligen 3.OG der TRG Oncology für die freundliche und herzliche Arbeitsatmosphäre und die Hilfestellungen bedanken.

Ein weiteres Dankeschön geht an Frau Dr. Boukamp vom DKFZ, die mir freundlicherweise die tumorigen HaCaT-Derivate zur Verfügung gestellt hatte. Ohne diese Zellen wäre diese Arbeit um ein Vielfaches erschwert worden!!!

Zu guter letzt möchte ich mich bei meinem Partner Christoph bedanken, der mir auch zu später Abendstunde nützliche Ratschläge zu Versuchen gegeben hat, mich oftmals wieder aufgemuntert und motiviert hat, wenn ein Versuch mal wieder so gar nicht funktionieren wollte und der nicht Müde geworden ist diese Arbeit korrekturzulesen!!!

9 LIST OF ORIGINAL PUBLICATIONS

9.1 Papers

I Rac1 is required for oncolytic NDV replication in human cancer cells and establishes a link between tumorigenesis and sensitivity to oncolytic virus
Puhlmann J, Puehler F, Mumberg D, Boukamp P, Beier R.; Oncogene 2010. Epub 2010 Jan 25.

II Generation of a recombinant oncolytic Newcastle disease virus and expression of a full IgG antibody from two transgenes
Pühler F, Willuda J, Puhlmann J, Mumberg D, Römer-Oberdörfer A, Beier R.; Gene Ther. 2008 Mar;15(5):371-83. Epub 2008 Jan 17.

III Expression of porcine endog enous retroviruses (PERVs) in melanomas of Munich miniature swine (MMS) Troll
Dieckhoff B, Puhlmann J, Büscher K, Hafner-Marx A, Herbach N, Bannert N, Büttner M, Wanke R, Kurth R, Denner J.; Vet Microbiol. 2007 Jul 20;123(1-3):53-68. Epub 2007 Feb 27.

9.2 Posters

I Malignant progression in a human cell transformation model correlates with increasing suceptibility to oncolytic Newcastle disease virus
Jenny Puhlmann, Florian Puehler, Petra Boukamp, Dominik Mumberg, Rudolf Beier
Third European Congress of Virology, Nürnberg, Germany, 2007

II Identification of oncolytic virus-sensitizing genes by an siRNA based screen
Jenny Puhlmann, Florian Puehler, Petra Boukamp, Dominik Mumberg, Rudolf Beier
ASGT 11th Annual Meeting, Boston, Massachusettes, USA, 2008

10 CURRICULUM VITAE

(deleted)

11 EIDESSTATTLICHE ERKLÄRUNG

Hiermit versichere ich, dass ich die vorliegende Arbeit selbstständig durchgeführt und verfasst habe. Dabei wurden keine anderen als die angegebenen Quellen und Hilfsmittel verwendet.

Berlin, 20.10.2009

Jenny Sarah Puhlmann